A STUDY OF SUBSTITUENT EFFECTS AND EXCHANGE REACTIONS OF PROTONATED ANILINES AND OF HINDERED ROTATION ABOUT THE C-N BONDS IN PROTONATED BENZYLAMINES BY PROTON MAGNETIC RESONANCE

by

William F. Reynolds

THE UNIVERSITY OF MANITOBA ELIZABETH DAFOE LIBRARY

A Thesis Presented to

The Faculty of Graduate Study and Research

University of Manitoba

In Partial Fulfillment of the Requirements

for the Degree

Doctor of Philosophy

TO MY PARENTS

ACKNOWLEDGEMENTS

I would like to thank Dr. T. Schaefer for his advice given during the course of this research project and also for his patience in answering the many questions which I have asked him.

I would like to thank Dr. J. Martin for providing a copy of his thesis and also Drs. G. Fraenkel and R. Drago for supplying preprints of publications.

Mr. E. Erickson has been most helpful in the maintenance of the NMR spectrometer. The preparation and sealing of sample tubes was done by Mr. George Epp.

Finally I would like to express my gratitude to The National Research Council of Canada for their financial assistance.

ABSTRACT

The ring proton shifts of a large number of ring- and N-substituted anilines in an inert solvent (CCl_4) and a protonating solvent (CF_3COOH) are given. It is shown that aniline is protonated in CF_3COOH. The ammonio group causes a low field chemical shift (relative to benzene) of 0.3 ppm for all ring protons of aniline and para-substituted anilines. The effect of the ammonio group is estimated by field effect calculations. The effect of ion pair formation upon ring proton shifts is estimated. The observed chemical shifts can be rationalized by field effect calculations if, (a) the E^2 term in Buckingham's equation is too large by a factor of four, or (b) anilinium trifluoracetate exists in solution largely as intimate ion pairs. It is concluded that the latter explanation is more reasonable. The ring proton shifts of some of the protonated N,N-dialkylanilines are not equal. This is attributed to steric hindrance of ion pair formation.

The effects of substituents upon chemical shifts of protonated and unprotonated para-substituted anilines are shown to be additive. This is attributed to "saturation".

The shifts of protons ortho to substituents can be rationalized by reasonable combinations of inductive, field, mesomeric, anisotropic, and dispersive effects. The meta proton shifts sometimes cannot be accounted for because anomolous high field shifts are sometimes noted.

The effect of steric hindrance upon the mesomeric inter-

action of the amino group is established. Steric hindrance only effects shifts of substituted anilines when (a) at least three of the four N and ortho positions are substituted or (b) a tertiary amine contains at least two phenyl groups.

An apparent direct relationship between substituent effects and amino proton shifts is noted. The amino proton shifts of meta - and para- substituted anilines are related to the appropriate Hammett reactivity parameters. The amino proton shifts of ortho-substituted anilines are shifted to low field. These shifts probably arise from dispersive and/or anisotropic effects.

The effect of hindered rotation upon methylene and ammonio proton shifts and coupling constants of eight protonated benzylamines has been determined. It is shown theoretically and confirmed experimentally that the necessary and sufficient condition for methylene proton asymmetry in protonated benzylamines is the absence of a plane of symmetry along the $C_6H_5CH_2$-N bond axis. It is established that the maximum value of the gauche H-C-N-H^+ coupling constant is 3.15 c/s and that the minimum value of the trans H-C-N-H^+ coupling constant is 9.45 c/s. From the relative values of the rotationally averaged coupling constants, it is established that the steric effect of the substituent decreases in the following order:

$$\left.\begin{array}{l}\text{isopropyl}\\ \text{phenyl}\end{array}\right\} \gtrsim \text{benzyl} \approx \text{ethyl} > \text{methyl}$$

It cannot be decided from the available evidence whether the phenyl group or the isopropyl group causes greater steric hindrance.

The proton exchange reactions of a large number of halo-substituted anilines in trifluoracetic acid have been investigated. The lifetimes of acid protons in these solutions have been determined by measuring the acid proton signal width. In addition, the exchange rate of protonated N,N-dimethylaniline in trifluoracetic acid has been determined by measuring the effect of temperature upon the apparent H_3C-N-H^+ coupling constant . It is concluded that proton exchange probably occurs via the following reaction:

$$\emptyset NH_3^+ + A^- \underset{k-1}{\overset{k_1}{\rightleftharpoons}} \emptyset NH_2 + HA .$$

The forward reaction has the smaller rate constant and it determines the overall exchange rate. The reaction is believed to occur in two steps: the oppositely charged ions form ion pairs which then transfer protons internally. Experimental evidence indicates that the ion pair dissociation constant is less than, or equal to one.

The activation energies of proton transfer of the various solutions are determined from the temperature dependence of the lifetimes of the acid protons. They range from 10 to 24 Kcal/mole. It is shown that the experimental activation energies are somewhere in between the activation energies for the over-

all reactions and the ion pair reactions.

The rate constants at 25°C for the bimolecular reactions are calculated. Ionic activity coefficients are estimated by the Debye-Hückel equation. The corrected rate constants are calculated. Another set of rate constants is calculated, assuming that the ions exist partly as ion pairs and that the ion pair dissociation constant is equal to one. The rate constants for the ion pair reaction are also calculated, assuming that the ion pair dissociation constant has a value between zero and one.

The free energies, enthalpies and entropies of activation are also calculated for the ion pair reaction and for the overall biionic reaction. The free energies of activation range from 10 to 17 Kcal/mole. There is a definite relationship between the type and position of halogen and the value of the free energy of activation. All free energies of activation for haloanilines are less than that of aniline. In the ortho- and para-substituted anilines, $\Delta F^{\ddagger}$, in general, decreases with decreasing halogen electronegativity. $\Delta F^{\ddagger}$ values for meta-substituted anilines decrease with increasing substituent electronegativity. $\Delta F^{\ddagger}$ values are largest for para-haloanilines and smallest for ortho-haloanilines. It is shown that the $\Delta F^{\ddagger}$ values for haloanilines can be rationalized by reasonable combinations of inductive and mesomeric effects.

The values of entropies of activation are determined

largely by the positions of the substituents. $\Delta S^{\ddagger}$ values range from 35 eu to -10 eu with aniline and para-substituted anilines having the largest positive values and ortho-substituted anilines having negative values. The $\Delta S^{\ddagger}$ values are rationalized by assuming that there is an increase in the steric and electrostatic hindrance of solvation of ion pairs when a substituent is placed close to the charge centres.

It is shown that the collapse of the methyl doublet in protonated N,N-dimethylaniline is caused by the exchange of ammonio proton spins (T_1 relaxation) rather than just ammonio proton exchange. It is assumed that the rate of change of spin is one half of the total exchange rate. Possible errors in this assumption are considered. Free energies, enthalpies, and entropies of activation are calculated.

The value of $\Delta F^{\ddagger}$ for protonated N,N-dimethylaniline is larger than that for protonated aniline, as would be expected. Since the relative values appear to be reasonable, it is concluded that the same type of exchange reaction is being measured in each case. $\Delta S^{\ddagger}$ is quite small. This is attributed to steric hindrance of solvation of the dimethylanilinium ion.

TABLE OF CONTENTS

CHAPTER		PAGE
1	GENERAL INTRODUCTION.....	1
2	A STUDY OF PROTONATION OF ANILINES.....	4
	1. INTRODUCTION.....	4
	2. THEORETICAL DISCUSSION.....	5
	(A) Factors Affecting Proton Chemical Shifts.....	5
	3. EXPERIMENTAL.....	38
	4. RESULTS.....	40
	(A) In CCl_4.....	40
	(B) In CF_3COOH.....	43
	5. DISCUSSION OF RESULTS.....	44
	(A) Aniline.....	44
	(B) *Para*-Substituted Anilines.....	51
	(C) N-Alkyl-Substituted Anilines.....	67
	(D) Toluidines and Dimethylanilines...	71
	(E) Amino Proton Shifts.....	73
	6. SUMMARY AND CONCLUSIONS.....	76
3	A STUDY OF HINDERED ROTATION IN PROTONATED BENZYLAMINES.....	90
	1. INTRODUCTION.....	90
	2. THEORETICAL DISCUSSION.....	91
	(A) Effect of Energy Levels Upon Relative Rotation Rates About Single Bonds and Upon Relative Populations of Rotation Isomers.....	91
	(B) Effects of Rotation Rate and Rotamer Populations Upon Methylene Proton Asymmetry.....	92

TABLE OF CONTENTS CONTINUED

CHAPTER		PAGE
	(C) Effect of Rotamer Population and Rotation Rate Upon Proton Coupling Constants.....	101
	(D) Effect of Proton Exchange Upon Methylene Proton Asymmetry and Observed Coupling Constants.....	107
	(E) Analysis of A_2X, ABX and A_2X_2 Proton Spectra When the X Proton Spectra Are Unmeasurable.....	108
	3. EXPERIMENTAL.....	110
	4. RESULTS.....	111
	5. DISCUSSION OF RESULTS.....	115
	(A) Effect of Proton Exchange.....	115
	(B) Type 1 Compounds.....	118
	(C) Type 2a Compounds.....	121
	(D) Type 2b Compounds.....	122
	(E) Possible Values of Jg and J_t...	124
	6. SUMMARY AND CONCLUSIONS.....	125
4	A STUDY OF PROTON EXCHANGE REACTIONS OF SUBSTITUTED ANILINES IN TFA.....	129
	1. INTRODUCTION.....	129
	2. THEORETICAL DISCUSSION.....	131
	(A) Spin-Lattice Relaxation Time T_1...	131
	(B) Spin-Spin Relaxation Mechanisms and Spin-Spin Relaxation Time.....	133
	(C) Spin-Lattice Relaxation Mechanisms	138

TABLE OF CONTENTS CONTINUED

CHAPTER		PAGE
	(D) An Alternative Treatment of Relaxation Times, the Bloch Formulation.....	141
	(E) Effect of Exchange Upon T_2 and Signal Line Widths.....	145
	(F) Ion Association or Ion Pair Formation.....	152
3.	EXPERIMENTAL.....	158
	(A) Aniline and Haloanilines in TFA...	158
	(B) N,N-dimethylaniline in TFA.....	163
4.	RESULTS.....	165
	(A) Aniline and Haloanilines in TFA...	165
	(B) N,N-dimethylaniline in TFA.....	168
5.	DISCUSSION OF RESULTS FOR ANILINE AND HALOANILINES.....	187
	(A) Factors Affecting the Shapes of Plots of Acid Proton Line Width Versus Temperature.....	187
	(B) Probable Reactions in Solution and Their Effect Upon the Observed Kinetics.....	191
	(C) Calculation and Discussion of Thermodynamic Data.....	202
	(D) Probable Errors in Measurements of Line Widths and Calculation of Exchange Rates.....	213
6.	DISCUSSION OF RESULTS FOR N,N-DIMETHYLANILINE.....	220

TABLE OF CONTENTS CONTINUED

CHAPTER		PAGE
	7. SUMMARY AND CONCLUSIONS.....	226
5	RECOMMENDATIONS FOR FUTURE RESEARCH.....	240
	BIBLIOGRAPHY.....	243

LIST OF FIGURES*

FIGURE PAGE

CHAPTER 2

1. Plot of the Distance, a, of the Effective Dipole of the C-X Bond in C_6H_5X from the Alpha Carbon Atom Versus the Value of the Geometric Factor at Four Points in the Phenyl Ring..... 28

2. Planar Projections of the Bonds and van der Waals Radii of Substituents of (A) CH_3X and (B) C_6H_5X Compounds..... 33

3. Ring Proton Spectra of p-Iodoaniline in (A) CCl_4 and (B) TFA..... 42

4. The Calculated Fields Due to the Ammonio Group and the Counter Ion at the Ring Protons of $C_6H_5NH_3^+$ Ions..... 50

5. (A) The Ortho and Meta Proton Shifts of Aniline and p-Substituted Anilines in CCl_4..... 56

5. (B) The Ortho and Meta Proton Shifts of Aniline and p-Substituted Anilines in TFA..... 57

6. Plot of Amino Proton Shifts of Aniline and Ring Substituted Anilines in CCl_4 Versus Hammett Constants..... 75

CHAPTER 3

1. A Typical Energy Level Diagram for Rotation About the C-C Bond of an Ethane-Type Molecule 93

2. The Three Possible Rotamers for a Protonated Compound of the Type XCH_2-$(NRSH)^+$..... 95

3. The Three Possible Rotamers for a Protonated Compound of the Type XCH_2-$(NR_2H)^+$..... 99

4. The Three Possible Rotamers for a Protonated Compound of the Type XCH_2-$(NRH_2)^+$..... 106

5. The Methylene Proton Spectrum of Protonated N-Methyldibenzylamine..... 113

---

* All figures in each chapter are numbered consecutively, starting from 1.

LIST OF FIGURES CONTINUED

FIGURE		PAGE
6.	The Methylene Proton Spectrum of Protonated N,N-dimethylbenzylamine.....	113
7.	The Methylene Proton Spectrum of Protonated N-isopropylbenzylamine.....	114
8.	The Methylene Proton Spectrum of Protonated Dibenzylamine.....	114
	CHAPTER 4.	
1.	The UV Spectra of Pure TFA and a One Mole Per Cent Solution of Aniline in TFA.....	170
2.	The UV Spectra of a Twenty Mole Per Cent Solution of Aniline in TFA Diluted 1:100 and 1:1000 in Acetonitrile.....	171
3.	Plot of Log (TFA Proton Line Width) Versus ($1/T^{o}K$) for a Four Mole Per Cent Solution of Aniline in TFA.....	172
4.	Plot of Log (TFA Proton Line Width) Versus ($1/T^{o}K$) for a Two Mole Per Cent Solution of p- Fluoroaniline in TFA.....	173
5.	Plot of Log (TFA Proton Line Width) Versus ($1/T^{o}K$) for a Three Mole Per Cent Solution of p-Chloroaniline in TFA.....	174
6.	Plot of Log (TFA Proton Line Width) Versus ($1/T^{o}K$) for a Two Mole Per Cent Solution of p-Bromoaniline in TFA.....	175
7.	Plot of Log (TFA Proton Line Width) Versus ($1/T^{o}K$) for a Two Mole Per Cent Solution of p-Iodoaniline in TFA.....	176
8.	Plot of Log (TFA Proton Line Width) Versus ($1/T^{o}K$) for a Two Mole Per Cent Solution of m-Iodoaniline in TFA.....	177
9.	Plot of Log (TFA Proton Line Width) Versus ($1/T^{o}K$) for a Two Mole Per Cent Solution of m-Bromoaniline in TFA.....	178

LIST OF FIGURES CONTINUED

FIGURE		PAGE
10.	Plot of Log (TFA Proton Line Width) Versus (1/T°K) for a Three Mole Per Cent Solution of m-Chloroaniline in TFA.....	179
11.	Plot of Log (TFA Proton Line Width) Versus (1/T°K) for a One Mole Per Cent Solution of m-Fluoroaniline in TFA.....	180
12.	Plot of Log (TFA Proton Line Width) Versus (1/T°K) for a One Mole Per Cent Solution of o-Fluoroaniline in TFA.....	181
13.	Plot of Log (TFA Proton Line Width) Versus (1/T°K) for a Two Mole Per Cent Solution of o-Chloroaniline in TFA.....	182
14.	Plot of Log (TFA Proton Line Width) Versus (1/T°K) for a One Mole Per Cent Solution of o-Bromoaniline in TFA.....	183
15.	Plot of Log (TFA Proton Line Width) Versus (1/T°K) for an Eight Mole Per Cent Solution of Aniline in TFA.....	184
16.	Plot of Log (TFA Proton Line Width) Versus (1/T°K) for an Eight Mole Per Cent Solution of m-Chloroaniline in TFA.....	185
17.	Plot of Log (Calculated Ammonio Proton Spin Exchange Rate) Versus (1/T°K) for a Ten Mole Per Cent Solution of N,N-Dimethylaniline in TFA.....	186
18.	Plot of TFA Proton Exchange Rate Versus $\frac{[\emptyset NH_3^+]^{1.2}}{[HA]} \times 10^2$.....	196
19.	Hypothetical Plot of Relative Enthalpies of Ions, Ion Pairs, Activated Complex and Free Molecules for a Solution of Anilinium Trifluoracetate in TFA.....	205

LIST OF FIGURES CONTINUED

FIGURE PAGE

20. Plot of Log (Additional Acid Proton Line Width) Versus (1/T°K) for a One Mole Per Cent Solution of p-Fluoroaniline in TFA..... 217

21. Theoretical Methyl Proton Spectrum of Protonated N,N-Dimethylaniline..... 222

LIST OF TABLES*

TABLE		PAGE
	CHAPTER 2	
I	Chemical Shifts of the Ring Protons of Substituted Anilines in CCl_4 and TFA.....	78
II	Ring Methyl Proton Shifts of Methyl-Substituted Anilines in CCl_4 and TFA.....	81
III	Amino Proton Shifts of Substituted Anilines in CCl_4.....	82
IV	Calculations of Field Effects Due to the Ammonio Group and the Trifluoracetate Ion...	83
V	Experimental and Predicted Shifts of p-Substituted Anilines in CCl_4 and Cyclohexane	84
VI	Experimental and Predicted Shifts of p-Substituted Anilines in TFA.....	85
VII	Calculated Chemical Shifts of p-Substituted Anilines in CCl_4.....	86
VIII	Estimated Ortho Proton and C^{13} Shifts of p-Substituted Anilines (Relative to Aniline) After Correction for Mesomeric Effects.....	87
IX	Predicted and Observed Ring Proton Shifts of Methyl-Substituted Anilines in TFA.....	88
X	Predicted and Observed Ring Proton Shifts of Methyl-Substituted in CCl_4.....	89
	CHAPTER 3	
I	Coupling Constants and Internal Chemical Shifts of Methylene Protons of Substituted Benzylamines in TFA.....	126
II	Chemical Shifts of Methylene Protons of Benzylamines in TFA.....	128

---

* All tables are numbered consecutively in each chapter, starting from I.

LIST OF TABLES CONTINUED

TABLE		PAGE
	CHAPTER 4	
I	Line Widths of TFA and Cyclohexane Protons in Two Solutions of Cyclohexane in TFA.....	165
II	Measured Acid Proton Line Widths and Acid Proton Exchange Rates of Solutions of Substituted Anilines in TFA.....	228
III	(A) Acid Proton Exchange Rates of Different Solutions of Aniline in TFA.....	233
	(B) Apparent and Corrected Rate Constants of Proton Exchange of Solutions of Aniline in TFA at 50.2°C.....	233
IV	Chemical Shifts of TFA Protons and Anilinium Ion Ring Protons in Different Solutions of Aniline in TFA.....	234
V	Acid Proton Line Widths of Solutions of Aniline and Trifluoracetic Anhydride in TFA at 25°C.....	235
VI	Measured Peak Separation of the Methyl Doublet of Protonated N,N-dimethylaniline and Calculated Values of the Proton Spin Exchange Rate of N,N-dimethylaniliniu m Ions.....	235
VII	Measured Activation Energies of Proton Transfer and Calculated Enthalpies of Activation of Proton Transfer of Solutions of Aniline and Substituted Anilines in TFA.....	236
VIII	Calculated Rate Constants for the Reactions of Solutions of Aniline and Substituted Anilines in TFA.....	237
IX	Calculated Values of Free Energies of Activation for the Reactions of Solutions of Aniline and Substituted Anilines in TFA....	238

LIST OF TABLES CONTINUED

TABLE PAGE

X Calculated Values of Entropies of Activation for the Reactions of Solutions of Aniline and Substituted Anilines in TFA..... 239

CHAPTER 1

GENERAL INTRODUCTION

The theory of nuclear magnetic resonance spectroscopy has been developed in detail in several monographs (1-5).* Therefore, the theory of NMR will not be developed in this chapter. Instead, the theory which is needed to consider the results given in any chapter will be developed in that chapter.

Numerous papers have been published which give results of experiments in which NMR spectroscopy has been used as a tool to study the nature of substituent effects. Usually, proton chemical shifts were correlated with substituent effects. NMR spectroscopy has also proved to be a very useful tool for investigating a fairly large number of physical and chemical processes which cannot be conveniently investigated using other physical methods. Among the types of processes which have been investigated are hindered rotation about single bonds in substituted ethanes and rapid proton chemical exchange reactions.

My original research project was the investigation of the effect of the ammonio ($-NH_3^+$) group upon proton chemical shifts of protonated anilines. This project was later expanded to include the investigation of hindered rotation about the C-N bonds in protonated benzylamines and the investigation of proton exchange

---

*No other reference numbers are given in this chapter. Any investigations which are mentioned in this chapter will be referred to in later chapters.

reactions of protonated anilines in trifluoracetatic acid. The three projects are discussed in separate chapters. The contents of the three chapters are outlined below.

The effects of substituents upon the ring proton shifts of mono- and di-substituted benzenes have been investigated by various workers. However, at the time that this project was started, there was very little published information about the effect of the ammonio group upon ring proton shifts. The information which was available indicated that the ammonio group affected all ring protons equally. This is not what one would intuitively expect. Therefore, the ring proton chemical shifts of a series of substituted anilines in trifluoracetic acid were determined. In addition, the proton shifts of the same anilines in a non-protonating solvent (CCl_4) were measured. A series of field effect calculations were carried out in order to theoretically predict the field effects of substituents and ion pairs upon proton chemical shifts. The results of these measurements and calculations are given in Chapter 2. The results are discussed in terms of the various substituent effects which may give rise to proton chemical shifts.

NMR spectroscopy has often been used to study hindered rotation about the C-C bonds of substituted ethanes. However, hindered rotation about C-N bonds in protonated bases has apparently not been studied previously. Therefore, it was

decided to investigate hindered rotation about the C-N bonds in various protonated benzylamines. The results are given in Chapter 3. The minimum substitution which is necessary to cause methylene proton asymmetry is determined. The relative magnitudes of steric effects of substituents and the limiting values of vicinal H-C-N-H coupling constants are determined.

The proton exchange reactions of ammonium and alkylammonium ions in aqueous solution have been extensively investigated by NMR. However, the exchange reactions of anilinium ions in aqueous solution have not been studied, presumably because the reactions are too rapid to be measured. It was decided to investigate the proton exchange reactions of substituted anilines in trifluoracetic acid, since it was found that the exchange reactions had measurable rates near room temperature. The exchange rate of protonated N,N-dimethylaniline at different temperatures was determined by measuring the separation of the methyl doublet. The exchange rates of protonated aniline and haloanilines were determined by measuring the line widths of the acid proton signals in the various solutions. The results are given in Chapter 4. The probable reactions which occur in solution are considered and thermodynamic data for the exchange reactions are calculated.

CHAPTER 2

A STUDY OF PROTONATION OF ANILINES

1. INTRODUCTION

It has been shown that aniline dissolved in acetic acid (6,7), and in many inorganic acids (8), has a ring proton NMR spectrum consisting of a single peak. This suggests that the ammonio group (NH_3^+) has either no effect or else an equal inductive effect upon all ring protons. The spectra of a large number of ring- and N-substituted anilines in trifluoracetic acid (TFA) have been studied in an effort to determine the effect of the ammonio group upon ring proton shifts. It is found that the ammonio group causes a low field shift of approximately 0.30 ppm for all ring protons of a series of substituted anilines. The effect of the field due to the ammonio group is calculated. The effect of ion pair formation is also considered. The results (based on certain assumptions) quantitatively predict the observed ring proton shifts.

For purposes of comparison, solutions of the various anilines in an inert solvent (CCl_4) have been prepared and the ring proton spectra measured. Differences in shielding between ring protons in substituted benzenes have been discussed in terms of additive substituent effects (9-12), Hammett reactivity parameters (9-11, 13-15), electric field

effects due to substituents (10,11,13,15,16), magnetic anisotropy of the substituents (13,15), and of special solvent effects (17). The ring proton shifts of the substituted anilines in both solvents are discussed in terms of the above effects and also in terms of the dispersive effects of the substituents. It is found that shifts of protons ortho to substituents can be accounted for by the effects mentioned above. However, meta proton shifts cannot be completely explained, since anomolous high field shifts are sometimes observed. It is shown that substituent effects are nearly additive for mono - substituted anilines in both solvents.

Steric hindrance of the mesomeric effect of the amino group is observed for some N-substituted anilines. The minimum substitution which will cause steric hindrance of the mesomeric effect is established.

2. THEORETICAL DISCUSSION

Factors Affecting Proton Chemical Shifts

For a fixed value of the RF field, there is a definite value of the main magnetic field H, at which a bare proton will resonate. If the proton is in an environment containing electrons, then the circulation of electronic charge caused by H will produce a secondary magnetic field which is proportional to the main field. The secondary field

generally acts in opposition to the main magnetic field, decreasing the field seen by the proton. Consequently the proton resonance occurs at a new field H_o, where

$$H_o - H = \sigma H_o . \qquad 2.1$$

σ, the shielding parameter, is a constant for a given proton and depends upon the electronic environment in the vicinity of the proton.

The chemical shift of a proton in any compound is the difference between the applied field at which resonance occurs and the field at which a bare proton resonates (H_o - H). It is usually more convenient to express chemical shift in terms of the difference in shift between the proton in question and a reference proton. Since the difference in shielding is a function of applied field, it is most useful to define the chemical shift by the following unitless expression:

$$\text{chemical shift} = \frac{H_o - H_r}{H_o} \qquad 2.2$$

where H_r = the field at which the reference proton resonates. This ratio is commonly expressed in parts per million (ppm). When this definition is used, the shift is the same regardless of the magnetic field strength and the frequency of the applied RF field.

The shielding parameter has been separated into three components by Pople (18,19) in his studies of electron circulations in molecules.

$$\sigma = \sigma_D + \sigma_P + \sigma_{ID}. \qquad 2.3$$

σ_D = contribution due to atomic diamagnetic currents.

σ_P = contribution due to paramagnetic currents.

σ_{ID} = contribution due to interatomic diamagnetic currents.

Consider an isolated atom. In the presence of a magnetic field, the circulation of electrons about the nucleus produces a secondary field which opposes the main field. This reduces the field seen by the nucleus, i.e., it increases the shielding of the nucleus. σ_D, the contribution due to this diamagnetic field, can be evaluated by the Lamb formula (20).

$$\sigma_D = \frac{e^2}{mc^2}\int \frac{\rho}{r}\, d\tau. \qquad 2.4$$

For a proton, $\rho \approx \lambda \psi_{1s}^2$, where λ measures the effective number of electrons in the hydrogen Is orbital. Evaluating the integral, we obtain

$$\sigma_D = 17.8\, \lambda \times 10^{-6}. \qquad 2.5$$

Since λ is a direct function of effective electron density, factors which alter the electron density should change the chemical shift in a corresponding manner.

The paramagnetic shielding component σ_p arises from the diamagnetic anisotropy of an atom in a molecule. As a result of this anisotropy, the ease of electron flow depends upon the orientation of the molecule in the magnetic field. In quantum mechanical terms this shielding corresponds to a mixing, under the influence of the applied field, of the ground state electronic configuration with low-lying excited states. The mixing only occurs for certain orientations of the molecule in the applied field.

It is difficult to evaluate σ_p since one must know all the necessary ground state and excited state wave functions. These are seldom known. However, since protons have no low-lying p orbitals, paramagnetic contributions should be small (21).

The third component σ_{ID} arises from interatomic circulation of electronic charge. This component is particularly important for aromatic molecules. The π electrons of aromatic molecules form closed loops through which current may flow. By assuming that the π electron system formed a closed loop, Waugh and Fessenden (22) calculated a low field shift of 2.2 ppm for benzene protons, due to interatomic circulations. They found an actual shift of -1.5 ppm (using the

ethylenic protons of 1, 3-cyclohexadiene as a reference).

As can be seen from the above discussion, proton chemical shifts depend upon the electronic environment. The introduction of substituents can alter the electronic environment by a number of mechanisms. Some of these are discussed below.

1. Changes in the electron density around the proton by substituents

The chemical shift is a function of effective electron density around the proton (see equation 2.5). Consequently, any alteration of the electron density by a substituent will cause a corresponding change in the chemical shift. For aromatic molecules it has been common practice to postulate two mechanisms by which substituents can alter electron density; inductive donation or withdrawal of electrons and mesomeric interaction between the substituent and the electron system of the aromatic ring. These two mechanisms have been subdivided into five mechanisms (23). The effects of these mechanisms upon chemical shifts are discussed below.

(a) Field effects - A substituent bonded to a ring carbon atom usually polarizes the C-X bond, forming a dipole. If the electric field E, associated with the dipole, has a component along the C-H bond axis, it will polarize the bond and cause a net shielding or deshielding of the proton.

There is also a deshielding effect proportional to E^2(16). This effect depends upon the component of the field perpendicular to the bond. This component destroys the axial symmetry of the bond, reducing the diamagnetic shielding.

(b) Primary inductive effect - A substituent can donate or withdraw electrons from the protons directly through the σ bonds. It is generally accepted that the σ inductive effect drops off exponentially with the number of bonds.

(c) π inductive effect - The withdrawal or donation of electrons by the substituent will set up an electrical charge at the alpha carbon atom. The electric field resulting from this charge will polarize the π electron system. As a result, the electron densities around the protons may be altered by field effects or σ inductive effects acting through the C-H bonds. If the substituent alters the π electron density at the alpha carbon atom, then an additional mechanism will alter the overall π electron density. According to the Pauli exclusion principle, the two sets of three π electrons with the same spin tend to align themselves as far apart as possible (24). For three electrons, this will be at the corners of an equilateral triangle. If the substituent concentrates π electron density at the alpha carbon, then there will be an increase in electron density

around the meta carbon atoms and a decrease at the ortho and para carbons. The opposite effect will result if there is a decrease in electron density around the alpha carbon atom.

(d) Mesomeric effect - According to the classical picture of the mesomeric effect, some substituents can form double bonds with the π electron system. Mesomeric interactions can only alter electron density at the ortho and para positions.

Two recent papers criticise many of the basic assumptions of the theory of mesomeric effects. Exner (25) has measured the ionization constants of a series of meta and para substituted benzoic acids. He concludes from his results that groups such as nitro, which are normally considered to be electron-withdrawing mesomerically, actually withdraw electrons only when direct substituent interactions are possible. However, groups which donate electrons mesomerically, do so even in the absence of substituent interactions.

Murrell (26) has determined the mesomeric effect of a number of electron donating substituents by UV spectroscopy. He finds that fluorine has almost no mesomeric effect while the rest of the halogens have approximately equal effects. He also finds that nitrogen has a larger mesomeric effect than any of the halogens. It is normally concluded from

chemical evidence that fluorine has the largest mesomeric effect of any of the halogens. However, Murrell claims that the mesomeric effect as measured chemically is actually a combined mesomeric and repulsive effect. The latter effect is caused by π electron repulsion by the lone pair electrons of the substituent. This repulsion is attributed to the Pauli exclusion principle rather than to electrostatic repulsion. If an orbital containing a pair of electrons overlaps with one containing a single electron, the electrons will be repelled since two electrons of the same spin are trying to occupy the same region of space. This should particularly apply to substituents with lone pair electrons in $2p$ orbitals, since these electrons will have the same spatial quantum numbers as two of the carbon π electrons.

The net effect will be a repulsion of π electrons from the <u>alpha</u> carbon atom. This will lead to a concentration of charge at the <u>ortho</u> and <u>para</u> positions for reasons outlined above. The classical model of the mesomeric effect would also predict this concentration of π electron density at the <u>ortho</u> and <u>para</u> positions.

There are at least two cases where experimental evidence indicates that mesomeric effects are more important than repulsive effects. Firstly, it is known that phenols are more acidic than alcohols. The increased acidity is

generally believed to be due to mesomeric donation of electrons by the hydroxyl group of the phenol to the phenyl ring. This withdrawal of electrons weakens the OH bond, increasing the acidity of the proton. Since Murrell's theory does not consider electron withdrawal from the substituent, it does not predict the increased acidity of phenols. Secondly, the steric hindrance of the mesomeric effect in substituted anilines cannot be explained by repulsive forces. The nitrogen valences in dimethylaniline are almost planar (27). The planarity is presumably due to overlap of the nitrogen lone pair electrons and the π electrons of the ring (see part 5 of the theoretical discussion). Bulky substituents tend to force the amino group out of the plane of the ring. If Murrell's theory of repulsive forces is correct, then the amino group should not be planar with the ring since electronic repulsion will produce a twisting moment about the C-N bond, forcing the amino group out of the plane of the ring.

Murrell suggests that mesomeric and repulsive effects occur simultaneously. Therefore, the above-mentioned two cases could be explained by assuming that the mesomeric effect is important in both cases. However, it is difficult to accept the suggestion that electrons could simultaneously overlap and be repulsed. On the other hand, it is difficult

to understand the disagreement between chemical and spectroscopic evidence if Murrell's theory is incorrect. Fortunately, chemical shifts should be affected in the same way by both mechanisms. Consequently no further attempt will be made to differentiate between the two mechanisms. The combined effect will hereafter be referred to as the mesomeric effect.

(e) Electromeric effect - Often mutual conjugation of two substituents through the ring π electrons is possible. Such an interaction would alter the effect which each substituent has upon ring proton shifts.

Martin (11) and Dewar (23) agree that the primary inductive effect is relatively unimportant in aromatic systems since it drops off rapidly with the number of bonds. This is confirmed by the results of Cavanaugh and Dailey (28). They found that substituent effects were much smaller at the gamma and delta positions of substituted aliphatic compounds than at the meta and para positions of substituted benzenes.

There is some disagreement regarding the relative importance of field effects and π inductive effects (11, 23). This disagreement is probably unimportant since in most cases the two effects are too closely interrelated to be considered separately. The difference is that the inductive effect may give rise to a periodic distribution of electron density about the ring while the field effect will not. Both effects may

work in opposition to the primary inductive effect.

Various quantitative and semi-quantitative methods for the estimation of expected chemical shifts have been devised. Some of these are discussed below.

(i) Molecular orbital calculations - Proton chemical shifts are related to electron density. Ideally, therefore, shifts should be estimated from molecular orbital calculations of molecular electronic distribution. Unfortunately, most MO calculations provide at best only crude quantitative estimates of electron density.

(ii) Electronegativity of the substituent- Various attempts have been made to correlate electronegativities and alpha proton shifts in alkyl halides (29-35). Electronegativity should be related to electron density and consequently to chemical shifts since it is a measure of the electron withdrawing power of the substituent. Schneider and Spiesecke (35) used such plots to estimate the magnitude of additional effects which alter proton shifts. In the absence of mesomeric effects, shifts of protons ortho to substituents in aromatic molecules might also be related to electronegativity. A severe criticism of the use of electronegativity as a criterion of chemical shifts has been advanced. It will be discussed in the next section.

(iii) C^{13}-H coupling constants - It has been postulated

that there is a direct linear relationship between C^{13}-H coupling constants and chemical shifts for compounds of the type $X(CH_3)_n$ (n=1 to 4) (36-39). Gutowsky and Juan (40) have derived an expression which correlates percentage "s" character of the C-H bond and the C^{13}-H coupling constant. The calculations of Hinze and Jaffe (41) indicate that the effective electronegativity of a carbon atom is also related to the percentage "s" character of its bonding orbitals. Since the inductive effect also depends upon the carbon electronegativity, there should be a direct relationship between chemical shifts and coupling constants. According to Drago (39), the hybridization of the carbon atom orbitals is determined by substituent electronegativity and by C-X bond strength. Bent has developed the concept of isovalent hybridization (42). According to this concept, an increase in substituent electronegativity will cause an increase in the "s" character of the other carbon bonding orbitals. Drago claims that a decrease in the C-X bond overlap (formation of a weaker bond) allows the carbon atom to use more "p" character in the C-X bond and consequently more "s" character in the C-H bonds. When X is a halogen atom, the two effects act in opposition since the weakest bond is formed by the least electronegative atom (iodine). Plots of chemical shifts versus coupling constants show high field deviations for the alkyl halide shifts (36-39) while plots

of chemical shifts versus electronegativity show low field deviations for the same compounds (35). It has been suggested that the discrepancy between the conclusions reached by the two methods may be due to the omission of overlap effects in the latter method (39).

(iv) Field effects calculations - Buckingham (16) has developed an equation which relates proton chemical shifts and electric field strength.

$$\Delta\sigma = -2\times10^{-12} E_z - 10^{-18} E^2. \qquad 2.6$$

E_z = the component of the field acting along the C-H bond. A substituent bonded to a ring carbon atom polarizes the C-X bond, forming an electric dipole. The field strength at the various protons is calculated by the standard equation for the field effect due to a dipole (43).

$$E = \frac{3\underline{\mu}\cdot\underline{r}}{r^5}\underline{r} - \frac{\underline{\mu}}{r^3}. \qquad 2.7$$

The expected chemical shift due to this field may be calculated by equation 2.6.

The dipole is usually considered to be situated at a point half way along the C-X bond. Considering the effect of the substituent as a point dipole is certainly only an approximation. Furthermore, the coefficients of equation 2.6 are only approximate.

An alternate treatment of the field effect has been developed by Dewar (23). He assumes that the net effect of the substituent is to place a point charge on the alpha carbon atom. Dewar considers that the effect of the charge upon reactivity parameters is proportional to $1/r$ since reactivity parameters depend upon potential rather than upon field strength. Shifts depend upon field strength and are therefore proportional to $1/r^2$ (16).

Dewar's method is not easily applied since it is difficult to estimate the charge on the alpha carbon atom. The C^{13} chemical shift is not a reliable estimate of the electron density at the alpha carbon atom since magnetic anisotropy also affects the chemical shift.

(v) Hammett reactivity parameters - For lack of a better criterion, Hammett reactivity parameters are often used to estimate chemical shifts. Hammett assumed that reactivity parameters were proportional to electron density (44).

Taft and coworkers determined a set of inductive and mesomeric reactivity parameters (45-47). Taft claimed that proton shifts depended upon several effects (47) and could be estimated by a linear equation

$$\Delta\sigma = \alpha\sigma_I + \beta\sigma_R + \gamma. \qquad 2.8$$

σ_I and σ_R are the inductive and mesomeric reactivity parameters. Equation 2.8 has doubtful significance because it

contains three independent variables.

Dewar and Grisdale (48) have subdivided reactivity parameters into two parameters, F and M, which depend upon field and mesomeric effects respectively. However, the individual parameters are calculated by assuming the appropriate σ constant. Consequently, Dewar's parameters and Hammett's parameters will predict the same shifts for substituted benzenes.

Various attempts have been made to obtain corrected σ constants which allow for the effect of mutual conjugation of substituents. However, Wepster (49) has shown that the extent of interaction depends upon the reaction involved and that σ constants may vary continuously over a considerable range. This observation is in agreement with Exner's observation that electron withdrawing mesomeric effects require substituent interaction.

There are three major objections to the use of Hammett constants as criteria for predicting chemical shifts. Firstly, Hammett constants are usually determined by kinetic measurements. The kinetic rates are related to the nature of the transition state complex, which depends upon the excited states of the reacting molecules and upon the polarizability of the molecules. Proton chemical shifts are characteristic of molecules in their ground states. The electron density distributions of molecules in the two states could differ appreciably.

Secondly, Hammett constants predict the effects of substituents upon the reactivity of a side chain bonded to the benzene ring. The substituents should have a different effect upon the chemical shifts of protons bonded directly to the benzene ring.

Thirdly, Hammett constants do not allow for other effects such as magnetic anisotropy which alter chemical shifts without altering reactivities.

Schneider and Spiesecke have shown that there is a general correlation between chemicals shifts and reactivities at the para positions of substituted benzenes (13). Both parameters are affected mainly by the π electron density at the para position, since other effects are insignificant.

(vi) Additivity principle - It has been postulated that the proton shifts of poly-substituted benzenes are equal to the algebraic sumsof the corresponding shifts of the appropriate mono-substituted benzenes (9-12). Martin (11) tested this postulate by measuring the shifts of a large number of di-substituted benzenes. He found that the additivity postulate was accurate to within 0.1 ppm for meta and para di-substituted benzenes. Deviations were greatest for substituents causing the largest shifts. The deviations appeared to follow a consistent pattern, suggesting the presence of an additional effect. Hückel MO calculations indicated that deviations might be due to mutual polarization

of the substituents. Since deviations occurred for both meta- and para- substituted compounds, it would appear that substituent interaction can occur without direct mutual conjugation.

2. Changes in ring current effects due to substituents

Molecular orbital calculations indicate that substituents donate or withdraw at most 0.1 π electrons per carbon atom (50-52). This represents a ten per cent change in π electron density. The low field shift due to the ring current effect in benzene is about 1.5 ppm (22). The substituent should therefore alter proton shifts in substituted benzenes by at most 0.15 ppm. Since the substituents which cause the largest change in π electron density also have large effects due to other mechanisms, the effect of changes in ring current is normally relatively unimportant.

3. Changes in shift due to the anisotropy of the substituent group

Pople (19) and McConnell(53) showed that the field-induced diamagnetic or paramagnetic electron circulation on a substituent might affect the chemical shift of neighbouring protons. McConnel considered the case of an anisotropic

substituent which had cylindrical symmetry along its bond axis. He assumed that the magnetic susceptibilities parallel and perpendicular to the group symmetry axis were respectively $\chi_{\parallel}$ and $\chi_{\perp}$. By considering that the magnetic moment induced in the group could be represented by a point dipole, he derived the following equation for the contribution to the chemical shift:

$$\Delta\sigma = \frac{(\chi_{\parallel}-\chi_{\perp})(1-3\cos^2\theta)}{3R^3} = \frac{\Delta\chi(1-3\cos^2\theta)}{3R^3} \qquad 1.9$$

R and θ give the position of the proton relative to the point dipole. The equation predicts a change in sign for the shift due to anisotropy when the angle between the symmetry axis and the line joining the point dipole to the proton exceeds 55°. Two different approaches have been used to estimate anisotropy effects. Guy and Tillieu (54), Pople (55), and Zürcher (56) theoretically calculated the anisotropy in the susceptibility of the C-C bond. The three values obtained for $\Delta\chi$ were respectively 1.21×10^{-6}, 0, and 1.04×10^{-6} cm^3 $mole^{-1}$. Zürcher (56) has also calculated that the anisotropy in the susceptibility of the C-H bond is -0.72×10^{-6} cm^3 $mole^{-1}$.

The anisotropy in the susceptibility of the C-C bond has been estimated from chemical shift measurements by several different workers. In all cases, McConnel's equation was

used to evaluate $\Delta\chi$. Bothner-By and Naar-Colin measured the chemical shift of the protons in cyclopentane and cyclohexane. They obtained a value of 3.3×10^{-6} cm^3 $mole^{-1}$ for $\Delta\chi$ (33). Narasimhan and Rogers (57) measured the difference in shift between the methyl and methylene protons in propane and from this data calculated that $\Delta\chi = 4.1 \times 10^{-6}$ cm^3 $mole^{-1}$. Musher (58) plotted screening constants versus the geometric factor in McConnel's equation $(3\cos^2-1)/3R^3)$ for a series of methyl-substituted cyclohexanols. From the slope of this plot, he obtained a value of 5.0×10^{-6} cm^3 $mole^{-1}$ for $\Delta\chi$. Goldstein and Reddy (37) plotted chemical shifts versus C^{13}-H coupling constants for a series of substituted methanes and ethanes. From the differences in shift for the two types of compounds, they estimated a value of 10×10^{-6} cm^3 $mole^{-1}$ for $\Delta\chi$.

It is obvious that the values of $\Delta\chi$ obtained from shift measurements are all much larger than those calculated theoretically. There are at least four possible reasons for this disagreement. Firstly, it is necessary to correct the experimentally determined values of $\Delta\chi$ by subtracting the value of $\Delta\chi$ for a C-H bond since in all cases a C-H bond was replaced by a C-C bond. Secondly, in view of the small distances involved, the point dipole approximation in McConnel's equation is probably no longer justified. Thirdly,

since the carbon atom is more electronegative than a proton, substitution of a C-C bond for a C-H bond should cause an inductive withdrawal of electrons from the remaining protons. Finally, it has been suggested by Abraham that van der Waals' dispersive forces may cause a low field shift of the methylene protons (59).

The large value of $\Delta\chi$ obtained by Goldstein and Reddy is particularily puzzling when one remembers that their method supposedly corrects for inductive effects (39). The alpha protons of substituted ethanes resonated at approximately one ppm to low field of the protons of the corresponding substituted methanes. They believed that this shift was caused by the anisotropy of the C-C bond. In view of the unusually large value of $\Delta\chi$ which they obtained, it would appear that their method may not be a particularly good one for estimating anisotropy shifts.

There is a basic disagreement in the literature concerning the sign and size of anisotropy shifts in alkyl halides. Drago and Matwiyoff (38,39) and Goldstein and Reddy (36,37) found high field deviations for methyl chloride, bromide, and iodide when they plotted shifts versus coupling constants for a series of substituted methanes. The approximate values obtained by Goldstein and Reddy were 0.4, 0.6 and 0.9 ppm for methyl chloride, bromide and iodide respect-

ively. Drago and Matwiyoff found much larger deviations; approximately 1.4, 2.0, and 2.4 ppm for the same three compounds. Schneider and Spiesecke found negative deviations for the same three compounds when they plotted shifts of methyl X compounds versus substituent electronegativity (35). Plots of this type have been criticised by Drago for reasons mentioned previously.

Since Drago and Matwiyoff obtained such different values, their method requires further consideration. They found that there was a linear relationship between shifts and coupling constants for compounds of the type $(CH_3)_nX$ (X= second row element). They assumed that shifts of compounds lying on this line contained approximately equal contributions from substituent anisotropy effects. Any deviations of other compounds from the straight line were assumed to be due to additional anisotropy effects.

One of the compounds lying on the line is $C(CH_3)_4$. Yet by essentially the same method, Goldstein and Reddy obtained a value of -1.0 ppm for the C-C bond anisotropy shift. When methane is plotted on Drago's graph, it is approximately one ppm to high field of the line of "constant" anisotropy. The value of -1.0 ppm represents the change in shift caused by replacing a C-H bond by a C-C bond. The calculations of Zürcher indicated that the anisotropy contribution from

a C-H bond should be small. Therefore, the line of zero anisotropy should pass through or near the point for methane. If it is assumed that the compounds lying on Drago's straight line are shifted equally by anisotropy, then the corrected values for the halogen anisotropy shifts will be 0.4, 1.0 and 1.4 ppm for methyl chloride, bromide and iodide respectively.

It is by no means certain that the anisotropy effects of the second row elements are constant. Since bond lengths and bond polarities change in an approximately linear manner as X is changed from C to F, one might also expect a linear change in bond anisotropy. However, the change is unlikely to be large and the points for the methyl halides would still lie to high field of any reasonably relocated line.

The proton signals of HCl, HBr, and HI are all to high field of the methane proton signal with the largest shift for HI (60). This indicates a high field shift due to anisotropy. The same conclusion is reached from the alpha carbon shifts of methyl and ethyl halides (35). This establishes that the sign of $\Delta\chi$ is negative. Cavanaugh and Dailey (61) have calculated the value of the geometric factor $((3\cos^2\theta-1)/3R^3)$ for the alpha and beta protons of substituted ethanes and methanes. Their calculations indicate that the alpha and

beta protons of ethyl and methyl halides should be shifted to high field as a result of anisotropy effects. However, two separate sets of experimental data indicate that the beta protons in ethyl halides resonate at lower fields than ethane protons (35,61). Since the low field shifts are greatest for iodine and least for fluorine, some additional mechanism must be responsible for at least part of the low field shift.

Schneider and Spiesecke found anomolous low field shifts of the ortho carbon^{13} atoms and protons in mono-substituted benzenes (13). Again iodine caused the largest low field shift. No reasonable combination of mesomeric and inductive effects could account for this observation. Martin considered in detail the probable effect of substituent anisotropy upon ring proton shifts (11). He constructed a plot (Figure 1) which showed the value of the geometric factor as a function of the distance, a, of the effective dipole from the alpha carbon, at four points of interest in a phenyl X molecule.

If the point dipole is located about one angstrom from the alpha carbon atom and if $\Delta\chi$ has a reasonable value of from -ten to - twenty cm^3 $mole^{-1}$, then negative shifts of the ortho protons of approximately the right magnitude are predicted. However if the point dipole is located closer to the substituent

FIGURE 1. Plot of the distance, a, of the effective dipole of the C-X bond in C_6H_5X from the alpha carbon atom versus the value of the geometric factor, $\frac{3\cos^2\theta-1}{3R^3}$, at four points in the phenyl ring. The four points are at the nuclei of the ortho, meta and para protons and the ortho carbon atom.

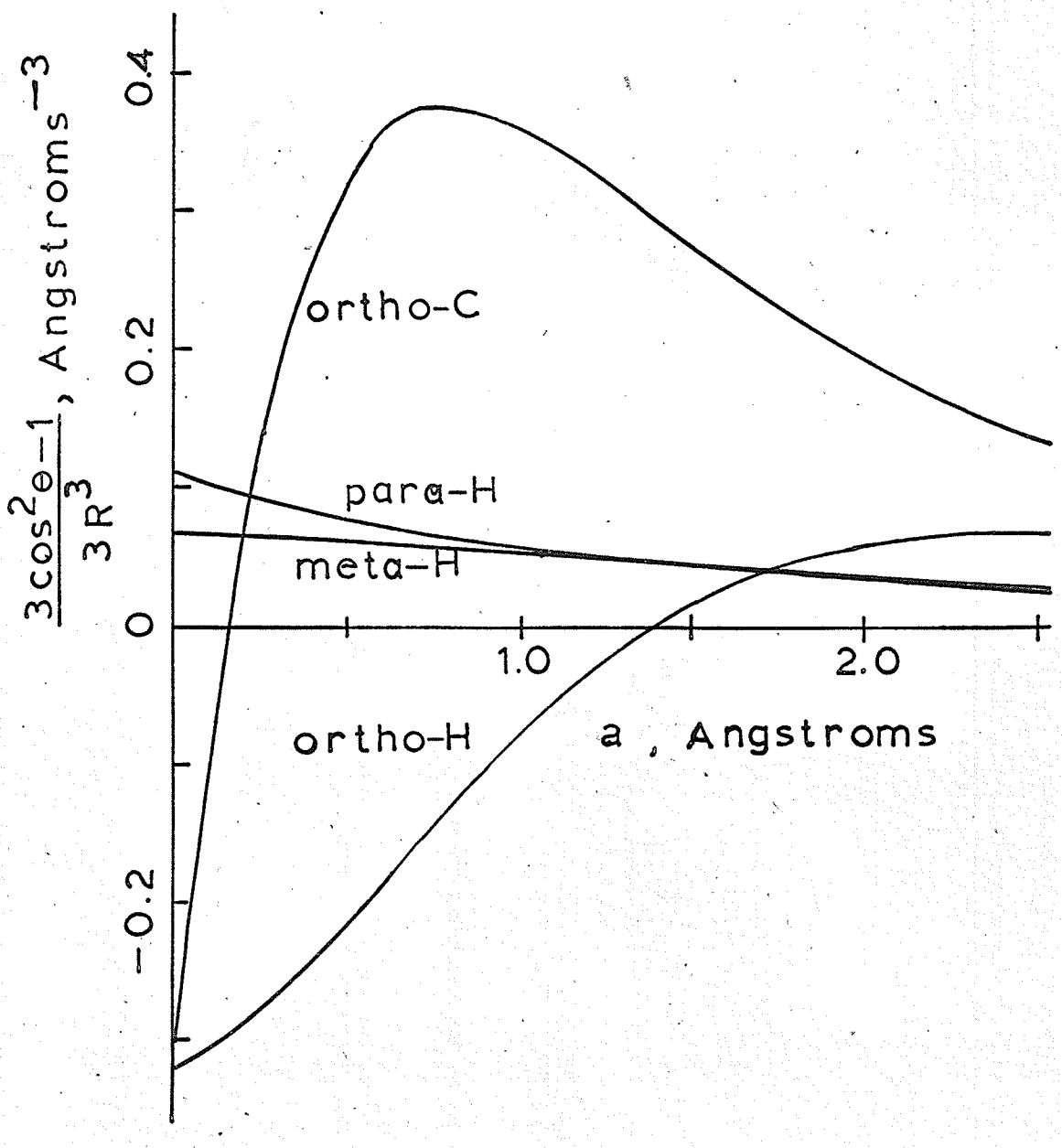
$\frac{3\cos^2\theta-1}{3R^3}$, Angstroms^{-3}
0.4
0.2
0
−0.2
ortho-C
para-H
meta-H
ortho-H
1.0
2.0
a , Angstroms

atom, then high field shifts would be predicted. Furthermore, a high field shift of the ortho C^{13} atoms would be expected for any reasonable location of the point dipole. However, negative shifts of several ppm have been observed for the ortho C^{13} atoms of halobenzenes, with the largest shift for iodobenzene (-9.9 ppm)(13). Some additional mechanism must cause the low field C^{13} shifts and probably at least part of the ortho proton shifts. The most plausible explanation for the low field shifts is that they are caused by van der Waals dispersive forces (62).

Since the relative magnitudes of the effects of bond anisotropy and dispersive forces upon alpha proton shifts in substituted methanes are unknown, it is impossible to determine the relative merits of the two methods for estimating additional shifts. Anisotropy probably causes high field shifts while dispersive forces cause low shifts. Therefore it cannot be determined whether a net high field or low field shift would be expected.

4. Intramolecular van der Waals forces

The previous discussion established that there was good evidence for the existence of anomolous low field shifts of the beta protons of ethyl halides and of ortho carbon^{13} atoms and protons in halobenzenes. It is possible that there

are similar low field shifts of alpha protons of methyl and ethyl halides, but this could not be definitely established.

Several additional examples of anomolous low field shifts of ortho protons in substituted benzenes have been reported in the literature. Martin found that the protons ortho to substituents in ortho di-substituted benzenes were strongly shifted to low field. The largest low field shift occurred in ortho diiodobenzene where the ortho proton signal was found at approximately 0.5 ppm to low field of the position predicted by additivity (11). Martin also pointed out that Fraser's results for 1-substituted 2,6-dimethylanilines (14) showed anomolous shifts for the 3 and 5 protons. Presumably, the additional shifts mentioned above occur because steric repulsion forces the substituents apart and consequently closer to the neighbouring protons.

Measurements by Fraser (14) and Diehl (9) of the methyl proton shifts of mesitylene halides showed that these shifts were proportional to and less than ($\approx 1/3$) the shifts of the ortho ring protons of the corresponding halobenzenes. As Diehl pointed out, this is difficult to explain if one assumes that the shifts are caused by substituent anisotropy. At least one of the methyl protons will be in a position such that anisotropy effects should shift it strongly to low field. Even after the effect of anisotropy is averaged over all poss-

ible positions of the methyl group, the low field shift due to anisotropy would be expected to be of the same order of magnitude as the shift of the ortho protons.

A recent communication reported the fluorine^{19} shifts for a series of X-pentafluorobenzenes (63). The ortho fluoro signals were strongly shifted to low field. Similar low field shifts have been noted for a series of perfluoroalkyl X compounds (64). In both articles it was suggested that the low field shifts were due to paramagnetic contributions to the screening parameters. These paramagnetic contributions were believed to be due to low-lying excited states in the substituent atoms. The largest shifts were noted for the substituent atoms which had the largest atomic numbers. This is reasonable since the largest atoms have the lowest excitation energies. However, the low field shifts could also be caused by dispersive forces since these forces should also be largest for the heaviest atoms. A similar suggestion was advanced by Tiers (65) in 1956 to explain the shifts for a number of similar compounds. He stated that "net electron displacement away from fluorine (and hydrogen) nuclei may be induced by repulsive interactions with neighbouring groups in the molecule".

It is known that intermolecular van der Waals forces between solvent and solute molecules can cause low field shifts (66). Therefore, it is reasonable to postulate that intra-

molecular van der Waals dispersive forces may also cause low field shifts. It is believed that intermolecular dispersive forces affect shifts via two mechanisms (66).

(a) Interaction between the solvent and the solute in its equilibrium configuration causes a distortion of the electronic environment of the nucleus. This distortion is probably an expansion, causing a low field shift.

(b) Molecular motion leads to a time-dependent distortion of the symmetry of the C-H bonds. When "side attack" of the bonds is possible, this second mechanism can be important. This distortion of the bond symmetry will increase the paramagnetic circulations in the vicinity of the nucleus and consequently decrease the shielding of the nucleus.

Presumably the same two mechanisms could act intramolecularly to alter shifts. The first mechanism is obviously possible. As can be seen from Figure 2, there is a definite overlap of the van der Waals radii of halogens and <u>alpha</u> methyl and ethyl protons or <u>ortho</u> phenyl protons. Vibrations and rotations of the substituent group could also induce a time-dependent distortion of the C-H bond symmetry. The extent of the deshielding should depend upon the number of electrons in the substituent group, the van der Waals radius of the substituent, and the distance between the substituent and the proton in question.

FIGURE 2. Planar projections of the bonds of (A)CH_3X and (B)C_6H_5X compounds where X is a halogen. The "long" C-H bond in CH_3X is the bond which lies in the plane of the diagram. The van der Waals radii are represented by the circles.

(A) CH_3X

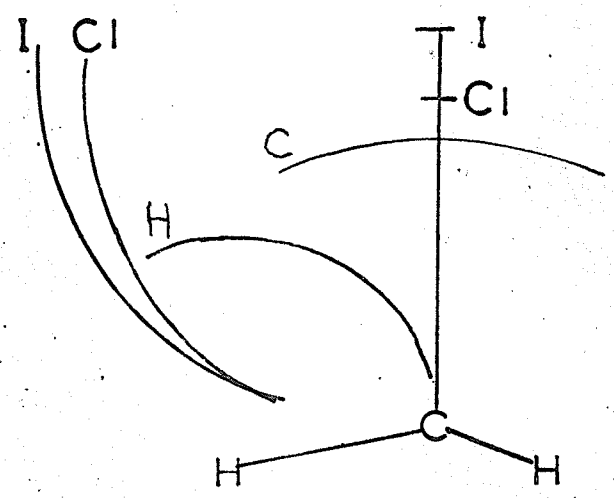

(B) C_6H_5X

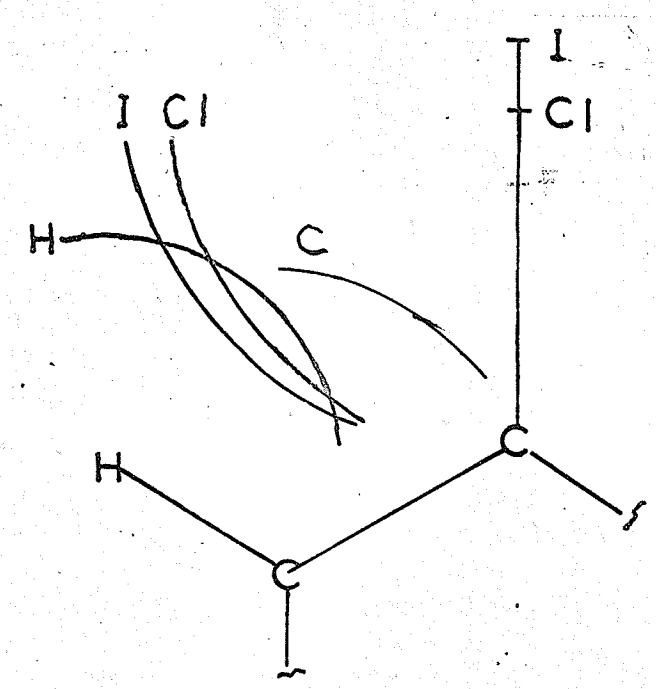

According to London, the energy of dispersive interaction between atoms is given by (67):

$$u_{Disp.} = -\frac{3\alpha^2 J_o}{4r^6} \text{ [volts]}. \qquad 2.10$$

J_o and α are respectively the ionization potential and the polarizability of the atom. Dispersive forces should be proportional to $1/r^7$. Stuart used London's equation to estimate the dispersive interaction energy of two atoms in a vacuum (68). He used average values of the atomic parameters and found an energy of about 2 kcal/mole at a distance of 3 Å. Creswell and Allred have measured hydrogen bond shifts with tetrahydrofuran of from -0.5 to -0.8 ppm for the haloforms. The enthalpies of formation were of the order of 2.5 kcal/mole (69). If it is assumed that hydrogen bond formation and dispersive interactions cause low field shifts by similar mechanisms, then low field shifts due to dispersive forces would be expected to be of the same order of magnitude as the shifts listed above.

Another estimate of the magnitude of intramolecular dispersive forces may be arrived at if it is assumed that they are of the same order of magnitude as intermolecular dispersive shifts in liquids. Linder and coworkers used a continuum model to consider dispersive shifts in liquids (70). They considered the experimental gas-to-solvent shifts of methane and found that no type of interaction other than dispersion need be considered to explain the solvent shifts

of nonpolar solutes in reasonably isotropic solvents. The dispersive shifts were as large as -0.7 ppm for solvents containing a large number of electrons (methylene iodide, for example). Therefore, it seems reasonable to assume that intramolecular dispersive forces could cause low field shifts of at least 0.7 ppm.

5. Steric hindrance of the mesomeric effect

The mesomeric effect of a substituent may be considerably reduced if steric hindrance forces the substituent out of its normal position relative to the ring. Often mesomeric interactions occur because a pair of p electrons from the substituent atom overlap with the π electrons of the ring, forming a double bond. When the p electron orbitals are perpendicular to the plane of the ring, maximum overlap of the electron orbitals (and consequently maximum mesomeric effect) occurs. If steric hindrance forces the substituent out of this position, then there will be a smaller mesomeric effect. If the substituent is forced to twist through an angle of 90°, overlap will decrease to zero and there will be no mesomeric effect. The overlap varies approximately as $\cos^2\theta$. If one assumes that the <u>para</u> proton shifts in benzenes depend solely upon mesomeric effects, then it is possible to calculate angles of twist of substituent groups.

6. Reaction field effect

If a polar molecule is dissolved, it will polarize the surrounding solvent molecules. This polarization causes an induced electrical field to act upon the solute molecule. If the solute molecule is sufficiently symmetrical, then the reaction field will be parallel to and proportional to the dipole moment of the solute molecule. An estimate of the value of the reaction field can be obtained from the Onsager model (16). In the case of a spherical solute molecule of radius r, with a point dipole, μ, at the center of the sphere, dissolved in a solvent of dielectric constant D, the reaction field is given by

$$\underline{R} = \frac{2(D-1)\,\underline{m}}{(2D+1)\,r^3}. \qquad 2.11$$

$$\underline{m} = \underline{\mu} + \alpha\,\underline{R}. \qquad 2.12$$

$\underline{m}$ = the total dipole moment of the solute in the solvent.
α = the polarizability of the sphere.

Similar calculations can be carried out for solute molecules of ellipsoidal shape (43). Shifts caused by the reaction field are estimated by equation 2.6.

The model described above obviously does not reproduce the actual situation in a solution. However, accurate estimates

of differences of chemical shifts can often be obtained from a combination of field and reaction field calculations (16). The absolute values of shifts are not predicted as accurately.

7. Effect of hydrogen bonds and counter ions

In some cases interactions between solvent and solute molecules are so strong that changes in molecular structure occur. A typical interaction of this type is that between a proton on one molecule and an electronegative atom on another. Such an interaction is referred to as hydrogen bonding. The interaction is primarily electrostatic in nature. An increase in the length of the bond joining the proton to its parent molecule is usually noted.

Hydrogen bonding causes a low field shift of the proton involved. The proton is electrostatically attracted to the electronegative group and the electron cloud around the proton is simultaneously repulsed. The decrease in electron density around the proton causes a low field shift. Anisotropy shifts due to electron circulations on the second atom are probably small. Anisotropic effects should give rise to high field shifts (see equation 2.9) for linear hydrogen bonds, but any high field shifts, if present, are hidden by the large low field shifts arising from electrostatic effects. Similarly, charge transfer reactions of the type

$$X\text{-}H{+}Y \longrightarrow X^{-} \text{---}H\text{---}^{+}Y \qquad 2.13$$

are probably also unimportant since they involve donation of electrons to the H-X bond and would be expected to cause high field shifts.

Charged ions can form similar bonds in solution. In such cases, there should be large electrostatic forces. The bond formation can be referred to as ion pair formation, counter ion attraction, or hydrogen bonding (if a proton is involved). It should be possible to carry out field effect calculations which would estimate the effect of the counter ion upon chemical shifts. If the counter ion is assumed to act as a point charge, then the field due to this monopole at each proton position can be calculated and the proton shifts can be estimated by using equation 2.6.

3. EXPERIMENTAL

Most substituted anilines were Eastman White Label grade chemicals. The various dimethyl anilines were obtained from Aldrich Chemicals and were believed to be of comparable purity. N-methylaniline and p-cyanoaniline were Eastman Practical grade chemicals. Trifluoracetic acid (TFA) was an Eastman White Label grade chemical. Carbon tetrachloride was a Baker Analyzed Reagent grade chemical. All chemicals were used without purification.

Solutions always contained 5.0 mole per cent base. p-Cyanoaniline and p-nitroaniline were almost insoluble in CCl_4. Therefore, solutions of the two anilines in CCl_4 were not prepared. Solutions were prepared by adding solvent to the anilines. A considerable amount of heat was evolved when TFA was added. Because substituted anilines are rapidly protonated, and also because they have much higher boiling points than TFA, negligible amounts of aniline should have evaporated. After the solution cooled, additional TFA was added to give the proper concentration. Five drops of TFA anhydride were added to each acid solution to absorb any water present.

It is known that alkylamines react photochemically with CCl_4 to form the corresponding amine hydrochlorides (71), which come out of solution as white precipitates. Of all the anilines studied, only p-anisidine formed a precipitate when dissolved in CCl_4. The precipitate formed only after the solution had been standing in sunlight for several hours. A fresh solution was prepared and kept in the dark until its spectrum was run. Presumably, the other anilines were not strong enough bases to undergo such reactions.

The spectra were measured at 60 Mc/sec. on a Varian DP60 spectrometer. Solutions were contained in ordinary 5mm O.D. sample tubes. All signals were measured relative to external chloroform. The chemical shifts of the benzene protons in 5 mole per cent solutions of benzene in TFA and CCl_4 were also measured relative to external chloroform. The bulk susceptibilities of the 5 mole

per cent solutions of substituted anilines and of benzene were assumed equal, since the bulk susceptibility of any dilute solution is essentially that of the solvent. The difference in chemical shifts between the substituted anilines and benzene in the same solvent were then taken as representing the shifts relative to benzene.

Chemical shifts were measured by placing sidebands of the external reference on both sides of the peak (s) under study. Frequencies were measured to within 0.1 c/s with a Hewlett-Packard 521C counter. All shifts were obtained from an average of six measurements.

4. RESULTS

(A) In CCl_4

In Table I* the shifts of the ring protons are given in ppm relative to benzene. The last column of Table I gives the difference in ring proton shifts in the two solvents. Table II gives the shifts of the ring methyl protons. The shifts for aniline and its N-alkyl derivatives were obtained by approximate analysis. The shifts were large enough in most cases to allow an estimation of the centers of gravity of the various proton signals. It is estimated that shifts are accurate to within 0.05 ppm. For aniline and

---

* All Tables are given at the end of the chapter

N-dimethylaniline in CCl_4, the shifts agree, within this limit, with the accurate results of Schneider and Spiesecke (13). The largest errors were probably in the ortho and para proton shifts of N-alkylanilines where these shifts were nearly equal.

The ring-substituted methylanilines were often somewhat simpler to analyze. The methyl groups couple slightly to the protons ortho to them and the resultant peak broadening facilitates the assignments of peaks to the various protons. Some of the symmetrically substituted dimethylanilines had simple spectra of the AB_2 type which could be analyzed exactly. The largest error probably occurred when two nonequivalent ortho or meta protons were present. It was generally impossible to separate the two signals. Therefore, only an average value of the two shifts could be obtained. Overall, an accuracy of 0.05 ppm is again claimed, although many of the shifts are probably known more accurately.

The p-substituted anilines could be analyzed exactly. They were all of the A_2B_2 type. The spectra reduced nearly to AB spectra since only the ortho couplings had appreciable magnitude, (see Figure 3). For purposes of analysis, the spectra were assumed to be of the AB type. The shifts are estimated to be accurate to within 0.02 ppm (1.0 c/s).

The amino proton resonance peaks were always broad. The broadening was probably caused by a combination of coupling

FIGURE 3. Reproductions of the ring proton spectra of p- iodoaniline in (A) CCl_4 and (B) TFA. The chemical shifts (in ppm relative to benzene) are given below each spectrum.

(A)

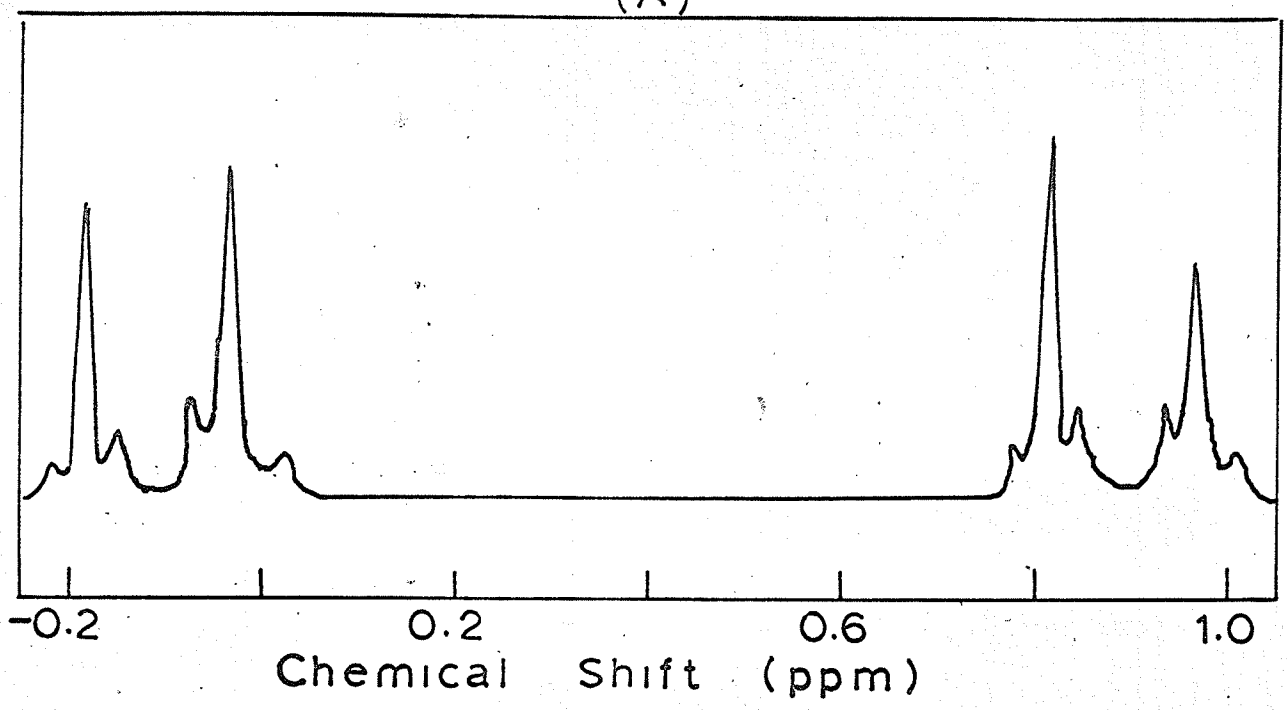

(B)

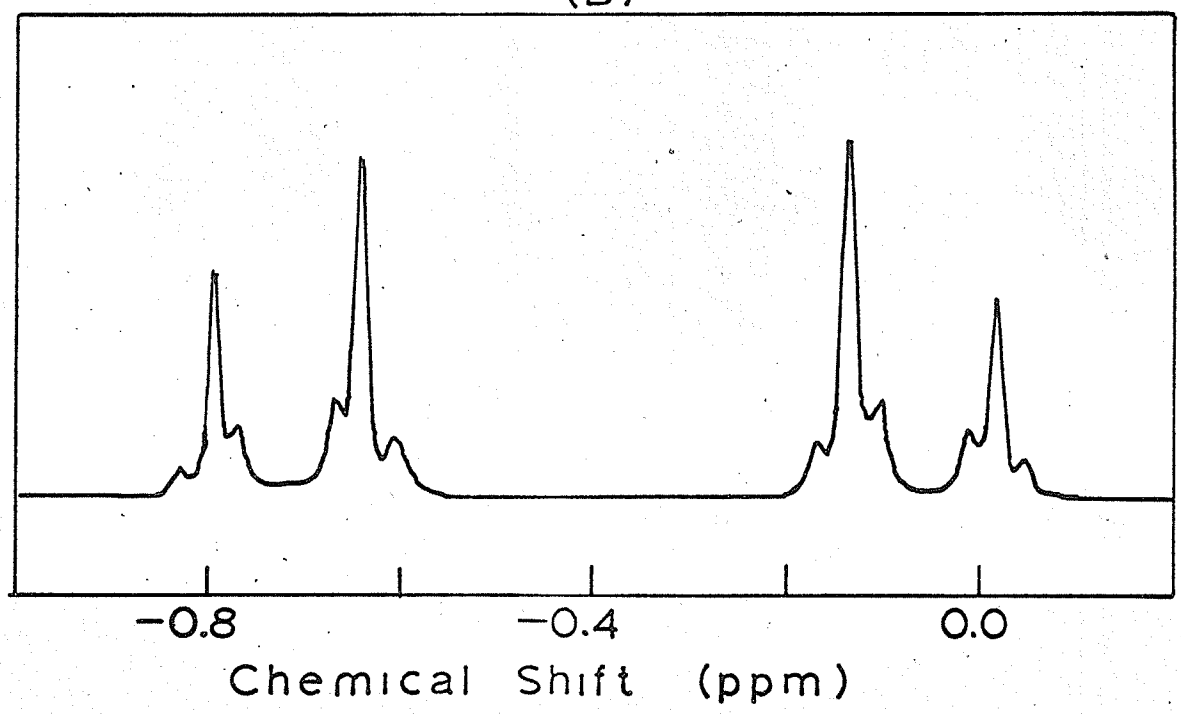

of amino protons to the N^{14} nuclei and quadrupole relaxation of amino protons by the N^{14} nuclei. It is estimated that the amino proton shifts are accurate to within 0.03 ppm. These shifts are listed in Table III.

(B) In CF_3COOH

Aniline and most of the N-alkylanilines had single peak ring proton spectra. The collapse may not have been complete in all cases. It was considered that all shifts were equal when a single peak was observed. Actually the proton shifts may vary by as much as 0.1 ppm but the real difference is impossible to determine.

The ring-substituted anilines usually had multi-peak spectra. The proton shifts were dominated by the effect of the substituent group. Para-substituted anilines again gave spectra of the A_2B_2 type.

The ammonio (NH_3^+) proton shifts were not measured accurately since the peaks were always very broad (of the order of 0.4 to 1.0 ppm). The protons usually resonated between 1.0 and 1.5 ppm to low field of benzene.

The alkyl groups of N-alkylanilines always showed couplings of 5.2 to 5.6 c/s. to the ammonio protons. For example, the spectrum of N-methylaniline in TFA contained a triplet peak due to the methyl group with a measured splitting of 5.5 ± 0.1 c/s. This indicates that N-methylaniline in TFA has the structure $C_6H_5NH_2^+(CH_3)$ since one should find

a doublet for the methyl group of unprotonated N-methylaniline. The lifetime of the protonated N-methylaniline in TFA at 25°C must exceed 0.03 seconds. The exchange rates and lifetimes for various protonated anilines are given in Chapter 4.

5. DISCUSSION OF RESULTS

(A) Aniline

(1) In CCl_4

The chemical shifts of the ring protons of aniline in CCl_4 (see Table I) indicate that the amino group has a strong mesomeric effect since the *ortho* and *para* proton shifts are much larger than the *meta* shifts. Since nitrogen has a low atomic number, anisotropic and dispersive effects should be relatively unimportant.

The *meta* shifts are not as easily explained. The shifts are to high field. It is not obvious why the amino group should donate electrons to the ring inductively. High field shifts of this type have been explained by Hine (72) in terms of the inductive effect (at the *meta* position) of a charge concentration at the *ortho* or *para* positions. A similar explanation has been advanced by Schug and Deck (73). They evaluate the effect of the π electron density at the *ortho* and *para* positions upon the *meta* proton shifts of a series of hydroxybenzenes. The Wheland (W) technique (74) used in molecular orbital calculations predicts the same trend of

results as the above mentioned explanations. All three would predict high field shifts for the meta protons of aniline.

It is interesting to note that calculations of the field and reaction field effects upon proton shifts also indicate high field shifts for the meta protons. For aniline in CCl_4, the predicted ortho shift is 0.19 ppm and the predicted meta shift is 0.16 ppm, relative to benzene. The calculation does not allow for mesomeric effects acting upon the ortho protons. However, the predicted meta shift agrees quantitatively with the experimentally measured value (0.2 $\pm$ 0.05 ppm). Therefore it is unnecessary to invoke any effect other than field effects to explain the meta proton shifts.

(2) In TFA

Aniline in TFA has a single peak ring PMR spectrum identical to its spectrum in acetic acid (6,7) and other acids (8). The sole apparent effect of the ammonio group is a low field shift of 0.3 ppm for all ring protons. The ammonio group should not have any mesomeric interaction with the phenyl group. However, one would expect it to exert a combined π inductive (field) effect and σ inductive effect, with the largest effect upon the ortho protons.

A series of calculations were carried out in an attempt to evaluate the effect of the ammonio group upon ring proton shifts. As a first approximation, it was assumed that a posi-

tive charge of 4.8×10^{-10} esu (1 electron charge) was located on the nitrogen atom. The field due to a monopole was calculated for the various proton positions. Using equation 2.6, the predicted shifts are -1.11 ppm, -0.49 ppm, and -0.38 ppm, relative to benzene, for the ortho, meta and para protons. The shift contributions due to the E_z term are -0.62, -0.43, and -0.34 ppm relative to benzene. Even if the E^2 term is ignored, agreement with experimental shift values is quite poor.

Dewar assumed that the field effect due to a substituent resulted mainly from an induced charge on the alpha carbon atom. A calculation based on this assumption gave shift values which were much larger than the experimental values.

Gutowsky measured the effect of the ammonium group in crystals (75). He assumed that the charge was evenly divided between the four protons. It was decided to make a similar assumption for the ammonio group, i.e., a charge of 1.6×10^{-10} esu on each of the protons. The field effect caused by this charge distribution was calculated for two possible positions of the ammonio group: (a) with one proton in the plane of the ring, adjacent to the ortho and meta protons under consideration, (b) with one proton in the plane of the ring, opposite to the ortho and meta protons being considered. The net result of this calculation is the consideration of

the effect of a charge averaged over six possible positions. This should represent a close approximation to integration over all possible positions.

The components of the field along the bond axes were precisely calculated. However, the complete calculation of the resultant of the total field acting at the protons was carried out only for the ortho protons, since the complete calculation is complex and tedious. The total field acting at the meta and para protons was approximated by assuming that the total charge was concentrated at the center of the circle circumscribed by the ammonio protons. Since the meta and para protons are relatively far removed from the ammonio group, this assumption should introduce only a slight error.

The results of the calculation are given in Table IV. If equation 2.6 is used in unmodified form, agreement with experiment is better than for the previous calculations but still not particularly good. It is interesting to note that the estimated effect of E_z is now least at the ortho position. This suggests that a lower value of the coefficient of E^2 in equation 2.6 would give better agreement between measured and predicted results, since the E^2 term is largest at the ortho position. As shown in column 5 of Table IV, predicted shifts agree, within experimental error, with those determined experimentally if one assumes a value of 0.25×10^{-18} for the

coefficient of the E^2 term. Since the coefficients estimated by Buckingham were not claimed to be exact, alteration of the E^2 coefficient is permissible.

Fraenkel (8) postulated that the collapse of the ring proton spectra of anilinium salts in polar solvents occurred because the anilinium ions and acid anions formed intimate ion pairs. He presented the following evidence in support of his postulate: (a) the shapes of the ring proton spectra of anilinium salts depend upon the nature of the accompanying anion, (b) the ring proton spectra of trimethylanilinium salts are always complex and are independent of the nature of the accompanying anion. These observations can be rationalized by assuming that anilinium salts exist in solution as ion pairs. The bulky trimethylammonio group must keep the anion so far away from the ring that it has little effect upon the ring proton shifts.

It was decided to test Fraenkel's postulate that the counter ion equalizes ring proton shifts by carrying out field effect calculations. In crystalline aniline hydrochloride, three chloride ions are coordinated with each nitrogen atom, at a distance of about 3.1 Å (76). The distance between the cone traced out by the ammonio protons and the chloride ions is approximately 2 Å. Therefore, it was assumed that the effective charge of the trifluoracetate counter ion was located 2 Å from the plane of the ammonio protons and in

the plane of the C-N bond (see Figure 4). The counter ion was considered to have an electrical charge of 4.8×10^{-10} esu. The net field caused by the counter ion and the ammonio group was calculated. The field contributed by the ammonio group was calculated by the "six position" method described previously.

The counter ion produces a field which is almost perpendicular to the plane of the ortho C-H bond. The fields arising from the ammonio protons and the counter ion partly cancel (Figure 4). There is little change in the component along the C-H bond but the total field is reduced to almost half of that caused by the charge on the ammonio protons. Consequently, the E^2 contribution to proton shifts is reduced to approximately one quarter of its value in the absence of the counter ion. The shifts of the meta and para protons become less negative as a result of the effect of the counter ion. The results of the field effect calculation are given in Table IV. If the charge separation is less than 2.0 Å, then all values of shifts will be less negative. If it is larger than 2.0 Å, all values will become more negative.

There is a 0.2 ppm difference between predicted ortho proton shifts and meta and para proton shifts. However, the presence of the ion pair should polarize the surrounding acid molecules, causing a reaction field. This reaction field will increase ortho proton shifts and decrease meta and para

FIGURE 4. The calculated fields due to the ammonio group and the counter ion at the ring protons of $C_6H_5NH_3^+$ ions. The fields arising from the two groups are represented by the light arrows and the resultant fields are represented by the heavy arrows.

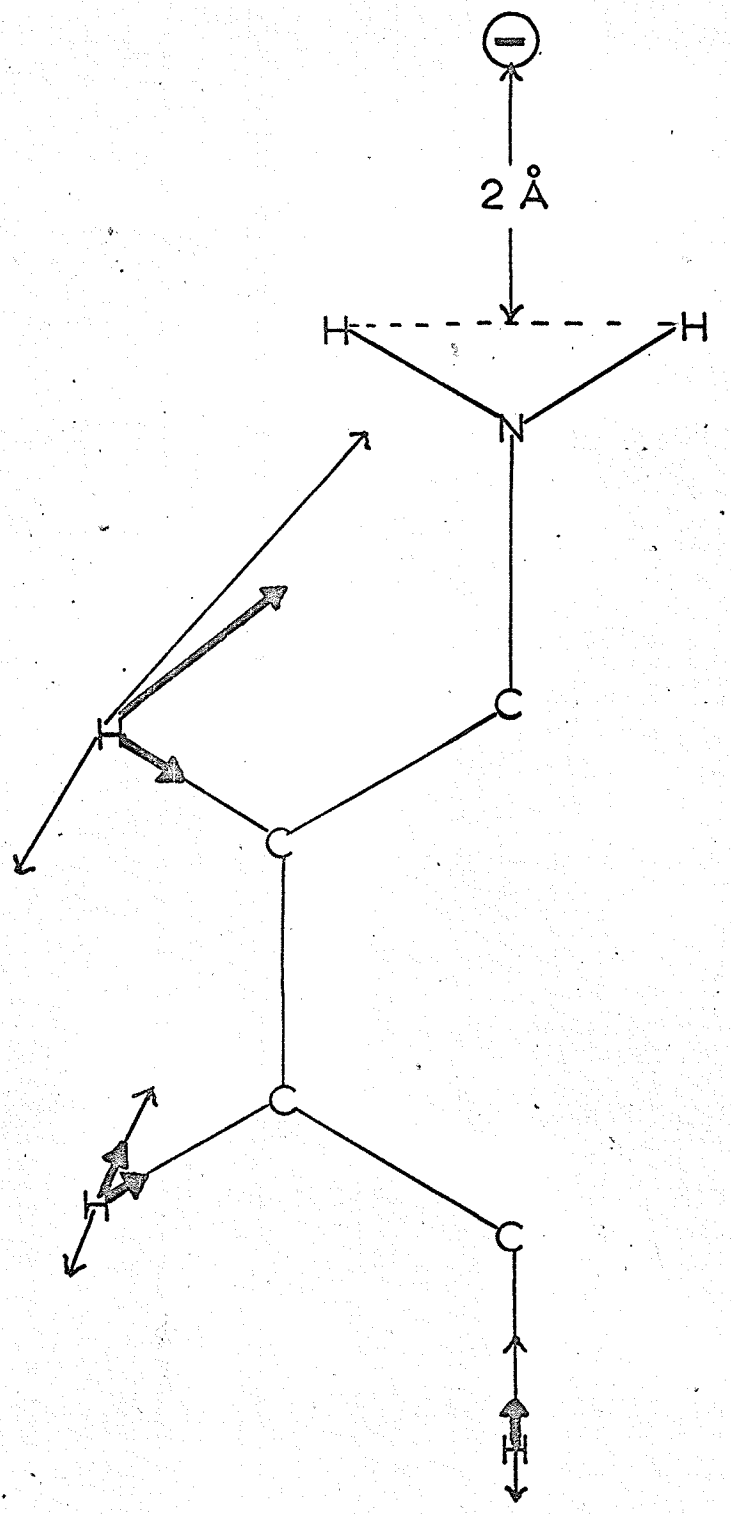
2 Å
H
H
N
C
C
C
C
H
H
H

proton shifts. The expected shifts resulting from the reaction field cannot be calculated since necessary data are not available. However, if the reaction field causes proton shifts of the same order as those estimated for haloanilines in CCl_4 (see Table VII), the predicted ortho, meta and para shifts will be nearly equal.

These calculations show that the collapse of the ring proton spectra of anilinium ions can be predicted if one assumes that the coefficient of the E^2 term in equation 2.6 is too large or if one assumes that anilinium salts exist in solution almost entirely as ion pairs. There is no guarantee that either one of the explanations is correct. However, the above discussion does show that it is possible to predict the collapsed ring proton spectrum of aniline in TFA, with a minimum number of assumptions. The second explanation is perhaps the more satisfactory of the two since it requires no alteration of equation 2.6. Certainly it is difficult to explain Fraenkel's results if one assumes that ion pairs do not exist in solution.

(B) Para Substituted Anilines

(1) Additivity

Martin (11) determined the infinite dilution shifts of a number of disubstituted benzenes dissolved in cyclohexane.

Among the compounds which he investigated were some of the para- substituted anilines whose shifts were also measured in the course of this investigation. Martin found that substituent effects were nearly additive and that deviations (of chemical shift) from additivity were at most 0.1 ppm. He found that the shifts of para- disubstituted benzenes could be predicted more accurately by the following relationship:

$$\sigma_2 = d_o(R_1) + \gamma(R_1)d_m(R_4) \qquad 2.14$$

$\gamma(R_1)$ is a constant characteristic of the substituent on carbon 1 and is a measure of the deviation from additivity. d_o and d_m are the substituent parameters which measure the effect of the substituents upon chemical shifts.

The shifts of para- substituted anilines in CCl_4 which were obtained in this study are given in Table V. The shifts measured by Martin, the shifts predicted by Martin from his substituent parameters, and the shifts predicted from the results of Schneider and Spiesecke (13) (assuming additivity) are also given. The RMS deviations of our shift measurements from the predicted shifts of Martin are 0.05 ppm for protons ortho to the amino group and 0.03 ppm for meta protons. It is felt that the shift measurements are more accurate than the deviations would indicate. Part of the deviation is probably due to the use of a different solvent and part due to the measurements of shifts of 5 mole per cent solutions

rather than of infinitely dilute solutions. The ortho proton shifts in CCl_4 are definitely lower than in cyclohexane while the meta shifts appear to be slightly lower. This deviation is probably largely caused by intermolecular dispersive forces and possibly partly by specific solvent - solute interactions (71).

Table VI, column 1 gives the ring proton shifts of para-substituted anilines in TFA. Shifts predicted from the results of Schneider and Spiesecke and of Martin are given. For the purpose of prediction, it was assumed that the ammonio group caused a low field shift of 0.30 ppm for all ring protons. Shifts were predicted from the results of Martin by using his substituent parameters and γ constants in equation 2.14. It was assumed that $\gamma_{NH_3^+} = 1$.

The two sets of predictions agree quite closely with the results in column 1. For example, the RMS deviation between experimental results and the predictions based on Martin's substituent parameters is 0.05 ppm. This includes relatively large deviations for the ortho protons of p-anisidine (-0.11 ppm) and p-nitroaniline (0.12 ppm). These compounds represent the extremes of strongest and weakest bases and the deviations may be due to alterations of the effect of the ammonio group by the substituents.

No particular trend is evident in the difference between predicted and observed results. This indicates that

the value of -0.30 ppm for the shifts of the ortho and meta protons caused by the ammonio group is accurate for para-substituted anilines as well as for aniline itself.

The last column of Table I gives the differences in shift of the ring protons in the two solvents. The sum of ortho plus meta shift changes is quite constant for most of the para- substituted anilines. The deviation of p-phenylenediamine from this constant value may be due to incomplete protonation of the two amino groups. The reason for the deviation of p-anisidine is not obvious. The spectra of this compound were remeasured since it was felt that one or more of the shift values might be inaccurate. No substantial change was found. It is interesting to note that deviations are in general greater for the individual shift differences than for the sums of the differences. This would indicate that the substituent redistributes the effect of the amino and/or ammonio group (s) without changing their overall effect.

In summary, the results for the para- substituted anilines indicate that the additivity principle provides a semi-quantitative method for predicting shifts of para- substituted anilines. The agreement between the results for para- substituted anilines in CCl_4 and the results of Martin confirms the additivity principle and the consistency of the two sets of

results. The results in TFA have greater significance because they show that the ammonio group has equal effects upon the ortho and meta proton shifts of para- substituted anilinium ions.

(2) Ortho and meta proton shifts.

Figures 5A and 5B show the proton shifts of aniline and para- substituted anilines in CCl_4 (Figure 5A) and TFA (Figure 5B). Since substituent effects are nearly additive, the differences in shift between the equivalent protons in aniline and the para- substituted anilines represent the additional shifts caused by the para substituents. These substituent effects appear to be nearly solvent independent (for the two solvents used) and will be discussed without reference to the solvent. The effects of the amino and ammonio groups have been discussed previously and will not be further discussed in this section.

Since this section is concerned with shifts caused by the para substituents, the normal nomenclature will be reversed and the proton adjacent to the substituent will be referred to as the ortho proton, etc.

(i) Meta proton shifts - In the absence of polar groups and/or large concentrations of charge at other ring positions, meta shifts relative to aniline are very small (see Figure 5). This is confirmed by the small shifts relative to benzene of meta protons in monosubstituted benzenes (13) and

FIGURE 5A. The <u>ortho</u> and <u>meta</u> proton shifts of aniline and p-substituted anilines in CCl_4. Chemical shifts are in ppm relative to benzene. The aniline proton shifts are represented by the lines which run the length of the diagram. Protons are labelled relative to the 4 position in aniline.

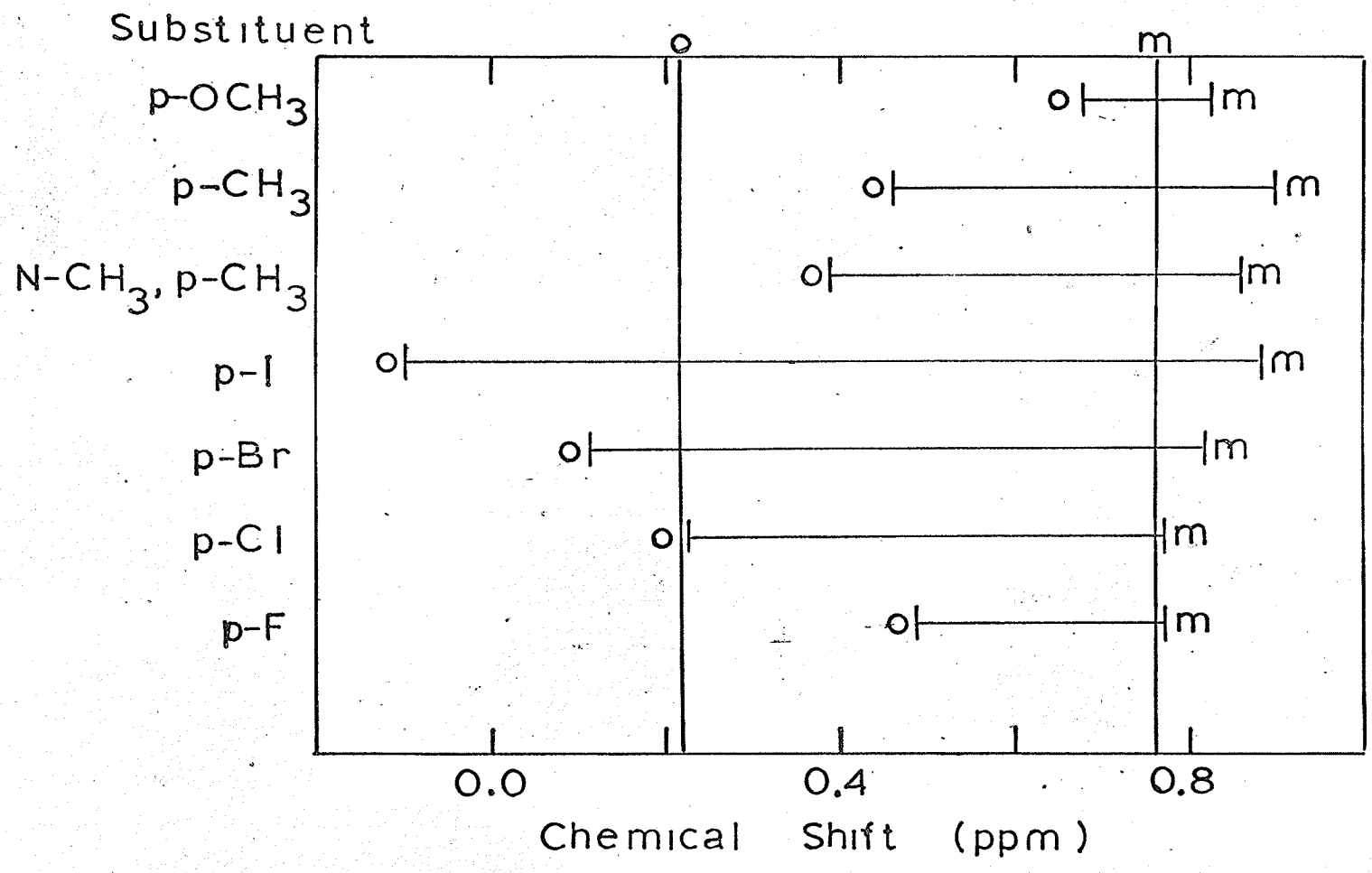
Substituent
o
m
p-OCH3
p-CH3
N-CH3, p-CH3
p-I
p-Br
p-Cl
p-F
0.0
0.4
0.8
Chemical Shift (ppm)

FIGURE 5B. The <u>ortho</u> and <u>meta</u> proton shifts of aniline and *p*-substituted anilines in TFA.

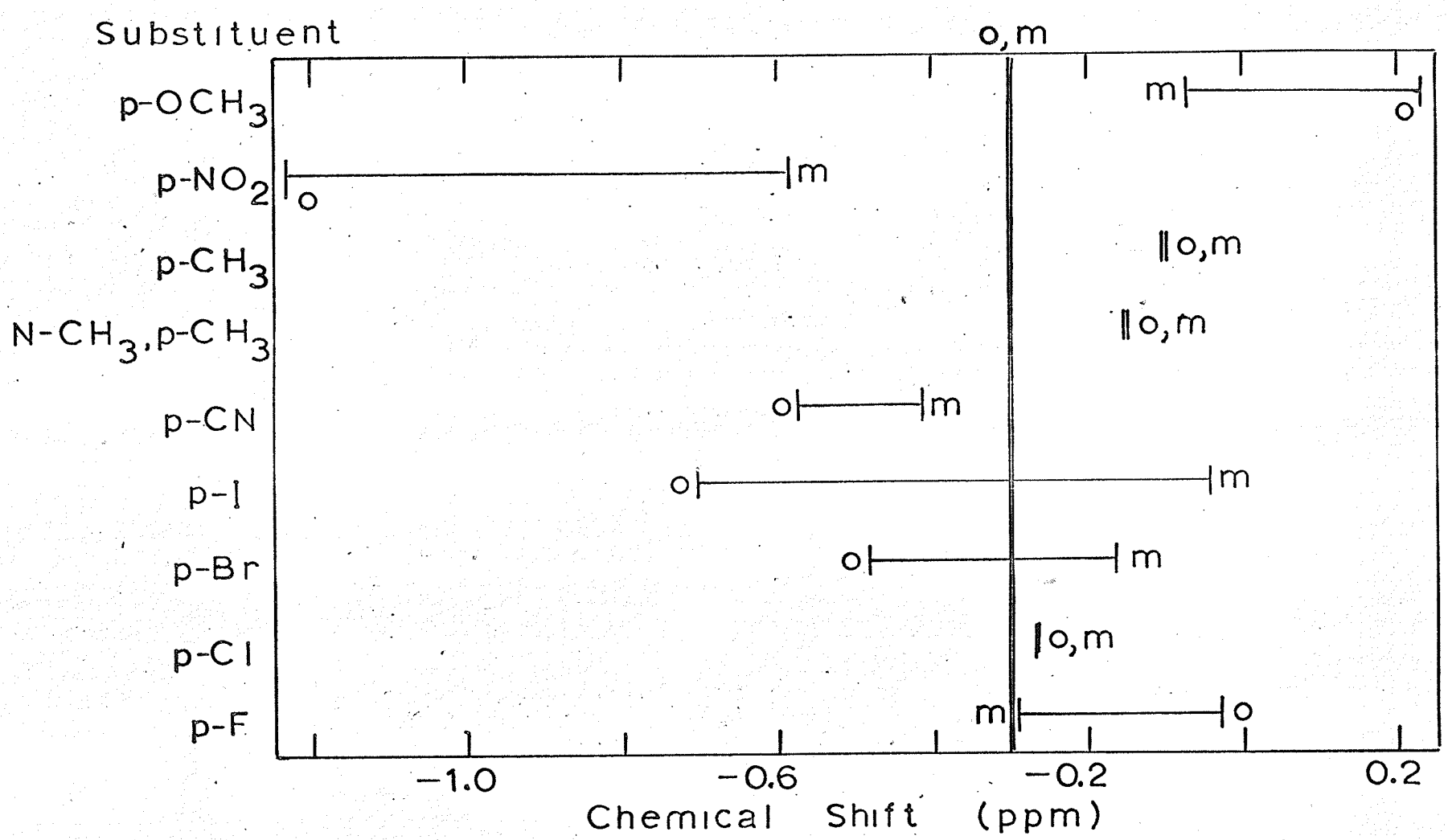
Substituent
o,m
p-OCH3
p-NO2
p-CH3
N-CH3,p-CH3
p-CN
p-I
p-Br
p-Cl
p-F
m
o
o
m
o,m
o,m
o
m
o
m
o
m
o,m
m
o
−1.0
−0.6
−0.2
0.2
Chemical Shift (ppm)

by the small values of meta substituent parameters in di-substituted benzenes (11). This strongly suggests that primary inductive effects are unimportant and that large meta shifts only occur when π inductive effects and/or field effects are important.

It is evident from Figure 5 that the meta proton signals of p-haloanilines all occur to high field of the corresponding aniline proton signals, with the largest shift for p-iodoaniline. Since the halogens are electron-withdrawers, the induced positive charges on the alpha carbon atoms would be expected to cause low field shifts of the meta protons by primary and π inductive mechanisms. Consequently the high field shifts must be caused by some other mechanism.

It has been suggested that the positive (high field) shifts of protons meta to halogens may be due to field effect contributions(13). An attempt was made to calculate shifts of some p-substituted anilines in CCl_4. The field (2.6) and reaction field (2.11) equations of Buckingham were used. Dipole moments were obtained from a standard compilation (77). Field and reaction field effects were assumed to be additive. The results are given in Table VII. Agreement with experimental values is quite poor. After correction for additional ortho shifts, the differences in shift would show the right trend. Presumably these calculations do not allow for mesomeric effects. The important point to be noted is that the

calculations predict negative shifts for the meta protons, relative to the equivalent protons in aniline. This agrees with what one would intuitively expect, but is opposite to what is found experimentally. The calculations apparently disprove the postulate that there are positive contributions to the meta shifts from field effects.

The dipole moments indicate that there is a net electron withdrawal from the phenyl ring by the halogens. The overall decrease in electron density should decrease the ring current effect and consequently increase the ring proton shielding. However, the shifts would be expected to be small and should be partly or wholly counteracted by the inductive withdrawal of electrons. In any case, the positive shifts should be least for iodoaniline. The largest shifts are observed for iodoaniline. Consequently, changes in ring current effects must be relatively unimportant.

It is tempting to assume that the high field shifts are due to substituent anisotropy contributions. The shifts should be largest for iodoaniline because $-\Delta\chi$ is largest for iodine. It can be seen from Figure 1 that if $-\Delta\chi$ has values of ten to twenty cm^3 $mole^{-1}$, then the predicted high field meta shifts will agree with the experimentally measured shifts. However, there should be nearly equal positive anisotropy shifts of the para protons. It has been shown that para proton shifts are small (in the absence of mesomeric effects)

and correlate well with Hammett reactivity parameters (13). This indicates that effects other than mesomeric effects are unimportant at the *para* position. Equation 2.9 would have to be grossly altered before it would predict significant *meta* shifts and insignificant *para* shifts. Therefore, the postulate that positive *meta* shifts are caused by substituent anisotropy must be rejected unless a reasonable explanation for the small *para* shifts can be proposed. This is unfortunate since there is no other obvious and plausible explanation for the large positive *meta* shift of p-iodoaniline.

Most of the other p-substituted anilines which were studied had large positive or negative *meta* proton shifts relative to aniline. These shifts can easily be rationalized. There are negative contributions to the *meta* proton shifts of p-cyano- and p-nitroaniline from the field effect of the substituents and from the π inductive effect of the large concentrations of positive charge at the *ortho* and *para* positions. The high field shift of the *meta* protons of p-anisidine must occur because positive field and π inductive effects overcome the primary inductive effect of the methoxy group.

Meta shifts can be rationalized when they result largely from inductive and field effects. In the p-haloanilines, where these effects are small, an unexplained high field shift

is found. The positive shifts have been discussed in general terms in this section, but an actual explanation of the shifts would require more complete knowledge of the nature of anisotropic, ring current, inductive, and field effects and possibly other effects not yet recognized.

(ii) Ortho proton shifts - The ortho proton shifts are in general much larger than the meta proton shifts. Mesomeric effects are at least partly responsible for the large ortho shifts of most of the compounds studied. Primary inductive effects are probably relatively unimportant. The much smaller meta shifts do not appear to contain any appreciable contributions from primary inductive effects. Therefore, it is unlikely that this effect will have a major role in the determination of the much larger ortho shifts. When the shifts cannot be accounted for by π inductive effects and mesomeric effects, anisotropic, dispersive and field effects are the most likely contributors to the additional shifts. In methyl halides, overlap effects of the type suggested by Drago must be less important than primary inductive effects since the alpha proton shifts are modified rather than dominated by overlap effects. Consequently, if primary inductive effects are considered to be relatively unimportant in substituted benzenes, then overlap effects need not be considered.

The ortho proton shifts of p-haloanilines vary from pos-

itive (relative to aniline) for fluoroaniline to strongly negative for iodoaniline. The positive ortho shift of fluoroaniline is undoubtedly caused by mesomeric interactions between the fluorine atom and the ring π electrons. It is known that the para proton and C^{13} shifts of halobenzenes (other than fluorobenzene) are small (13). Experiments and calculations by Karplus and Das (78) indicate that halogens other than fluorine have no significant mesomeric effect upon F^{19} shifts of fluorobenzenes. This strongly suggests that halogens other than fluorine will have little mesomeric effect upon ortho proton shifts. Therefore, the ortho shifts cannot be accounted for by a combination of σ inductive and mesomeric effects because iodine has the lowest electronegativity of the halogens and should have the smallest inductive effect.

Schneider and Spiesecke have postulated that anisotropy contributions were at least partly responsible for similar low field shifts in halobenzenes (13). This possibility was considered in detail in the theoretical introduction. It was concluded that the negative ortho proton shifts might be caused by substituent anisotropy. However, the low field shifts of the ortho C^{13} atoms (13) could not be caused by anisotropy.

Since the halogens withdraw electrons from the phenyl ring, the polar C-X bond should cause a negative ortho proton

shift. Field effect calculations indicate that the halogens cause negative ortho proton shifts of 0.25 to 0.32 ppm (see Table VII). Reaction field effects should reduce the predicted shifts slightly. If it is assumed that half of the total reaction field effects shown in Table VII are caused by the halogen atoms, then the predicted shifts are -0.2 to -0.26 ppm with the largest negative shift for fluoroaniline. These values are probably too large, since shifts caused by the substituents were estimated separately. The shift proportional to E^2 must be estimated from the total field since the field components due to the individual substituents partly cancel. Field effects will certainly contribute to the negative ortho shifts. However, some other mechanism must cause the large negative shifts of the ortho protons of p-bromo- and p-iodoaniline.

Pitcher and coworkers (64) have postulated that low field alpha F^{19} shifts of fluoroalkanes are due to paramagnetic contributions from the substituent. They supported this postulate by pointing out that alkyl tin IV compounds do not exhibit negative alpha F^{19} shifts. Tetravalent tin has no unfilled d orbitals. Consequently it should have no low-lying excited states and small paramagnetic contributions to shifts. Beta F^{19} shifts are apparently not altered by paramagnetic effects. This suggests that there may possibly be appreciable paramagnetic contributions to ortho C^{13} shifts but not to

ortho proton shifts, particularly since protons have no low-lying excited states.

It has been postulated that negative ortho F^{19} shifts in mono-substituted fluorobenzenes are also due to paramagnetic contributions (63). However, fluorinated dimethyl, diphenyl tin also exhibits large negative ortho F^{19} shifts. This suggests that the low field shifts may be caused by some other mechanism.

The negative ortho shifts of substituted anilines can also be accounted for by assuming that they are caused by intramolecular dispersive forces. Dispersive forces should have appreciable magnitudes at the ortho positions since the van der Waals radii of the substituents and the ortho protons and carbon atoms overlap (see Figure 2). Dispersive effects should be unimportant at the meta and para positions since they drop off rapidly with distance.

An attempt was made to obtain a semi-quantitative estimate of the magnitudes of low field shifts contributed by the three effects. A plot of chemical shifts versus C^{13}-H coupling constants could not be constructed since the necessary information was not available. However, a study of the C^{13}-H coupling constants of poly-substituted benzenes showed that the values of the coupling constants changed only slightly as the substituents were changed (79). The coupling constants appeared to be partially related to electronegativity since

they increased in the order H > Cl > Br > NO_2 for compounds of the type 1,3,5-triXaniline where X was one of the four substituents listed above. Therefore, it was considered that a plot of shifts versus electronegativity would give an accurate estimate of shifts arising from additional effects. The plot was constructed but it proved to be unsuitable for estimating shifts arising from additional effects because many of the proton shifts were determined largely by mesomeric effects.

An attempt was made to obtain shifts which had been corrected for mesomeric effects. The accurate data of Schneider and Spiesecke for mono-substituted benzenes (13) were used since this eliminated errors introduced by deviations from additivity in di-substituted benzenes. Shifts due to effects other than mesomeric effects were estimated by subtracting the <u>para</u> shifts from the <u>ortho</u> shifts. It was assumed that the <u>para</u> shifts were caused entirely by mesomeric effects and that mesomeric effects were equally important at the <u>ortho</u> and <u>para</u> positions. The estimated ortho proton and C^{13} shifts are given in Table VIII.

Inductive, field, dispersive, and possibly anisotropic effects contribute to the negative <u>ortho</u> proton shifts of the p-haloanilines. Only dispersive and possibly anisotropic effects should be largest for iodoaniline. Therefore, either or both of these effects must dominate the <u>ortho</u> proton shifts

in p-haloanilines. The large negative ortho C^{13} shifts of bromo- and iodobenzene (13) must be caused by dispersive forces and/or by paramagnetic deshielding by the substituent.

The ortho proton shifts of p-methoxy-, p-nitro-, p-methyl-, and p-cyanoaniline can be accounted for by reasonable combinations of mesomeric, inductive, field, anisotropic, and dispersive effects. Hydrogen bonding between the nitro group and the ortho protons in p-nitroaniline may cause an additional low field shift of the ortho protons of that compound.

The ortho proton shifts of all the p-substituted anilines can be rationalized by combinations of the five effects mentioned above. Unfortunately, it is impossible to determine the relative magnitudes of the various effects. The probable signs and sizes of inductive, mesomeric, and field effects can be estimated from reactivity parameters and dipole moments. Dispersive forces obviously cause low field shifts but the size of the shifts cannot be determined. It is known that intermolecular dispersive forces can cause shifts of as much as -0.7 ppm (70). Therefore, it is quite conceivable that intramolecular dispersive forces could cause shifts as large as those shown in Table VIII. Both the signs and sizes of the anisotropy contributions to ortho shifts are unknown.

The above discussion in no way proves the existence of appreciable dispersive effects upon ortho proton and C^{13}

shifts. However, the postulate that dispersive forces cause at least part of the negative ortho shifts in substituted anilines is consistent with experimental evidence. Also, it appears that the experimental results can be more easily explained if it is assumed that significant dispersive forces are present. All the ortho proton shifts can be rationalized by combinations of the five possible effects discussed above.

(C) N-alkyl-Substituted Anilines

The spectra of the N-alkylanilines in CCl_4 were generally of the A_2B_2C type and were not rigorously analyzed. Shift values are only approximate. Usually they are nearly equal to the corresponding shifts in aniline. However, some of the shifts differ sufficiently from the aniline proton shifts to require explanations.

(1) Steric hindrance of the mesomeric effect - There is conclusive evidence that steric hindrance affects the shifts of N,N-di-methyl-o-toluidine and N-methyl-N-phenylaniline in CCl_4.

The ortho and para protons of N,N-dimethyl-o-toluidine resonate at much lower field than the corresponding protons in N,N-dimethylaniline. Molecular models indicate that the presence of a methyl group in the ortho position prevents the dimethylamino group from lying in the plane of the ring. No abnormal shifts are noted for N,N-dimethyl-o-toluidine in TFA. This strongly suggests that the abnormal shifts in CCl_4

result from a decrease in the mesomeric effect. The ammonio group has no mesomeric effect.

In unsubstituted N,N-dimethylaniline the nitrogen valences are probably nearly in a trigonal planar configuration (27). The lone pair electrons are in p orbitals at right angles to the plane of the ring. When steric hindrance forces the group out of the plane of the ring, the spatial arrangement of the nitrogen valences alters until they are in a pyramidal configuration when the dimethylamino group is twisted through an angle of 90°. As the group is forced out of the plane of the ring, the overlap between the lone pair electrons and the π electrons of the ring decreases and the mesomeric effect becomes smaller.

It is possible to estimate the angle of twist if one assumes that <u>para</u> shifts arise entirely from mesomeric effects. Subtraction of the substituent parameter for the ring methyl group from the observed shift leaves a value of 0.2 ppm for the <u>para</u> shift of N,N-dimethyl-o-toluidine while N,N-dimethylaniline has a <u>para</u> shift of 0.7 ppm. Since the overlap varies as $\cos^2\theta$, a ratio of 2/7 corresponds to an angle of twist of 57°. The same value is obtained for the angle of twist of N-methyl-2,6-dimethylaniline, if the shift values of Fraser are used (14). Obviously this method provides only a very crude estimate of the angle of twist.

Angles of twist have been estimated from the electronic spectra of substituted anilines (80). The angle of twist

obtained from the electronic spectrum of N,N-dimethyl-o-toluidine was 50°. The agreement between the two values of angle of twist is about as good as could be expected.

In N-phenylaniline the lone pair overlaps with two rings and one might naively expect a two-fold decrease in shielding, as is roughly true. The addition of a methyl group to the nitrogen causes hindrance and apparently decreases overlap almost to zero, since the shifts decrease to zero. This implies that the nitrogen atom is in a tetrahedral configuration.

From the experimental data it can be concluded that steric hindrance only affects shifts appreciably when (a) at least three of the four N and ortho positions are substituted or (b) a tertiary amine contains at least two phenyl groups.

(2) Low field shifts of ring protons in N-alkylanilines- In general, the ring protons of N-alkyl and N,N-dialkylanilines in CCl_4 are shifted to low field of the corresponding aniline protons. The ortho and meta protons are appreciably shifted to low field while the para proton shifts are not altered significantly. These trends are not obvious in the crude shift results for N-alkylanilines. They can be observed in the shifts of p-toluidine and N-methyl-p-toluidine in CCl_4 and also in the results of Schneider and Spiesecke for aniline and N,N-dimethylaniline (13).

The presence of the N-methyl groups would be expected to increase the mesomeric effect of the amino group, increasing the ortho and para proton shifts. The low field shift cannot be caused by steric hindrance of the mesomeric effect since this should decrease the para shift as well as the ortho shift.

The low field shift of the ortho protons may be partly due to the dispersive effect of the methyl groups adjacent to the ortho protons. This is unlikely to account for the negative shift of the meta protons since it is unlikely that the dispersive effect is important at so great a distance. A more plausible explanation for the low field shifts is that they are caused by a decrease in the field effect of the amino group. The presence of the methyl groups allows the charge on the amino group to spread over a larger volume, and the field due to the amino group is reduced.

(3) The ring proton spectra of N,N-dialkylanilines in TFA are not completely collapsed if at least one of the alkyl groups is larger than methyl. The ring protons seem to be slightly shifted to low field of the ring protons of aniline in the same solvent. These observations can be accounted for if one assumes that anilinium trifluoracetate forms ion pairs in TFA. The bulky dialkylammonio group must prevent the close approach of the trifluoracetate ion. Consequently the low field ring pro-

ton shifts are no longer counteracted by the counter ion.

(D) Toluidines and Dimethyl Anilines

(1) Ring proton shifts - The experimental results indicate that methyl groups cause high field shifts of 0.10 to 0.25 ppm for protons *ortho* to the methyl groups and 0.05 to 0.15 ppm for *meta* and *para* protons. These values agree with Martin's substituent parameters for p-substituted toluenes (11). His substituent parameters had values of 0.183 ppm for *ortho* protons and 0.107 ppm for *meta* protons.

Some of the unsymmetrically substituted anilines contained two *ortho* or *meta* protons of unequal shift. In these cases the spectra were not sufficiently resolved to allow estimation of both shifts and only average values were obtained. This should introduce a small error since, as indicated by the predicted values of shifts in Tables IX and X, the difference in shift should be small. In TFA, almost all ring proton spectra were single, collapsed peaks. All shifts were considered to be equal in these cases. This possibly introduces an error which is larger than the normal expected error.

A comparison of experimental shift values of protonated methyl anilines and shift values predicted by the use of Martin's substituent parameters is given in Table IX. The RMS deviation is 0.04 ppm. Much of the error probably is

introduced by the assumption of equal shifts for single peak ring proton spectra.

Table X shows calculated and observed shifts of several methylanilines in CCl_4. The calculated shifts are consistently too high. The RMS deviation is approximately 0.1 ppm. This is certainly larger than the experimental error. The deviations are probably caused by a breaking down of the additivity relationships for trisubstituted benzenes. In dimethylanilines, three substituent groups are trying to push electrons into the ring. This may lead to a "saturation" effect. As a result actual shifts may be smaller than predicted shifts. There should be no saturation effect in protonated dimethylanilines because the ammonio group has an electron withdrawing tendency which is approximately equal to the combined electron donating tendencies of the two methyl groups.

(2) Methyl proton shifts - The chemical shifts of the methyl protons are given in Table II. The shifts for methylanilines in CCl_4 fall into two distinct groups. The <u>meta</u> and <u>para</u> methyl proton shifts are equal within experimental error. The <u>ortho</u> methyl protons definitely resonate at higher field than the other methyl protons.

In TFA there are no obvious trends. However, it appears that the <u>ortho</u> protons resonate at lowest field, since both 2,4- and 2,5-dimethylaniline in TFA show two distinct

methyl proton signals. It cannot be definitely concluded that the low field peak is the ortho methyl peak, but the assignment seems reasonable in view of the methyl proton shifts of the three monomethylanilines. Also, the low field peak is higher in both cases. Since the meta and para methyl proton signals are broadened by coupling to two protons while the ortho methyl protons are coupled to only one proton, the low field peak is most probably due to the ortho methyl protons.

The high field shift of the ortho methyl protons in CCl_4 is probably due to a combination of field dipole effects and inductive effects caused by the mesomeric concentration of charge at the ortho carbon atom.

The methyl proton shifts in TFA are nearly analogous to the ring proton shifts in the same solvent, since the shifts of the different types of methyl protons are almost equal. One would have to compare shifts with those of toluene in the same solvent in order to obtain a value of the actual negative shifts caused by the ammonio group.

(E) Amino Proton Shifts

The amino proton shifts in CCl_4 are listed in Table III. Included in the list are values of the amino proton shifts of ortho- and meta-bromoaniline. Ring proton shifts of these two compounds could not be determined since the

spectra were too complicated for first order analysis. All of the amino proton signals were single peaks of a few cycles width. Coupling to the N^{14} nuclei should split the amino proton signals into triplets. Rapid quadrupole relaxation by the N^{14} nuclei must cause the proton signals to collapse to single peaks.

The amino proton shifts can be correlated to Hammett reactivity parameters. Figure 6 shows a plot of shifts versus Hammett σ constants (81). For the ortho-substituted anilines Taft σ^* constants were used (82). These constants do not correct for any "steric" (dispersive) effects. σ constants were assumed to be additive for di-substituted anilines.

Most points deviate from the straight line by no more than the estimated experimental error (0.3 ppm). Only the amino proton shifts of 2,6-dimethylaniline and o-bromoaniline deviate markedly from the straight line. Schematic diagrams indicate that there should be a positive shift of the amino protons of 2,6-dimethylaniline due to the "C-C" bond anisotropy (if the experimental estimates of anisotropy are correct) and a negative shift of the amino protons of o-bromoaniline due to the anisotropy of the C-Br bond. Dispersive forces should cause low field shifts in both cases.

Presumably, the size of reactivity parameters depends upon the electron density about the side chain proton whose reactivity is being measured. In the absence of ortho substituent effects, the amino proton shifts depend largely upon the

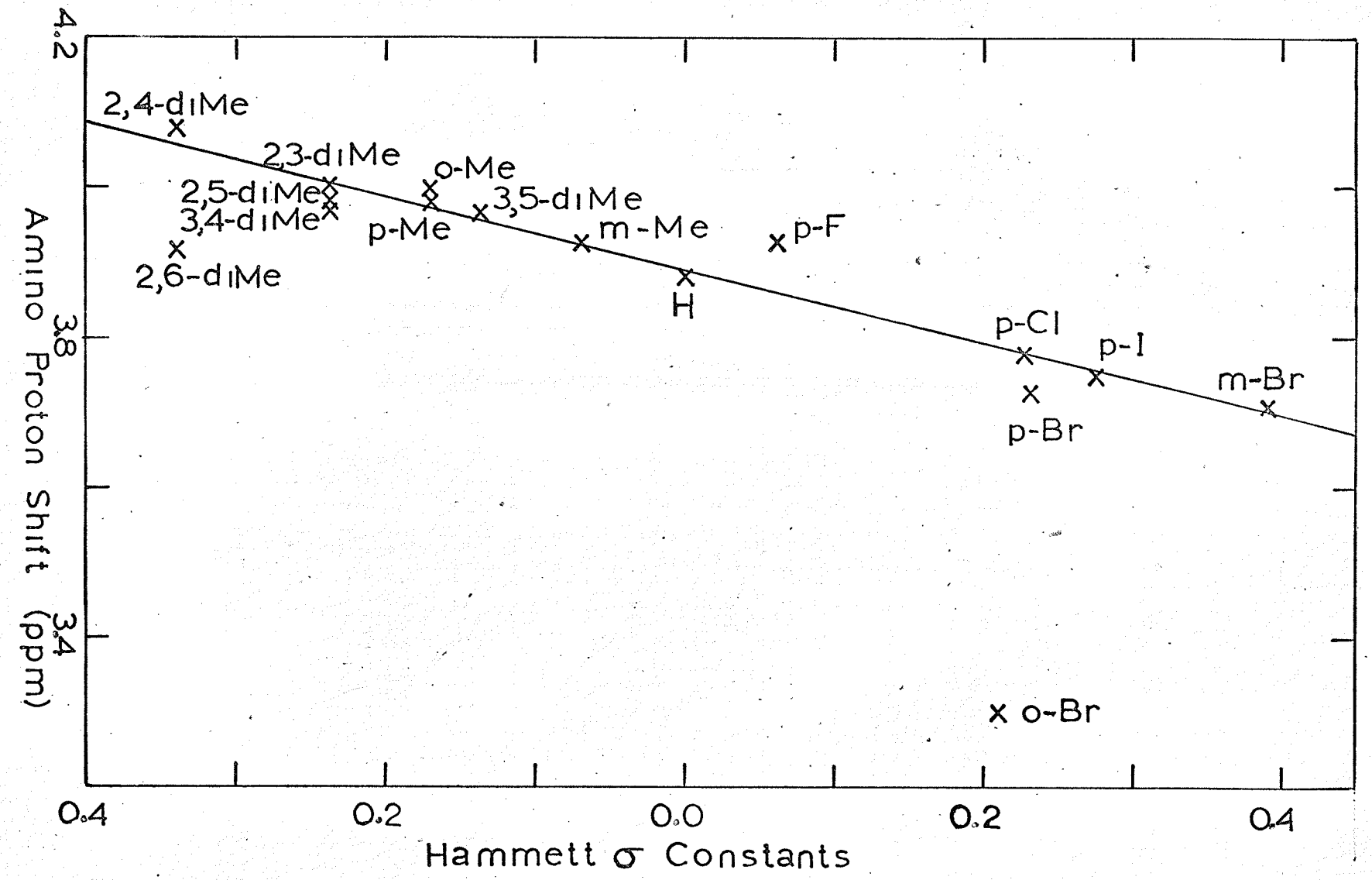
4.2
3.8
3.4
Amino Proton Shift (ppm)
2,4-diMe
2,3-diMe
o-Me
2,5-diMe
3,5-diMe
3,4-diMe
p-Me
m-Me
p-F
2,6-diMe
H
p-Cl
p-I
m-Br
p-Br
o-Br
0.4
0.2
0.0
0.2
0.4
Hammett σ Constants

electron density of the amino protons. Therefore, the straight line relationship between shifts and Hammett constants is not surprising. Plots of this type may prove quite useful for estimating anisotropic and dispersive effects.

Taft has obtained a set of constants which measure the extent of steric alteration of reactivity by ortho substituents (82). He has shown that the differences between the E_s values of fluorine and other substituents vary in the same manner as the differences between the van der Waals radii of fluorine and other substituents. This suggests that steric effects and dispersive effects are essentially equivalent.

6. SUMMARY AND CONCLUSIONS

Measurements of the ring proton spectra of substituted anilines in TFA have shown that the ammonio group causes a low field shift of 0.30 ppm of all ring protons. N,N-dialkylammonio groups cause unequal proton shifts. These results can be explained if it is assumed that anilinium ions and trifluoracetate ions exist in solution as ion pairs. Calculations of the effect of ion pair formation indicate that the ring proton shifts of anilinium ions can be accounted for by the combined field and reaction field effects of the ion pairs in solution. The bulkier dialkylammonio groups must prevent close approach of the trifluoracetate ions and therefore decrease the field

effects of these ions.

It has been confirmed that substituent effects are nearly additive in protonated and unprotonated *para*-substituted anilines. Substituent effects in disubstituted anilines are, in general, not additive.

Chemical shifts of protons *ortho* to substituents can be more easily rationalized if one assumes that intramolecular dispersive forces cause low field shifts. *Meta* proton shifts cannot be completely explained.

It has been shown that steric hindrance reduces the mesomeric effects of the amino groups of N-methyl-N-phenylaniline and N,N-dimethyl-o-toluidine. Steric hindrance only affects shifts of substituted anilines appreciably when (a) at least three of the four N and *ortho* positions are substituted or (b) a tertiary amine contains at least two phenyl groups.

It has been shown that there is an apparent relationship between Hammett σ constants and amino proton shifts of *meta*- and *para*- substituted anilines. Amino proton shifts of some *ortho*-substituted anilines cannot be correlated with Taft σ^* constants.

TABLE I

Chemical Shifts in ppm Relative to Internal Benzene of the Ring Protons in Substituted Anilines; 5 mole % Solutions in Carbon Tetrachloride and Trifluoroacetic Acid

		Chemical Shift*									
		CCl_4 Solution			CF_3COOH Solution			CCl_4 - CF_3COOH			
	Substituent	ortho	meta	para	ortho	meta	para	Δortho	Δmeta	Δpara	$\Delta o + \Delta m$
1.	4-NH_2	0.897	0.897	--	-0.550	-0.550	--	1.447	1.447	--	1.45 †
2.	4-OCH_3	0.825	0.677	--	-0.072	+0.232	--	0.897	0.445	--	1.34
3.	4-NO_2		insoluble		-0.585	-1.232	--				-
4.	4-CH_3	0.897	0.460	--	-0.10	-0.10	--	0.997	0.560	--	1.56
5.	4-CH_3,N-CH_3	0.860	0.390	--	-0.15	-0.15	--	1.010	0.540	--	1.55
6.	4-I	0.882	-0.097	--	-0.042	-0.705	--	0.924	0.608	--	1.53
7.	4-Br	0.817	0.112	--	-0.167	-0.483	--	0.984	0.595	--	1.58
8.	4-Cl	0.772	0.227	--	-0.267	-0.267	--	1.039	0.494	--	1.53
9.	4-F	0.773	0.487	--	-0.293	-0.030	--	1.066	0.517	--	1.58
9a.	4-CN		insoluble		-0.414	-0.574					
10.	3,5-di-CH_3	1.1	--	1.0	0.2	--	0.05	0.9	--	0.95	-
11.	2,6-di-CH_3	--	0.47	0.77	--	-0.02	-0.02	--	0.49	0.79	-
12.	2,3-di-CH_3	0.90	0.52	0.80	0.03	0.03	0.03	0.87	0.49	0.77	-

continued

† 1.45 = $(\Delta_o+\Delta_m)/2$. $(\Delta_o+\Delta_m)$ is divided by two because there are two amino (or ammonio) groups in the molecule.

TABLE I continued

	Substituent	Chemical Shift* CCl_4 Solution ortho	meta	para	CF_3COOH Solution ortho	meta	para	CCl_4 - CF_3COOH Δortho	Δmeta	Δpara
13.	2,4-di-CH_3	0.90	0.5	--	0.02	0.02	--	0.88	0.48	--
14.	2,5-di-CH_3	0.95	0.5	0.9	-0.05	-0.05	-0.05	1.0	0.55	0.95
15.	3,4-di-CH_3	1.0	0.5	--	0.0	0.0	--	1.0	0.5	--
16.	3-CH_3	1.0	0.4	0.8	-0.1	-0.1	-0.1	1.1	0.5	0.9
17.	2-CH_3	0.8	0.4	0.7	-0.2	-0.2	-0.2	1.0	0.6	0.9
18.	H	0.8	0.2	0.6_5	-0.3	-0.3	-0.3	1.1	0.5	0.9_5
19.	N-CH_3	0.8	0.2	0.7	-0.3	-0.3	-0.3	1.1	0.5	1.0
20.	N-CH_3,2-CH_3	0.8	0.3	0.7_5	-0.2	-0.2	-0.2	1.0	0.5	0.9_5
21.	N-di-CH_3	0.6	0.1	0.7	-0.4	-0.4	-0.4	1.0	0.5	1.1
22.	N-di-CH_3,2-CH_3	0.3_5	0.3	0.4	-0.3	-0.3	-0.3	0.6	0.6	0.7
23.	N-C_2H_5	0.7	0.2	0.7	-0.4	-0.4	-0.4	1.1	0.6	1.1
24.	N-di-C_2H_5	0.7	0.2	0.7	-0.4	-0.4	-0.4	1.1	0.6	1.1
25.	N-C_2H_5,CH_3	0.7	0.2	0.7	-0.4	-0.4	-0.4	1.1	0.6	1.1
26.	N-(n-C_3H_7)$_2$	0.7	0.2	0.8	-0.3	-0.3	-0.3	1.0	0.5	1.1

continued

TABLE I continued

	Substituent	Chemical Shift*								
		CCl_4 Solution			CF_3COOH Solution			CCl_4 - CF_3COOH		
		ortho	meta	para	ortho	meta	para	Δortho	Δmeta	Δpara
27.	N-(n-C_4H_9)	0.8	0.2	0.7	-0.3	-0.3	-0.3	1.1	0.5	1.0
28.	N-C_6H_5	0.3	0.1	0.2	-0.3	-0.3	-0.3	0.6	0.4	0.5
29.	N-C_6H_5,CH_3	0.1	0.0	0.0	-0.3	-0.3	-0.3	0.4	0.3	0.3

* the ring protons are labelled relative to the amino group

TABLE II

Ring Methyl Proton Shifts of Methyl-Substituted Anilines in CCl_4 and TFA (Relative to Benzene in the Same Solvent)

Substituent(s)	Methyl Proton Shifts (ppm) In CCl_4			Methyl Proton Shifts (ppm) in TFA		
	ortho	meta	para	ortho	meta	para
4-CH_3	--	--	5.09	--	--	4.84
3-CH_3	--	5.09	--	--	4.82	--
2-CH_3	5.26	--	--	4.79	--	--
2-3-Di-CH_3	5.27	5.05	--	(4.76	)	--
2,4-di-CH_3	5.19	--	5.06	4.83	--	4.88
2,5-di-CH_3	5.19	5.05	--	4.83	--	4.88
2,6-di-CH_3	5.16	--	--	4.77	--	--
3,4-di-CH_3	--	(5.11)		--	(4.88)	
3,5-di-CH_3	--	5.09	--	--	4.86	--

TABLE III

Amino Proton Shifts of Substituted Anilines in CCl_4 (Relative to Benzene in the Same Solvent

Substituent	Chemical Shift (ppm)
H	3.88 ± 0.03
p - I	3.75
p - Br	3.73
m - Br	3.70
o - Br	3.30
p - Cl	3.78
p - F	3.93
p - CH_3	3.98
m - CH_3	3.93
o - CH_3	4.00
2,3-di-CH_3	4.00
2,4-di-CH_3	4.08
2,5-di-CH_3	3.98
2,6-di-CH_3	3.92
3,4-di-CH_3	3.97
3,5-di-CH_3	3.97

TABLE IV

PART A
Calculation of the Field Effect Due to the Ammonio Group

Position	E_z(esu)	E^2(esu^2)	$\left(\begin{matrix}-2\times10^{-12}E_z \\ -10^{18}E^2\end{matrix}\right)$ ppm	$\left(\begin{matrix}-2\times10^{-12}E_z \\ -0.25\times E^2\times10^{-18}\end{matrix}\right)$ ppm
ortho	1.15×10^5	2.77×10^{11}	-0.51	-0.30
meta	1.44×10^5	0.35×10^{11}	-0.32	-0.30
para	1.39×10^5	0.20×10^{11}	-0.29	-0.28

PART B
Calculation of the Net Field Effect Due to the Ammonio Group and the Trifluoracetate Ion

Position	E_z(esu)	E^2(esu^2)	$\left(-2\times10^{-12}E_x-10^{-18}E^2\right)$ ppm
ortho	1.17×10^5	0.97×10^{11}	-0.33
meta	0.71×10^5	0.25×10^{11}	-0.17
para	0.51×10^5	0.14×10^{11}	-0.12

TABLE V

Experimental and Predicted Shifts of p-substituted Anilines in CCl_4 (This Study) and Cyclohexane (11)(Relative to Benzene in the Same Solvent

Substituent	Chemical Shift in ppm (protons labelled relative to substituent)							
	Experimental Results				Predicted Chemical Shifts			
	This Study		Martin (11)		From Results of Schneider and Spiesecke (13)		From Substituent Parameters of Martin (11)	
	ortho	meta	ortho	meta	ortho	meta	ortho	meta
OCH_3	.677	.825	.643	.790	.637	.795	.659	.844
CH_3	.460	.897	.418	.823	--	--	.430	.843
I	-.097	.882	-.055	.968	-.197	1.033	-.065	.954
Br	.112	.817	.130	.877	-.020	.840	.120	.862
Cl	.227	.772	.275	.808	.183	.780	.271	.814
F	.487	.773	--	--	.558	.778	--	--
NH_2	.897	.897	--	--	.952	.952	.958	.958

TABLE VI

Experimental and Predicted Shifts of p-Substituted Anilines in TFA (relative to benzene in TFA)

Substituent	Chemical Shift in ppm (Protons labelled relative to substituent)					
	Experimental Results		Predicted Chemical Shifts*			
	This Study		From Results of Schneider and Spiesecke (13)		From Substituent Parameters of Martin (11)	
	ortho	meta	ortho	meta	ortho	meta
CH_3	-0.10	-0.10	--	--	-0.09	-0.19
OCH_3	+0.23	-0.07	+0.13	-0.26	+0.28	-0.18
I	-0.71	-0.04	-0.70	-0.05	-0.69	-0.04
Br	-0.48	-0.17	-0.52	-0.22	-0.49	-0.17
Cl	-0.27	-0.27	-0.28	-0.32	-0.30	-0.24
F	-0.03	-0.29	+0.01	-0.28	--	--
CN	-0.57	-0.41	--	--	-0.58	-0.40
NO_2	-1.23	-0.58	-1.25	-0.51	-1.32	-0.46
NH_3^+*	-0.55	-0.55	--	--	--	--

* It is assumed that $\gamma_{NH_3^+} = 1$, $d_{NH_3^+} = -0.30$ ppm.

TABLE VII

Chemical Shifts of p-Substituted Anilines in CCl_4 as Calculated by the Field and Reaction Field Equations (16)

Substituent	Chemical Shift in ppm (relative to benzene)						
	Field Dipole Effect				Reaction Field Effect		Difference in Shift ($\nu_m - \nu_o$)
	NH_2		X				
	ortho	meta	ortho	meta	ortho	meta	
I	$.08_5$	0.28	-0.26	-0.07	0.08	-0.09	0.21_5
Br	"	"	-0.31	-0.07_5	0.08	-0.10	0.26_5
Cl	"	"	-0.32	-0.08_5	0.09	-0.12	0.22
F	"	"	-0.31	-0.09	0.11	-0.13	0.17_5
CH_3	"	"	+0.07	+0.02	$+0.02_5$	-0.03	0.09

TABLE VIII

Estimated Ortho Proton and C^{13} Shifts (13) of -Substituted Benzenes (relative to benzene) after Correction for Mesomeric Effects

Substituent	Chemical Shift (in ppm)	
	Ortho H^1	Ortho C^{13}
F	+ .091	+ 9.9
Cl	- .137	- 2.2
Br	- .253	- 4.3
I	- .433	-10.3
OCH_3	+ .067	+ 6.6
NH_2	+ .130	+ 2.9

TABLE IX

Predicted and Observed Ring Proton Shifts of Methyl-Substituted Anilines in Trifluoroacetic acid, Relative to Benzene in the Same Solvent.

Substituents	Chemical Shift* (in ppm)					
	Predicted			Observed		
	ortho	meta	para	ortho	meta	para
2,6-di-CH_3	--	0.04	-0.08	--	-0.02	-0.02
3,5-di-CH_3	0.04	--	0.07	-.2	--	0.05
2,3-di-CH_3	-0.03	-0.03	-0.01	0.03	0.03	0.03
2,4-di-CH_3	-0.08	(-0.04) (-0.06)	--	0.02	0.02	
2,5-di-CH_3	-0.01	-0.01	-0.01	-0.05	-0.05	-0.05
3,4-di-CH_3	(-0.03) (-0.01)	-0.01	--	0.0	0.0	--
2-CH_3	-0.19	(-0.14) (-0.12)	-0.19	-0.2	-0.2	-0.2
3-CH_3	(-0.14) (-0.12)	-0.19	-0.12	-0.1	-0.1	-0.1

* Ring protons are labelled relative to the ammonio group.

TABLE X

Predicted and Observed Ring Proton Shifts of Methyl-Substituted Anilines in CCl_4

Substituent	Chemical Shift (relative to benzene) in ppm					
	Experimental Results This Study			Shifts Predicted from Substituent Parameters of Martin (11)		
	ortho	meta	para	ortho	meta	para
2-CH_3	0.8	0.4	0.7	0.88	0.43 0.45	0.78
3-CH_3	1.0	0.4	0.8	0.95 0.93	0.38	0.85
2,3-di-CH_3	0.90	0.52	0.80	1.04	0.54	0.96
2,4-di-CH_3	0.90	0.50	-	0.98	0.64 0.61	-
2,5-di-CH_3	0.95	0.5	0.9	1.06	0.56	0.96
2,6-di-CH_3	-	0.47	0.37	-	0.61	0.88
3,4-di-CH_3	1.0	0.5	-	1.06 1.04	0.56	-
3,5-di-CH_3	1.1	-	1.0	1.11	-	1.04

CHAPTER 3

A STUDY OF HINDERED ROTATION IN PROTONATED BENZYLAMINES

1. INTRODUCTION

Considerable work has been done on the problem of configurational isomerism of substituted ethanes, using high resolution nuclear magnetic resonance (83-92). There was some misunderstanding in the early literature about the roles of asymmetry and conformational populations in producing magnetic non-equivalence of nucleii (86,87). This confusion has lately been cleared up (93-95).

From the temperature dependence of coupling constants involved, (89), or from an observed averaged coupling constant at one temperature and a value of energy differences between isomers obtained from vibrational spectra, (91), values of vicinal coupling constants have been estimated as 10 to 18 c/s for trans coupling constants and 1 to 3.5 c/s for gauche coupling constants of protons attached to saturated carbon atoms in substituted ethanes.

In the course of investigating a series of protonated anilines and related compounds, it was noted that the methylene protons of certain protonated benzylamines were non-equivalent. Protonated benzylamines ($\emptyset H_2C\text{-}NHRR$)$^+$ are analogous to triply-substituted ethanes ($XH_2C\text{-}CHYX$). It was decided to investigate a series of substituted benzylamines and dibenzylamines in a protonating solvent (TFA) in order to

FIGURE 6. Plot of amino proton shifts of aniline and ring-substituted anilines in CCl_4 versus Hammett σ constants. σ constants of disubstituted anilines are assumed to be additive. Taft polar substituent constants have been used for <u>ortho</u>-substituted anilines.

determine the magnitudes of coupling constants, asymmetry shifts, and isomer population differences for this type of compound.

The equivalence or non-equivalence of rotamer population is established for the series of compounds studied. The predictions of Gutowsky (95) about the effect of substitution upon methylene proton asymmetry are confirmed. Maximum values of the gauche coupling constants and minimum values of the trans coupling constants are established. A qualitative estimate of the relative steric hindrance caused by several substituents is made. There is not sufficient data available to allow the determination of exact values of the vicinal coupling constants and the energy differences between the various isomers.

2. THEORETICAL DISCUSSION

(A) Effect of Energy Levels Upon Rotation Rates About Single Bonds and Upon Relative Populations of Rotational Isomers

Steric hindrance of rotation about single bonds in saturated hydrocarbons has often been considered to be due to van der Waals forces of repulsion between substituents (96). Since this repulsion will generally be greatest when substituents are in eclipsed positions and least when they are in staggered configurations, it is usually assumed that hydrocarbon molecules exist in their three possible staggered configurations. These are often called rotational configurations or rotamers.

The relative populations of rotamers depend solely upon their relative energy levels. A typical energy level plot would have the form shown in Figure 1. The relative populations are given by the Boltzmann equation.

$$\frac{N_i}{N_j} = e^{-\Delta E_{ij}/kT} \quad (i \neq j = 1,2,3) \qquad 3.1$$

An increase in temperature will cause the relative populations to approach equality.

The rotation rate about a single bond depends upon the heights of the energy barriers ($\Delta E_n'$). The rotation rate will increase with increasing temperature because a larger percentage of rotamer molecules will have sufficient energy to jump the barriers. If one of the energy barriers is very high, a rocking motion will occur instead of rotation. Since this normally will have the same effect upon the proton spectrum as rotation, further discussion will be based upon the assumption that rotation occurs about the single bond. If two of the barriers are much higher than the other barrier, then this assumption will no longer be justified.

(B) <u>Effect of Rotation Rate and Rotamer Population Upon Methylene Proton Asymmetry</u>

The conditions which cause methylene proton asymmetry were sometimes misunderstood in the early literature in this field (86,87). The confusion has since been cleared up. Waugh and Cotton (93) and Bishop (94) pointed out a fundamental

FIGURE 1. A typical energy level diagram for rotation about the C-C bond of an ethane-type molecule.

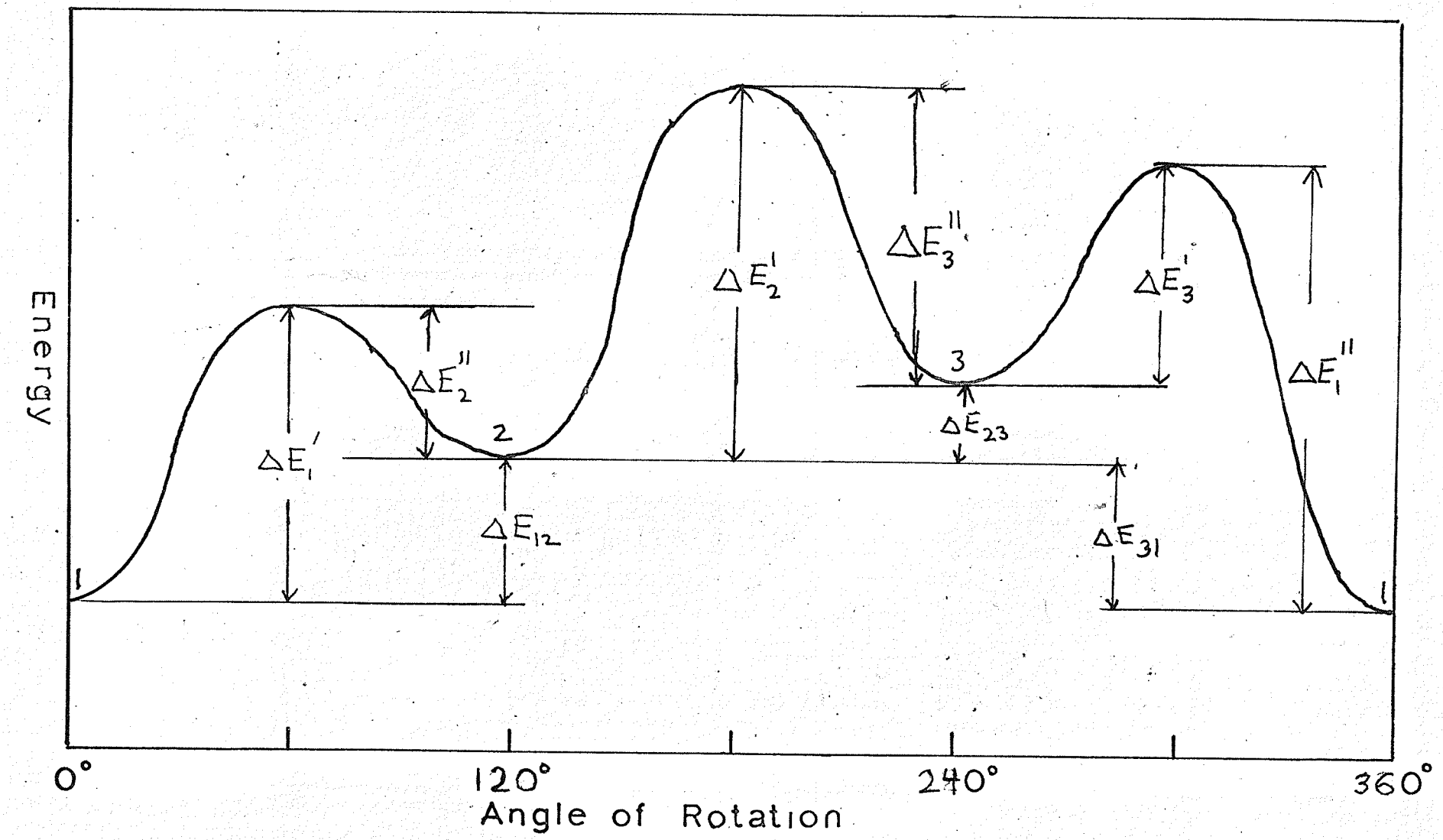
Energy
0°
120°
240°
360°
Angle of Rotation
1
2
3
1
$\Delta E_1'$
$\Delta E_2''$
ΔE_{12}
$\Delta E_2'$
$\Delta E_3''$
ΔE_{23}
ΔE_{31}
$\Delta E_3'$
$\Delta E_1''$

error in the reasoning of previous workers. Gutowsky has established algebraically the minimum substitution required to cause non-equivalence of methylene protons in compounds of the substituted ethane type (95). His treatment will be applied here to the methylene groups of protonated benzylamines. These compounds are analogous to substituted ethanes: ($\emptyset CH_2$-(NHRS)$^+$).

(1) <u>Type 1</u> - Consider a compound of the general type XH_2C-($NRSH_X^1$)$^+$. The possible rotational configurations are shown in Figure 2, using standard diagrams. There are three more possible rotamers which are mirror images of the three shown.

The rotationally averaged proton shifts are

$$\overline{\nu}_A = \sum_n X_n \nu_n^A \qquad \text{and} \qquad \overline{\nu}_B = \sum_n X_n \nu_n^B \qquad 3.2$$

or in general,

$$\overline{\nu}_i = \sum_n X_n \nu_n^i \qquad 3.3$$

where X_n= mole fraction of rotamer n and ν_n^i= the chemical shift of the ith nucleus of rotamer n. The shift of proton H_X is not considered for reasons outlined in the section on results. It can be seen from the configuration diagrams that all three rotamers are identical if X=H. Therefore,

$$\overline{\nu}_A = \overline{\nu}_B = \sum_n \frac{1}{3} \nu_n^A = \sum_n \frac{1}{3} \nu_n^B \qquad 3.4$$

FIGURE 2. The three possible rotamers for a protonated compound of the type XCH_2-$(NRSH)^+$ (Type 1). The methylene carbon atom lies outside the plane of the diagram and the nitrogen atom lies inside the plane of the diagram.

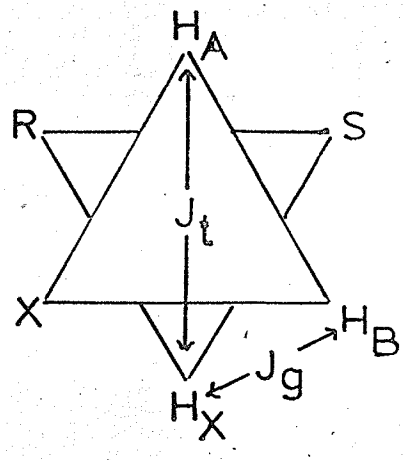

(1)

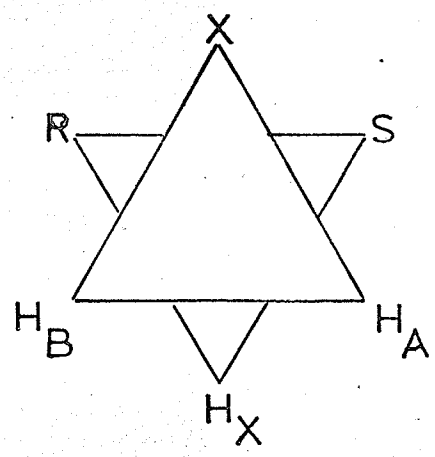

(2)

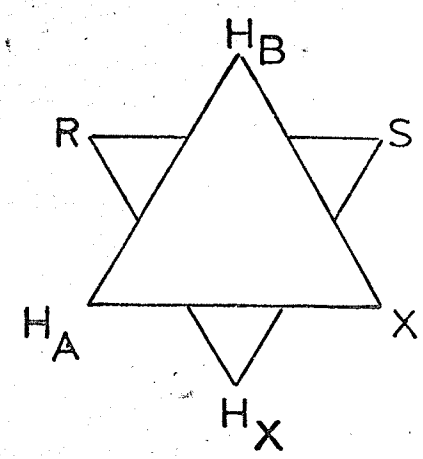

(3)

i.e., $(\overline{\nu_A - \nu_B}) = 0.$

All A and B protons are equivalent only if rapid rotation occurs about the C-N bond axis. Equation 3.4 is obtained by noting that $\nu_1^A = \nu_3^B$, etc. However, there is still an intrinsic asymmetry which would be observed if rotation were stopped, since $\nu_1^A \neq \nu_2^A \neq \nu_3^A$, etc.

If X ≠ H, then three different rotamers are present. The presence of X changes all six proton shifts ν_n^A and ν_n^B. The net result is a chemical shift between H_A and H_B,

$$\overline{\Delta\nu}_H = \sum_n X_n (\nu_n^A - \nu_n^B) = (\overline{\nu_A - \nu_B}). \qquad 3.5$$

This may be rewritten as

$$\overline{\Delta\nu}_H = \sum_n X_n (\Delta\nu_n^0 + \delta\nu_n) \qquad 3.6$$

where $\Delta\nu_n^0$ = the shift between the protons of rotamer n of the parent compound (where X=H) and $\delta\nu_n$ = the change in $\Delta\nu_n^0$ caused by the substitution of X for H. But from equation 3.4 we find that

$$\sum \frac{1}{3}\Delta\nu_n^0 = 0. \qquad 3.7$$

Substitution of this result in equation 3.6 yields

$$\overline{\Delta\nu}_H = \sum_n (X_n - \tfrac{1}{3})\Delta\nu_n^0 + \sum_n \left[(X_n - \tfrac{1}{3})\delta\nu_n + \tfrac{1}{3}\delta\nu_n\right]. \qquad 3.8$$

Equation 3.8 can be rearranged in terms of equation 3.5 to give

$$\Delta\overline{\nu}_H = \sum_n (X_n - \tfrac{1}{3})(\nu_n^A - \nu_n^B) + \sum_n \tfrac{1}{3}\delta\nu_n. \qquad 3.9$$

The first term depends upon relative populations and upon differences in chemical shifts in the three rotamers. The second term depends solely upon the additional shifts caused by the substitution of X for H. This additional shift has been referred to as the asymmetry effect (95).

Equations 3.1 to 3.9 can be used to predict what types of spectra would be expected for type 1 compounds for different populations of rotamers and for different rates or rotation about the C-N bond. There are three basic situations which must be considered. These are: (1) no rotation - slow rotation, (2) rapid rotation with equal rotamer population, (3) rapid rotation with unequal rotamer populations. If the compound does not rotate about the C-N bond, the spectra of the individual rotamers will be obtained, if they are sufficiently populated to be observed. As the rotation rate increases the spectra of the individual rotamers collapse to a single, averaged spectrum. Collapse is complete when the rotation rate exceeds $2\pi(\nu_1^A - \nu_2^A)\,SEC.^{-1}$, etc. The theories of the effects of rotation and chemical exchange upon chemical shifts are essentially identical. The effect of exchange is considered in detail in Chapter 4. Since none of the compounds studied showed evidence of slow rotation about the C-N bond, there will be no further discussion of this possibility.

Equation 3.9 indicates that the methylene protons of type 1 compounds are non-equivalent even when rapid rotation

occurs about the C-N bond. The averaged shift will alter with changing temperature until the populations of the three rotamers are equal. At this point a small shift will remain (the asymmetry effect) which will not alter with increasing temperature. It was originally believed that the methylene protons would become equivalent when populations became equal (87). Cotton and Waugh (93), Bishop (94) and Gutowsky (95) were the first to point out the error in this assumption. The asymmetry effect is a second order effect, which results from different interactions between the various substituent groups. It is impossible to predict the expected value of the asymmetry effect. It is also difficult to obtain experimentally, because equalized populations normally are obtained only at very high temperatures.

(2) <u>Type 2</u> - Type 2 compounds are those with two identical groups bonded to the nitrogen (other than the benzyl group). There are two possibilities: $XH_2C-(NR_2H)^+$ (type 2a) and $XH_2C-(NRH_2)^+$ (type 2b). In terms of the asymmetry of the methyl group they are both of the general type $XH_2C-(NRS_2)^+$ and therefore may be considered together. The diagrams in Figure 3 represent the type 2a rotamers. These can be considered as a trans form (2), referring to X and H_X, and two gauche forms (1 and 3). It can be seen that $\nu_1^A = \nu_3^B$, $\nu_3^A = \nu_1^B$, $\nu_2^A = \nu_2^B$ and $x_1 = x_3$ since rotamers 1 and 3 are sterically equivalent. Substitution of the above relationships into equation 3.2, yields

FIGURE 3. The three possible rotamers for a protonated compound of the type $XCH_2-(NR_2H)^+$ (Type 2a).

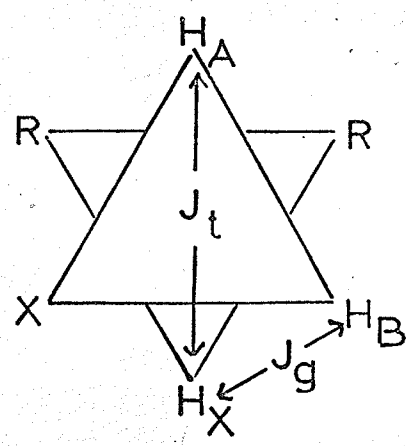

(1)

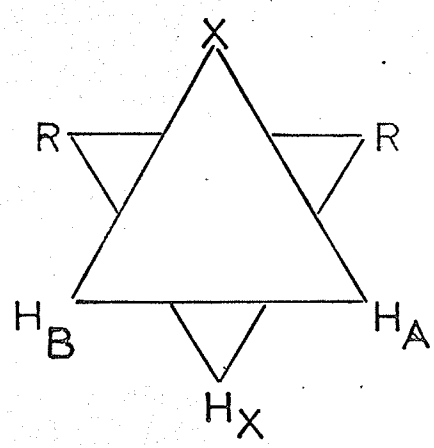

(2)

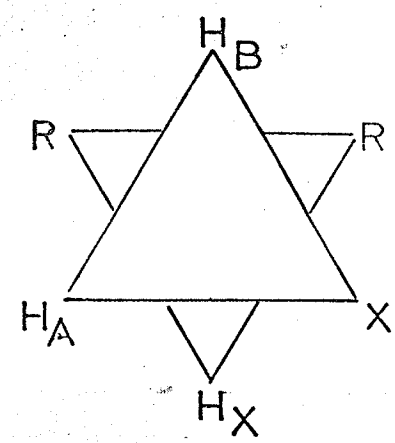

(3)

$$\bar{\nu}_A = \bar{\nu}_B = x_2 \nu_2^A + 2x_1 (\nu_1^A + \nu_1^B) \qquad 3.10$$

or

$$\bar{\nu}_A = \bar{\nu}_B = x_t \nu_2^A + x_g (\nu_1^A + \nu_1^B) \qquad 3.11$$

where $x_g = x_1 + x_3$. Equations 10 and 11 predict that protons H_A and H_B are equivalent, regardless of the relative populations of the trans and gauche rotamers, if rotation is rapid enough to average chemical shifts. The averaged shifts will vary with temperature until rotamer populations are equal, and then will remain constant.

(3) Type 3 - If the $(NRS_2)^+$ group is changed to $(NH_3)^+$ (type 3), it can easily be shown that all rotamers are equivalent and that no shift differences will be found, regardless of the rate of rotation about the C-N bond.

From the above discussion it can be seen that only type 1 compounds show methylene proton asymmetry when rapid rotation occurs about the C-N bond. This asymmetry persists even for free rotation (equal populations). The methylene protons of type 2 and type 3 compounds are always equivalent when rotation is rapid enough to average the differences in shift of the individual rotamers. Therefore, methylene proton asymmetry occurs when three different groups, other than the benzyl group under observation, are bonded to the nitrogen atom. In other words, the necessary condition for methylene proton

asymmetry is the absence of a plane of symmetry along the C-N bond axis. Complete nitrogen asymmetry is a sufficient condition but not a necessary condition since some substituted dibenzylamines should show methylene proton asymmetry. For example, protonated N-methyldibenzylamine should show methylene proton asymmetry because it has three different groups, other than the benzyl group under consideration, bonded to the nitrogen: $(C_6H_5\text{-}CH_2\text{-}N(CH_3)(C_6H_5CH_2)(H^+))$. There is no plane of symmetry along the $C_6H_5CH_2\text{-}N$ bond. Thus the methylene protons will be asymmetric even though the nitrogen atom is not asymmetric.

(C) <u>Effect of Rotamer Population and Rotation Rate Upon Proton Coupling Constants</u>

There are two basic types of coupling constants between methylene protons and ammonio protons of molecules in staggered configurations: J_{gauche} (J_g) and J_{trans} (J_t). The values of J_g and J_t will vary slightly for the different rotamers for the same reason that there is an asymmetry effect. It is normally assumed that all values of each type of coupling constants within a given molecule are equal (97). It is known that trans and gauche F-F coupling constants can vary by as much as 4 c/s within a given molecule (98,92). The constancy of the different trans and gauche H-H coupling constants within a given ethane-type molecule has apparently never been measured.

It has been suggested that F-C-C-F coupling constants are determined by a "through space" mechanism which principally involves non-bonded F-F interactions (99). On the other hand, H-H coupling constants are believed to depend upon the electron distribution in the intervening bonds (100). If these theories are correct, then vicinal H-H coupling constants should be determined largely by the electronegativity of the substituents while vicinal F-F coupling constants should be determined largely by steric effects which alter the separation of the fluorine atoms. Since steric factors probably cause different F-F distances in the various rotamers, it is quite possible that vicinal fluorine coupling constants are less constant within a given molecule than the corresponding proton coupling constants. In any case, it will be assumed that the values of J_g and J_t are the same for all the rotamers of a given molecule. It is necessary to make this assumption, since without knowledge of the energy levels of the three rotamers, it is impossible to determine the constancy of J_g and J_t (92).

From the previous equations and diagrams, it is possible to predict the effect of population changes upon proton coupling constants.

(1) <u>Type 1</u> - This type of compound is expected to give an ABX spectrum for the methylene protons and the ammonio proton with the methylene protons being A and B. The AB

coupling constant is measurable. It should be nearly independent of rotation rate since geminal coupling constants of saturated carbon atoms depend upon molecular geometry (100). A slight change in J_{AB} can occur if sufficient steric hindrance is present to cause a change in geometry as the rotation rate changes.

The possible values of $\overline{J}_{AX}$ and $\overline{J}_{BX}$ can be obtained from the rotamers illustrated in Figure 2. For fast rotation, the averaged coupling constants are:

$$\overline{J}_{AX} = x_1 J_t + (x_2 + x_3) J_g \qquad 3.12$$

$$\overline{J}_{BX} = (x_1 + x_2) J_g + x_3 J_t. \qquad 3.13$$

The difference between the two coupling constants depends only upon the relative mole fractions of rotamers 1 and 3 and the values of J_g and J_t.

$$\overline{J}_{AX} - \overline{J}_{BX} = (x_1 - x_3)(J_t - J_g). \qquad 3.14$$

In general, $\overline{J}_{AX} \neq \overline{J}_{BX}$ except by coincidence (when $x_1 = x_3$). If it is assumed that J_g and J_t are constant, then it is possible to determine the relative populations and consequently the relative stability of the two rotamers. As populations approach equality, both $\overline{J}_{AX}$ and $\overline{J}_{BX}$ approach a limiting value of $(2/3\ J_g + 1/3\ J_t)$. Inequality of $\overline{J}_{AX}$ and $\overline{J}_{BX}$ definitely indicates unequal rotamer populations. Equality of $\overline{J}_{AX}$ and $\overline{J}_{BX}$ indicates that $x_1 = x_3$ and that possibly all populations are

equal. The situation where $x_1 = x_3 \neq x_2$ might exist if the steric effects due to R and S were approximately equal, because there would then be little energy difference between rotamers 1 and 3. This corresponds to type 2a discussed below.

(2) Type 2a - Compounds of this type should give A_2X spectra when rapid rotation occurs about the C-N bond axis. Since the methylene protons are equivalent, it is impossible to measure the geminal coupling constant (101).

The values of $\overline{J}_{AX}$ and $\overline{J}_{A'X}$ can be obtained from Figure 3 ($H_{A'} \equiv H_B$ in Figure 3). The rotationally-averaged coupling constants are:

$$\overline{J}_{AX} = X_1 J_t + (X_2 + X_3) J_g = \frac{X_g}{2} J_t + \left(1 - \frac{X_g}{2}\right) J_g \qquad 3.15$$

$$\overline{J}_{BX} = X_3 J_t + (X_1 + X_2) J_g = \frac{X_g}{2} J_t + \left(1 - \frac{X_g}{2}\right) J_g . \qquad 3.16$$

The averaged coupling constants are therefore equal. The magnitudes of $\overline{J}_{AX}$ and $\overline{J}_{A'X}$ will vary with relative populations up to a limiting value of $(2/3\ J_g + 1/3\ J_t)$.

(3) Type 2b - The rotamers for compounds of this type are shown in Figure 4. It can be seen from the diagram that $\overline{J}_{AX} \equiv \overline{J}_{A'X'}$ and $\overline{J}_{A'X} \equiv \overline{J}_{AX'}$ since rotamers 1 and 3 are sterically equivalent. Taking into account that there are two coupling constants of each type per rotamer, the averaged values of the coupling constants are:

$$\overline{J}_{AX} = \frac{(1+x_2)J_g + (x_1+x_3)J_t}{2} = \frac{(1+x_t)J_g + x_g J_t}{2} \qquad 3.17$$

$$\overline{J}_{A'X} = (x_1+x_3)J_g + x_2 J_t = x_g J_g + x_t J_t . \qquad 3.18$$

In general, $\overline{J}_{AX} \neq \overline{J}_{A'X}$. Both will alter with temperature up to a limiting value of ($2/3\ J_g + 1/3\ J_t$) when populations are equal.

Experimentally, the sums and differences of $\overline{J}_{AX}$ and $\overline{J}_{A'X}$ are measured. These two variables have the following values:

$$\overline{J}_{AX} + \overline{J}_{A'X} = \left(1 + \frac{x_g}{2}\right) J_g + \left(1 - \frac{x_g}{2}\right) J_t \qquad 3.19$$

$$\overline{J}_{AX} - \overline{J}_{A'X} = \left(x_t - \frac{x_g}{2}\right)(J_t - J_g) . \qquad 3.20$$

If it is assumed that the gauche rotamers are sterically less favorable than the trans rotamer, then it is found that ($\overline{J}_{AX} - \overline{J}_{A'X}$) varies by ($J_t - J_g$) when the relative rotamer populations change from $x_t = 1$ to $x_t = 1/2\ x_g$. ($\overline{J}_{AX} + \overline{J}_{A'X}$) varies by only $1/3\ (J_t - J_g)$ for the same change in relative populations. Consequently the measured difference in coupling constants should be more temperature dependent than the sum of the coupling constants for type 2b molecules. The limiting values for the two variables are 0 for ($\overline{J}_{AX} - \overline{J}_{A'X}$) and ($4/3\ J_g + 2/3\ J_t$) for ($\overline{J}_{AX} + \overline{J}_{A'X}$).

FIGURE 4. The three possible rotamers for a compound of the type $XCH_2-(NRH_2)^+$ (Type 2b).

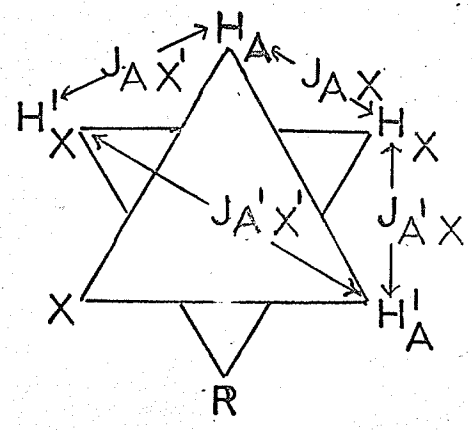

(1)

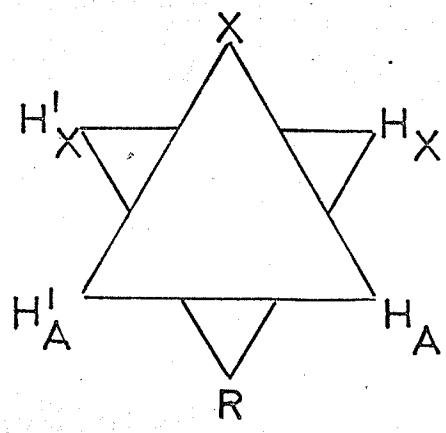

(2)

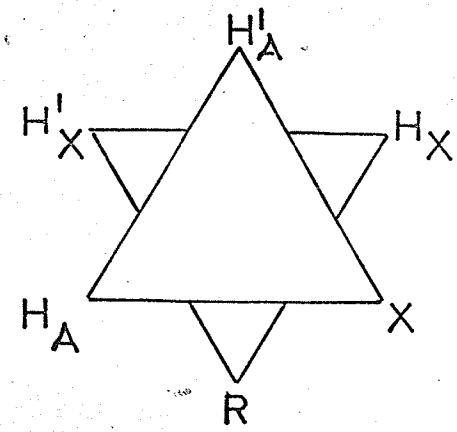

(3)

(4) Type 3 - Regardless of temperature, rotation rate, etc., a single, averaged value of $(2/3\ J_g + 1/3\ J_t)$ will be obtained for $\overline{J}_{AX}$.

The most notable feature of the effect of temperature upon coupling constants is the constancy of the limiting value of the average coupling constants obtained for the three types of molecules. In Type 2 compounds the methylene protons are equivalent and changes in chemical shift can only be measured relative to a reference signal. However, definite values of coupling constants can always be obtained. Definite values of coupling constants are preferable to relative values of chemical shifts since there is always uncertainty whether the reference and/or the methylene protons may show additional shifts due to factors other than changes in rotamer populations as the temperature changes.

(D) Effect of Proton Exchange Upon Methylene Proton Asymmetry and Observed Coupling Constants.

Exchange alters the shape of the observed methylene proton spectrum by two mechanisms. Firstly, exchange between the protonated and unprotonated forms of the substituted benzylamine produces an averaged methylene proton spectrum. Experimental evidence will be presented in Chapter 4 which shows that aniline in TFA is almost completely protonated. Benzylamines are stronger bases and should be even more completely protonated in solution. Since the concentration of

free base is much smaller than that of the protonated base, the observed spectrum should be little different than that of protonated benzylamine in the absence of exchange (see equation 4.89). Secondly, the exchange of a proton bonded to a nitrogen atom may be accompanied by an inversion of the nitrogen atom valences. This inversion effectively interchanges the A and B protons of the methylene group of a type 1 molecule. Consequently exchange will cause the AB spectrum to collapse to an A_2 spectrum since the protons become indistinguishable. If the lifetime of unprotonated benzylamine in solution is long compared to the time taken for rearrangement of the nitrogen valences, then every second exchange will invert the nitrogen atom valences.

Exchange will also alter the observed values of $\bar{J}_{AX}$ and $\bar{J}_{BX}$. As the X proton exchanges, there is an increasing uncertainty about the X proton spin alignment. Only every second exchange will result in an interchange of the X proton spin.

(E) <u>Analysis of A_2X, ABX and A_2X_2 Proton Spectra When the X Proton Spectra are Unmeasurable.</u>

The X (ammonio) proton spectra of protonated benzylamines do not yield any useful information, for reasons discussed later. Consequently, the amount of useful information which can be obtained is limited.

(a) A_2X and A_3X spectra - Only the AX coupling constant

can be obtained. J_{AA} is not observable when the two protons are equivalent (101).

(b) ABX spectra - The AB part of an ABX spectrum consists of two quartets. The quartets are easily identified since they contain four spacings equal to J_{AB}. Since the X part of the spectrum cannot be measured, the spectrum cannot be analyzed. However, if it is assumed that $\bar{J}_{AX}$ and $\bar{J}_{BX}$ have the same sign, then it is possible to obtain absolute values of $\bar{J}_{AX}$, $\bar{J}_{BX}$, and the chemical shift. This is a reasonable assumption since it has been shown that the vicinal coupling constants in substituted ethanes have the same sign (89, 91,102). The values of $1/2\ |\bar{J}_{AX}+\bar{J}_{BX}|$ and $1/2\ |\bar{J}_{AX}-\bar{J}_{BX}|$ can be obtained from the spectrum (103). There are two possible values of the latter term, depending upon whether the defined constants $D^{+} \cos 2\theta^{+}$ and $D^{-} \cos 2\theta^{-}$ (103) have the same or opposite signs. Only one of the two possible values will give $|\bar{J}_{AX} + \bar{J}_{BX}| > |\bar{J}_{AX} - \bar{J}_{BX}|$. The above relationship must hold if $\bar{J}_{AX}$ and $\bar{J}_{BX}$ have the same sign. The chemical shift can also be obtained from the expressions defining $D^{+} \cos 2\theta^{+}$ and $D^{-} \cos 2\theta^{-}$. The signs of J_{AB}, $\bar{J}_{AX}$, and $\bar{J}_{BX}$ cannot be obtained. It is also impossible to decide which coupling constant is $\bar{J}_{AX}$ and which is $\bar{J}_{BX}$.

(c) A_2X_2 spectra - The theory of A_2X_2 spectra has been developed in general (104) and also for the specific case of

disubstituted ethanes with unequal rotamer populations (91, 92). The coupling constants are defined as shown in Figure 4. It is convenient to define the following quantities:

$$K = J_{AA'} + J_{XX'} \qquad 3.21$$

$$L = \overline{J}_{AX} - \overline{J}_{A'X} \qquad 3.22$$

$$M = J_{AA'} - J_{XX'} \qquad 3.23$$

$$N = \overline{J}_{AX} + \overline{J}_{A'X} \qquad 3.24$$

If $K \gg L$ and $M=0$, then the methylene proton spectrum will consist of five peaks: an intense doublet with spacing equal to N and a triplet whose outside peaks are L c/s apart. Both spectral groupings have the same centre of gravity. As L increases with respect to K, the central line of the triplet splits into a doublet. If $M \neq 0$, then the outside peaks of the triplet are split into doublets. The spacing from center to center of the two doublets is equal to $(M^2 + L^2)^{\frac{1}{2}}$ and the doublet spitting is equal to M. If L is small or M is large, the total spectrum collapses to a triplet. Only the value of N can definitely be obtained from an A_2X_2 spectrum.

3. EXPERIMENTAL

Eleven different protonated benzylamines were investigated. In three cases no useful results were obtained. All solutions

contained 5 mole per cent of the benzylamine being investigated and 2 mole per cent of cyclohexane as an internal reference. Trifluoracetic acid (TFA) was used as a protonating solvent. All chemicals were Eastman White Label grade and were used without further purification.

Proton resonance spectra were measured at 60 Mc/s on a Varian DP -60 spectrometer. Samples were degassed and sealed in thick-walled 5 mm glass sample tubes. Spectra were obtained at different temperatures with the aid of a variable temperature probe manufactured at NRC (105). Sample temperatures were measured by a copper-constantan thermocouple attached to a Varian G-11 recording potentiometer. The temperature measurements are believed accurate to within 2° K. Peak separations were measured by sideband techniques, using a Hewlett-Packard 521C frequency counter. All results are the average of at least six measurements.

The temperature range was limited by the high freezing points of the solutions and by their high volatility.

4. RESULTS

The calculated chemical shifts and coupling constants are given in Table I. The measured shifts of the centers of gravity of the methylene groups relative to internal cyclohexane are given in Table 2. Since these shifts do not appear to vary in any meaningful manner as temperature changes, they will not be further discussed.

Rapid proton exchange between N-N-dibenzylethylenediamine and TFA collapsed the methylene proton spectrum of that compound below room temperature, preventing the observation of coupling constants. Proton exchange also collapsed the methylene proton spectra of N-ethyl-N-phenylbenzylamine and N-phenyldibenzylamine at temperatures above room temperature.

Separate peaks were observed for the benzyl and ethyl protons of N-ethyl-N-phenylbenzylamine and 2-benzylamino-6-methylheptanol-6. Presumably, the anisotropy of the phenyl groups caused a low field shift of the benzyl methylene protons relative to the ethyl methylene protons (106). However, in the spectra of N-benzylethanolamine and N-benzyldiethanolamine, the ethyl and benzyl methylene protons overlapped, rendering these compounds useless for investigation.

Four main types of methylene proton-ammonio proton spectra were observed. Since the methylene protons resonated at more than 4 ppm to high field of the ammonio protons, the types of spectra can be classified as A_2X, A_3X, A_2X_2, and ABX. Typical spectra are shown in Figures 5 to 8. The analysis of the spectra was complicated by the fact that the ammonio proton spectra always consisted of single broad peaks. A combination of slow proton exchange and N^{14} quadrupole relaxation presumably caused the collapse of the X proton spectra. The analysis of the types of spectra mentioned above has been discussed in the theoretical introduction.

FIGURE 5. Reproduction of the methylene proton spectrum of protonated N-methyldibenzylamine. This is the AB part of an ABX spectrum (Type 1).

FIGURE 6. Reproduction of the methylene proton spectrum of protonated N,N-dimethylbenzylamine. This is the A_2 part of an A_2X spectrum (Taype 2a).

FIGURE 5

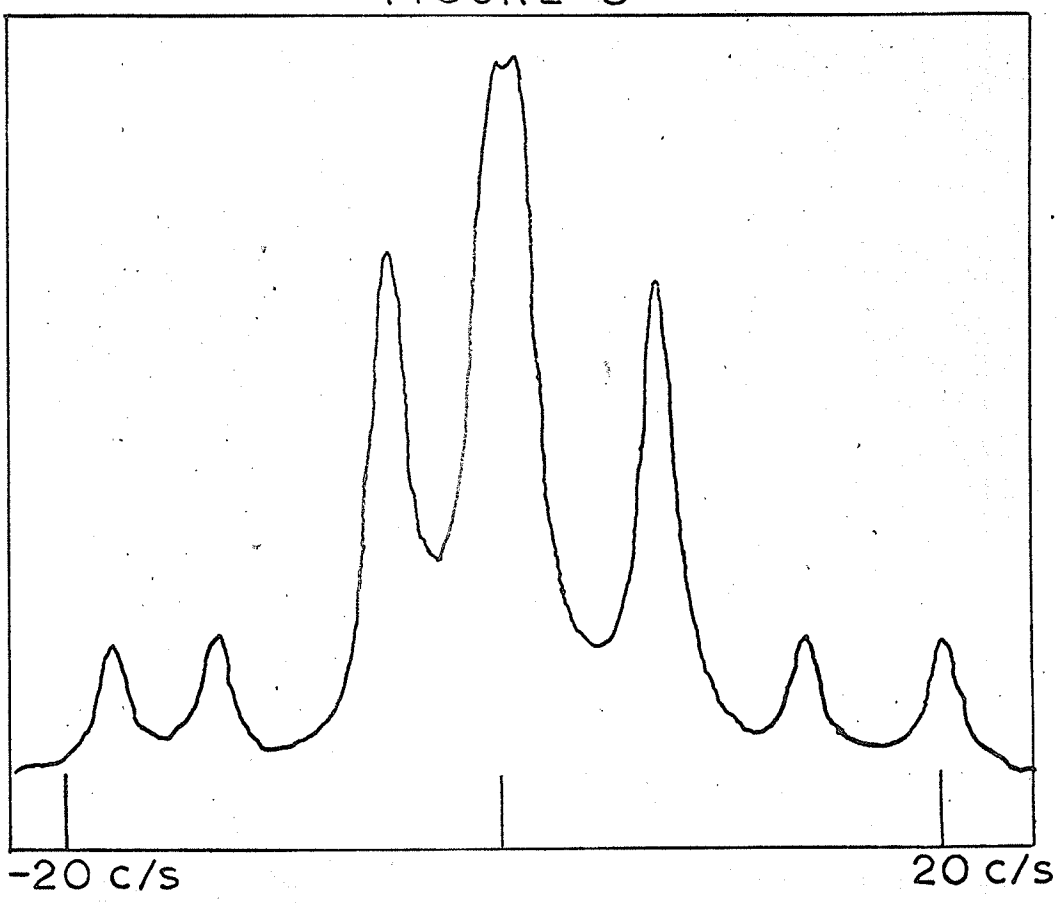

FIGURE 6

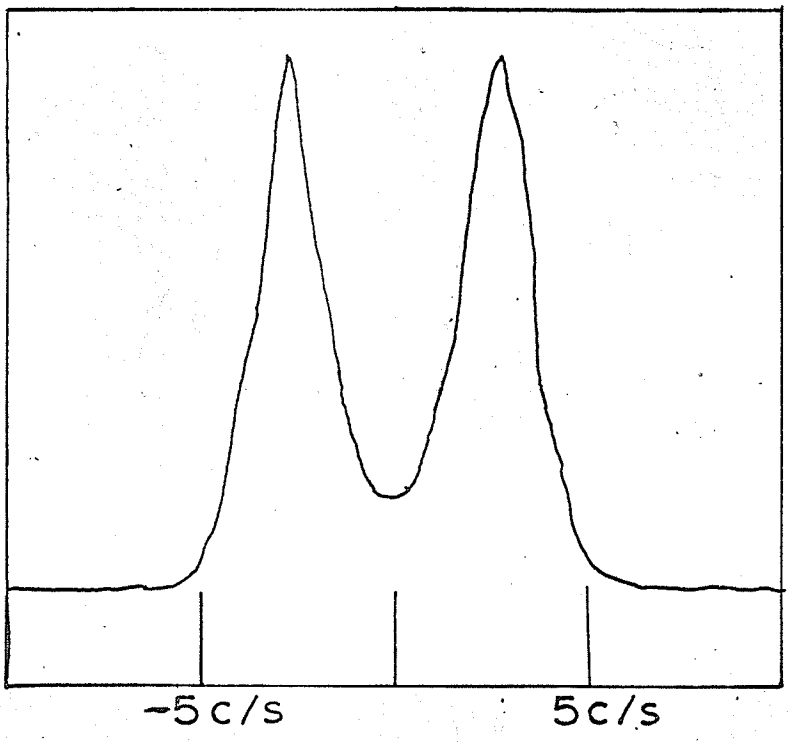

FIGURE 7. Reproduction of the methylene proton spectrum of protonated N-isopropylbenzylamine. This is the A_2 part of an A_2X_2 spectrum (Type 2b).

FIGURE 8. Reproduction of the methylene proton spectrum of protonated dibenzylamine. This is the A_2 part of an A_2X_2 spectrum (Type 2b).

FIGURE 7

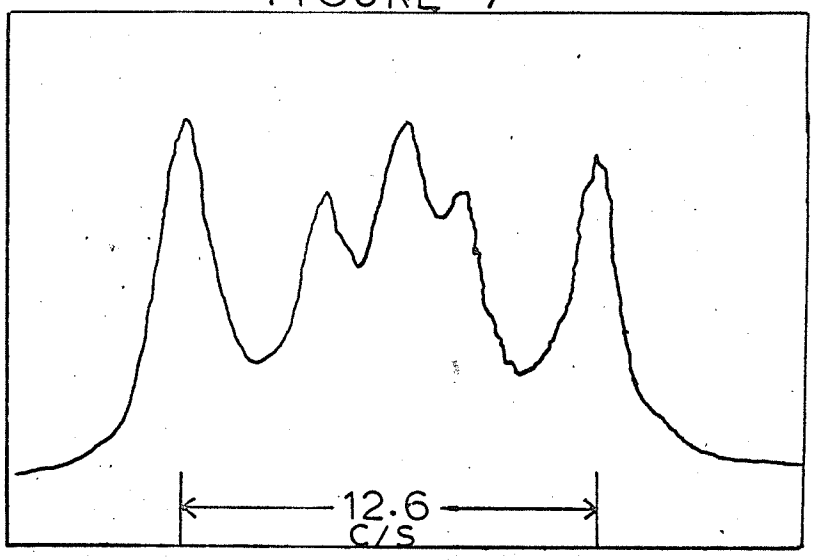

FIGURE 8

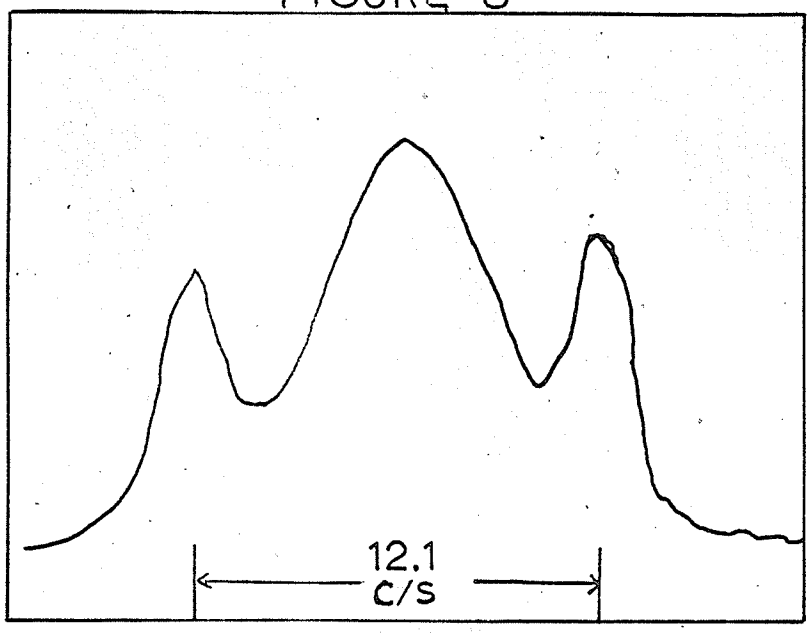

The estimated errors in measurements are given in Tables I and II. In the case of ABX spectra, the derived values of chemical shift and coupling constants are not as accurately known as other values of coupling constants since they are obtained by the differences of other derived values.

Two major factors limited the accuracy of the measurements. The individual peaks were quite broad due to the high viscosities of the solutions. Also, the thick-walled sample tubes and the temperature probe reduced the sensitivity of the spectrometer so much that it was difficult to obtain signals. (The sensitivity of the spectrometer has since been increased by a factor of 2 in the signal to noise ratio). The benzylamine concentration used represented a compromise between too much viscosity broadening and too little signal amplitude. The solution of 2-benzylamino-6-methylheptanol-6 was so viscous that the spectrum could not be accurately measured at room temperature.

5. DISCUSSION OF RESULTS

(A) Effect of Proton Exchange

Rapid proton exchange caused the methylene proton spectrum of protonated N,N-dibenzylethylenediamine to collapse to a single peak, below room temperature. Collapse of the methylene proton spectra of N-ethyl-N-phenyldibenzylamine and

N-phenyldibenzylamine occurred at elevated temperatures. Since proton exchange alters the observed coupling constants and chemical shifts, it was considered necessary to determine whether or not appreciable ammonio proton exchange was occurring in the other solutions studied.

Benzylamines should be stronger bases than aniline. Consequently, the activation energies of proton exchange should exceed 25 kcal/mole (see Chapter 4). Therefore, the collapse of the methylene proton spectra should occur over a narrow temperature range. Depending upon the peak separations, the spectra should collapse over a temperature range of 15 to 30° K. This can be shown in the following way: the rate of collapse of a doublet as a result of exchange is approximately given by (107)

$$\frac{\text{Separation of peaks}}{\text{Separation of peaks for large } \tau} = \left[1 - \frac{1}{2\pi^2\tau^2(\nu_A - \nu_B)^2}\right]^{\frac{1}{2}}. \qquad 3.25$$

τ = lifetime of protonated molecule in seconds.

For two peaks 10 c/s apart, the calculated separations are respectively 9.94, 9.75, 8.93, 4.36, and 0.00 c/s for exchange rates of 5.0, 10.0, 20.0, 40.0 and 44.4 exchanges/second. If the activation energy of exchange is 25 Kcal/mole and if exchange takes place at a temperature of 330°K, then the exchange rate will change from 4.4 to 44 exchanges/second over

a temperature range of approximately 22°K.

It is interesting to note that equation 3.25 predicts that there is little change in measured peak separations at low exchange rates. Consequently, only the measurements at the highest temperatures are likely to be in error since if appreciable exchange were occurring at lower temperatures, the methylene proton spectra would be completely collapsed at higher temperatures.

Exchange causes a broadening of the spectral peaks as well as a decrease in peak separation. Such behaviour was not noticed for any solutions other than the three mentioned, even at the highest temperatures. However, this was not considered sufficient evidence to exclude the possibility of exchange. Additional evidence for the absence of appreciable exchange was provided by the two compounds containing N-methyl groups. These formed type 3 groupings due to rotation about the N-CH_3 bonds. In both cases the H-N-C-H coupling constants were temperature independent, as would be expected for type 3 groupings in the absence of exchange.

Of all the monoamino compounds studied, only those with a phenyl group bonded directly to the nitrogen atom showed evidence of appreciable proton exchange. Presumably, the withdrawal of electrons from the nitrogen atom by the phenyl group increased the acid strength of the ammonio group to such an extent that appreciable proton exchange occurred at higher

temperatures. The methylene proton spectra of N-ethyl-N-phenyldibenzylamine and N-phenylbenzylamine were only partly collapsed at 50°C. Because the collapse occurred over a narrow temperature region and because no evidence of proton exchange at room temperature was noted for either of the two compounds, it is assumed that the room temperature results for protonated N-ethyl-N-phenylbenzylamine and N-phenyldibenzylamine are reliable.

(B) Type I Compounds

All three compounds contain non-equivalent methylene protons. Protonated N-phenyldibenzylamine and N-methyldibenzylamine contain symmetric nitrogen atoms while protonated N-ethyl-N-phenylbenzylamine does not. All lack a plane of symmetry along the benzyl-nitrogen bond. This confirms the conclusion reached in the theoretical introduction that the absence of a plane or axis of symmetry along the bond axis is the sufficient condition for methylene proton asymmetry.

The chemical shifts between the methylene protons are small in all three compounds. In the case of N-methyldibenzylamine, the shift decreases when the temperature is increased, but appears to level off at higher temperatures. However, this cannot be true. If rotamer populations are equal at 407°K, then $\overline{J}_{AX}$ and $\overline{J}_{BX}$ should be equal (see equations 12 and 13). The non-equivalence of $\overline{J}_{AX}$ and $\overline{J}_{BX}$ in all three compounds

indicates that the rotamer populations are unequal in all three compounds. Presumably, the asymmetry shift would be found to be quite small if it could be determined. This is not surprising since the asymmetry shift arises from second order effects.

$|J_{AB}|$ has values of 12.75 ± 0.1, 12.95 ± 0.1, and 13.0 ± 0.2 c/s for N-ethyl-N-phenylbenzylamine, N-phenyldibenzylamine, and N-methyldibenzylamine respectively. Thus $|J_{AB}|$ is essentially constant for the three compounds. Karplus has calculated that $|J_{AB}| = 12.85$ for H-C-H bonds when the carbon valences are in a tetrahedral configuration (100). The agreement is quite good, suggesting that steric hindrance does not force the methylene carbon atom out of its tetrahedral configuration. It is probable that J_{AB} is negative and that $\overline{J}_{AX}$ and $\overline{J}_{BX}$ are positive, since the corresponding coupling constants in substituted ethanes have those signs (108).

As shown by equation 14, the difference between $\overline{J}_{AX}$ and $\overline{J}_{BX}$ is determined by the difference in mole fraction of rotamers 1 and 3. If it is assumed that J_g and J_t are the same for all three compounds, then it is possible to estimate the relative amounts of steric hindrance caused by the various substituents. It has been shown that the size of vicinal proton coupling constants in polyhaloethanes depend upon the electronegativity of the substituents (92,109,110). Since in all three compounds three carbon atoms are bonded to a

nitrogen atom, J_g and J_t probably do not alter appreciably from compound to compound. The bonding of a phenyl group to a nitrogen atom may cause some change in J_g and J_t since the bonding carbon atom is trigonally hybridized.

In all three compounds, rotamer 2 would be expected to be energetically least favoured since in this rotamer a phenyl group (X) is adjacent to two other bulky substituents (see Figure 2). The non-equivalence of $\overline{J}_{AX}$ and $\overline{J}_{BX}$ in N-methyldibenzylamine is presumably due to the fact that the benzyl groups are bulkier than the methyl group. The non-equivalence of the vicinal coupling constants in the other two type 1 compounds is most reasonably explained by assuming that the phenyl group causes more steric hindrance than either the ethyl or the benzyl group. If it is assumed that the phenyl group causes less steric hindrance than the other two groups, then one must conclude that it also causes less steric hindrance than the methyl group. This does not seem reasonable. Since the coupling constants of N-phenyldibenzylamine and N-ethyl-N-phenylbenzylamine are nearly identical, the ethyl and the benzyl groups must cause approximately the same amount of steric hindrance. Consequently one concludes from the differences between $\overline{J}_{AX}$ and $\overline{J}_{BX}$ for the three compounds that the steric hindrance of the substituents decreases in the following order: phenyl $>$ benzyl $\approx$ ethyl $>$ methyl. This order seems quite reasonable. This suggests that the assumption

that J_g and J_t do not alter from compound to compound is at least approximately correct.

The value of the H-N-CH_3 coupling constant of N-methyldibenzylamine is 5.25 ± 0.15 c/s. The constancy of the coupling constant confirms that no appreciable proton exchange occurs in the temperature range which is used. Since this is a type 3 grouping, 5.25 c/s should represent the value of $|2/3\ J_g + 1/3\ J_t|$. If the value of another combination of J_g and J_t could be obtained, then the values of J_g and J_t could be obtained algebraically.

(C) Type 2a Compounds

The value of the vicinal coupling constant of protonated N,N-dimethylbenzylamine changes very little over a temperature range of 90°K and is only slightly larger than the expected value when rotamer populations are equal. This indicates that the methyl groups cause only a slight hindrance of rotation about the C-N bond. The observed value of the H-N-CH_3 coupling constant is 5.25 c/s. It is independent of temperature. Therefore no appreciable ammonio proton exchange can be occurring in the temperature range studied.

The results for tribenzylamine are difficult to understand. The vicinal coupling constant is almost temperature independent and is identical, within experimental error, to the two values obtained for $|2/3\ J_g + 1/3\ J_t|$. This indicates

that all three rotamers have nearly equal energies and populations. It is difficult to visualize why a phenyl group situated between two benzyl groups should not be in a sterically less favorable position than a phenyl group adjacent to only one benzyl group. However, the results indicate that the two positions are equivalent.

The shifts of the methylene protons, relative to cyclohexane, do not change significantly as the temperature changes. Therefore, no conclusions can be drawn about the effect of changing rotamer population upon chemical shift.

The equivalence of the methylene protons in type 2 compounds confirms that the absence of an axis or plane of symmetry along the C-N bond axis is the necessary condition for methylene proton asymmetry.

(D) Type 2b Compounds

The methylene protons of the three compounds of this type give five line spectra corresponding to the A_2 parts of A_2X_2 spectra. The triplet splitting is measurable only in the spectrum of N-isopropylbenzylamine. In the spectra of dibenzylamine and 2-benzylamino-6-methylheptanol-6 the central peaks of the methylene proton spectra are broadened rather than split into distinct triplets. The spacing of the outside peaks of the triplet is equal to $M + (M^2 + L^2)^{\frac{1}{2}}$. If $M=0$, then values of $\overline{J}_{AX}$ and $\overline{J}_{A'X}$ can be obtained from the sums

and differences of the two coupling constants. It is difficult to determine whether geminal H-C-H and H-N-H coupling constants should be the same when both atoms are quadrivalent. Grant has shown that the size of the geminal H-C-H coupling depends upon the extent of π bonding between the carbon atom and substituents attached to it (111). It has also been shown that the size of vicinal coupling constants depends upon the electronegativity of substituents present in the molecule (92,109,110). Therefore, it is unlikely that M=0 in the compounds studied. All that can be stated with certainty is that the value of the triplet splitting represents an upper limit of L. The value of the triplet splitting changes more rapidly with temperature than the value of the doublet splitting. It was shown in the theoretical introduction that L should change three times as fast as M as temperature changes.

The value of N for N-isopropylbenzylamine appears to be temperature independent. N changes with temperature for dibenzylamine and is in general lower than the value of N for N-isopropylbenzylamine. This implies that the isopropyl group causes more steric hindrance than the benzyl group. This is not surprising when one notes that the results for type 1 compounds indicated that the benzyl and ethyl groups cause approximately equal amounts of steric hindrance.

The value of N for 2-benzylamino-6-methylheptanol-6

is independent of temperature within the limits of experimental error. It is slightly lower than the corresponding value for N-isopropylbenzylamine.

In all cases the rotamer populations must be unequal since N is always smaller than the expected value for equal populations ($|4/3\ J_g + 2/3\ J_t| = 10.5$ c/s).

(E) Possible Values of $|J_g|$ and $|J_t|$

If the energy difference between trans and gauche rotamers of a type 2b compound becomes very large, then most of the compound should exist as the trans rotamer (see Figure 4). If one assumes that protonated N-isopropylbenzylamine exists solely as the trans rotamer at room temperature, then $|J_g+J_t| = 12.6$ c/s. Using this value and the previously obtained value of $|2/3\ J_g + 1/3\ J_t|$, it can then be calculated that $|J_g| = 3.15$ c/s and $|J_t| = 9.45$ c/s. These values represent an upper limit of $|J_g|$ and a lower limit of $|J_t|$ since the actual value of $|J_g+J_t|$ may be larger than 12.6 c/s. J_g has been found to have values between 1.0 and 3.5 c/s in substituted ethanes while J_t has values between 10 and 18 c/s (89,91). Therefore, the estimated vicinal coupling constants for protonated benzylamines do not seem unreasonable.

It is possible to use values of $|J_g|$ and $|J_t|$ to calculate energy and population differences for the various rotamers. However, these values would be highly questionable, considering

the number of assumptions involved. Therefore, calculations of this type were not carried out.

6. SUMMARY AND CONCLUSIONS

(1) It has been shown theoretically and experimentally that the necessary and sufficient condition for methylene proton asymmetry in protonated benzylamines is the absence of a plane of symmetry along the $C_6H_5CH_2$-N bond axis.

(2) Rotamer populations are unequal for all compounds except protonated tribenzylamine.

(3) The maximum value of $|J_g|$ in protonated benzylamines is 3.15 c/s. The minimum value of $|J_t|$ is 9.45 c/s.

(4) The steric hindrance caused by the various substituents decreases in the following order:

$$\left.\begin{matrix}\text{isopropyl}\\ \text{phenyl}\end{matrix}\right\} > \text{benzyl} \approx \text{ethyl} > \text{methyl}$$

It cannot be decided from the experimental evidence whether the phenyl group or the isopropyl group causes greater steric hindrance.

TABLE I

Coupling Constants and Internal Chemical Shifts of the Methylene Protons of Substituted Benzylamines in TFA

(A) TYPE I COMPOUNDS

Compound	Temperature (°K)	Chemical Shift (c/s)	Coupling Constants (c/s) $\lvert J_{AB}\rvert$	$\lvert J_{AX}, J_{BX}\rvert$	$\lvert J_{H_X-CH_3}\rvert$
N-methyldibenzylamine	299± 2	14.8±0.2	12.85±0.15	6.5, 4.4±0.2	5.2±0.1
	305	14.9	13.05	6.6, 4.4	5.3
	317	14.75	13.0	6.5, 4.45	5.2
	325	14.6	13.1	6.55,4.6	5.35
	339	14.4	13.1	6.55,4.55	5.3
	353	14.2	13.2	6.45,4.65	5.2
	379	14.25	13.1	6.4, 4.55	5.15
	393	14.2	13.1	6.3, 4.55	5.3
	407	14.3	12.9	6.05,4.55	5.2
N-phenyldibenzylamine	298	12.1±0.2	12.95±0.1	7.85,3.75±0.2	-
N-ethyl-N-phenylbenzylamine	298	13.5±0.2	12.75±0.1	7.6, 3.65±0.2	-

(B) TYPE 2a COMPOUNDS

Compound	Temperature	Coupling Constants (c/s) $\lvert J_{AX}\rvert$	$\lvert J_{H_X-CH_3}\rvert$
N,N-dimethylbenzylamine	299±2	5.57±0.1	5.14±0.1
	309	5.58	5.30
	321	5.52	5.23
	335	5.50	5.28
	347	5.50	5.28
	372	5.48	5.26
	388	5.47	5.36

TABLE I CONTINUED

Compound	Temperature	Coupling Constants (c/s) $\lvert J_{AX} \rvert$	$\lvert J_{H_X-CH_3} \rvert$
Tribenzylamine	298	5.3 ±0.1	-
	323	5.22 ±0.1	-
	353	5.24 ±0.1	-
	382	5.19 ±0.1	-

(C) TYPE 2b COMPOUNDS

Compound	Temperature	Coupling Constants (c/s) $\lvert J_{AX}+J_{A'X} \rvert$	$M+(L^2+M^2)^{\frac{1}{2}}$
Dibenzylamine	298±2	11.99±0.15	-
	323	11.86±0.1	-
	353	11.80±0.2	-
	384	11.62±0.1	-
N-isopropylbenzyl-amine	299	12.50±0.1	4.10±0.1
	321	12.56±0.1	3.89±0.1
	351	12.50±0.1	3.61±0.1
2-benzylamino-6-methylheptanol-6	324	12.05±0.15	-
	351	12.12±0.2	-
	383	11.88±0.15	-

TABLE II

Chemical Shift of Methylene Protons of Benzylamines in TFA (Relative to Internal Cyclohexane)

Compound	Temperature (°K)	Chemical Shift (ppm)
N-methyldibenzylamine	299±0.2	-2.88± 0.03
	328	-2.90
	376	-2.87
	403	-2.86
N-phenyldibenzylamine	298	-2.85
N-ethyl-N-phenylbenzylamine	298	-2.90
N,N-dimethylbenzylamine	299	-2.93
	337	-2.92
	440	-2.88
Tribenzylamine	298	-3.13
	323	-3.12
	353	-3.12
	382	-3.04
Dibenzylamine	298	-2.87
	323	-2.89
	353	-2.91
	384	-2.88
N-isopropylbenzylamine	299	-2.88
	321	-2.88
	351	-2.87
2-benzylamino-6-methylheptanol-6	324	-2.90
	351	-2.92
	383	-2.88

CHAPTER 4

A STUDY OF PROTON EXCHANGE REACTIONS OF SUBSTITUTED ANILINES IN TFA

1. INTRODUCTION

The effect of chemical exchange upon NMR spectra was established theoretically several years ago (107, 112-115). Since then, NMR spectroscopy has been used by various workers as a tool to study exchange reactions in aqueous and alcoholic solutions (116-133).

In the course of investigating protonated anilines in TFA, it was noted that the observed H^+-N-CH_3 coupling constant of protonated N,N-dimethylaniline was temperature dependent. The temperature dependence of this coupling constant was measured and the exchange rate and thermodynamic properties of exchange were calculated. It was originally intended to investigate the exchange reactions of a number of ring substituted N-alkylanilines. This investigation would have provided information about the effects of substituents upon exchange rates and thermodynamic variables. However, because few of these compounds were commercially available and because there were experimental difficulties involved in the measurements of small coupling constants, it was decided to try an alternative method of investigating exchange reactions of anilines in TFA. It was found that the TFA proton signal width depended upon the

exchange rate of the protonated aniline in solution. The acid proton peak was intense and its width could be measured with minimum experimental difficulty. Therefore, the acid proton signal widths of a series of dilute solutions of haloanilines in TFA were measured at different temperatures. The haloanilines were chosen for study because they were all commercially available and because there seemed to be some confusion about the nature of halogen substituent effects (26).

Because the exchange reactions of haloanilines have been studied in detail, the experimental results of these investigations are considered first. The results for protonated N, N-dimethylaniline are discussed in terms of these results.

The acid proton exchange rates of solutions of haloanilines in TFA are given. The probable reactions occurring in solutions are considered. Thermodynamic data for the exchange reactions are calculated and, where possible, are interpreted in terms of the nature of the reaction and structural properties of the reactants. Possible errors in measurement of exchange rates are considered.

The exchange rates of protonated N,N-dimethylaniline at different temperatures are given. Thermodynamic data are calculated. It is found that the measured activation energy of exchange is lower than that of aniline. A possible explanation is suggested.

2. THEORETICAL DISCUSSION

(A) Spin-Lattice Relaxation Time T_1

(1) The Nuclear Magnet

The magnetic moment of a nucleus is given by

$$\mu = \gamma(I\hbar) \qquad 4.1$$

where μ = the maximum observable component of the magnetic moment of the nucleus and $\hbar I$ = the maximum observable component of angular momentum of the nucleus. γ is called the magnetogyric ratio. μ may also be expressed in terms of the nuclear magneton. The nuclear magneton is the magnetic moment which would be ascribed to a proton if it were a spinning spherical particle with mass and charge spread evenly over its surface. On this basis,

$$\mu = g\left(\frac{e\hbar}{2M_p c}\right) I \qquad 4.2$$

where M_p is the proton mass, c is the speed of light and e is the proton charge (134). g is a dimensionless constant which corrects for the inaccuracies in the postulated model.

(2) Distribution of Nuclear Spins in a Magnetic Field

If a nucleus of spin $\frac{1}{2}$ is placed in a uniform magnetic field, the energies of the two spin states are separated by $2\mu H_o$, where H_o is the applied magnetic field. In NMR experiments, transitions between the two levels are induced by the emission or absorption of energy quanta. The required

frequency of transition is given by the standard relationship

$$E = h\nu = 2\mu H_o. \qquad 4.3$$

The ratios of spin state populations are given by the Boltzmann factor, exponential $(2\mu H_o/kT)$. Since the value of $(2\mu H_o/kT)$ is usually of the order of 10^{-5}, the probabilities of a given nucleus being in the upper or lower spin state are, respectively, very nearly

$$\tfrac{1}{2}\left(1-\mu\frac{H_o}{kT}\right) \quad \text{and} \quad \tfrac{1}{2}\left(1+\mu\frac{H_o}{kT}\right). \qquad 4.4$$

(3) Spin-Lattice Relaxation Time

An ensemble of nuclear spins (spin $\frac{1}{2}$) placed in a magnetic field will seek a new thermal equilibrium characterized by the Boltzmann factors given in equation 4.4. At equilibrium, the number of transitions in both directions must be equal. Therefore,

$$n_+ U_{+\rightarrow -} = n_- U_{-\rightarrow +} \qquad 4.5$$

where n_+ = number of nuclei in lower energy state, $U_{+\rightarrow -}$ = the probability of transition from the lower to the higher energy state, etc. From equations 4.4 and 4.5,

$$\frac{U_{-\rightarrow +}}{U_{+\rightarrow -}} = 1 + \frac{2\mu H_o}{kT}. \qquad 4.6$$

If n is the number of nuclei per unit volume in excess in the lower energy state at any time t, n_{eq} is the value of n at thermal equilibrium, and U is the mean of $U_{- \rightarrow +}$ and $U_{+ \rightarrow -}$, then it may be shown that (134)

$$(n - n_{eq}) = (n - n_{eq})_0 e^{-2Ut} \qquad 4.7$$

where $(n-n_{eq})_o$ is the initial value of $(n-n_{eq})$. The excess number approaches its equilibrium value with a characteristic time constant 1/2 U, which is usually called T_1, the spin-lattice relaxation time.

Mechanisms which may cause spin-lattice relaxation are discussed in part C.

(B) <u>Spin-Spin Relaxation Mechanisms and Spin-Spin Relaxation Time.</u>

(1) <u>NMR Absorption</u>

The angular momentum and the magnetic moment are related by equation 4.1. By considering the effect of the main magnetic field upon the time rate of change of angular momentum, it can be shown that (134)

$$\omega = -\gamma H_o, \qquad 4.8$$

where ω is the angular velocity of the angular momentum vector, or

$$\nu = \frac{\gamma}{2\pi} H_o . \qquad 4.9$$

Therefore, the nucleus precesses around the main magnetic field with an angular velocity $-\omega$. The frequency of this precession is called the Larmor precession frequency.

Suppose one uses a coordinate system rotating with angular velocity $-\gamma H_o$. Then in the absence of other fields, the magnetic moment vector will remain stationary relative to the new coordinate system. Suppose a new field H_1 is introduced which is perpendicular to the original field H_o and rotating about H_o. H_1 exerts a torque $\underline{\mu} \times \underline{H}_1$ on the nucleus, tending to increase the angle between $\underline{\mu}$ and $\underline{H}_o$. If $\underline{H}_1$ is moving in the coordinate system, then the direction of the torque will vary rapidly and little overall effect will be noticed. However, if $\underline{H}_1$ is stationary in the rotating coordinate system, then a steady torque will be exerted and the angle between $\underline{\mu}$ and $\underline{H}_o$ will increase. There will be a net absorption of energy which can be detected by monitoring the strength of H_1. Classically, the absorption of energy is a resonance phenomenon, with maximum absorption of energy occurring when $\underline{H}_1$ rotates at the Larmor precession frequency.

The resonance experiment can also be treated quantum mechanically. Since energy level transitions are quantized, equation 4.3 shows that the transition from the low to the high energy state occurs only when $\underline{H}_1$ rotates with a frequency

$$\nu = 2 \frac{\mu H_o}{h} . \qquad 4.10$$

There is no finite probability of a transition at any frequency other than ν_0. It may easily be shown that equations 4.9 and 4.10 are identical and that the Larmor precession frequency and the transition frequency are identical. The difference between the two treatments is that the quantum mechanical treatment predicts absorption of energy only at the Larmor precession frequency while the classical treatment predicts absorption over a range of frequencies with a maximum at the Larmor precession frequency.

(2) Line Widths of NMR Signals, T_2

As mentioned above, the quantum mechanical treatment predicts resonance only at one frequency. In actual practice, resonance occurs over a range of frequencies, for reasons discussed in part B(3). The number of nuclei with a resonance frequency between ν and $\nu + d\nu$ will be given by

$$dN = N_0 g(\nu) d\nu \qquad 4.11$$

where $g(\nu)$, the line shape function, is proportional to the absorption at frequency ν. Therefore, $g(\nu)$ describes the shape of the resonance signal. Since N_0 is the total number of nuclei,

$$\int_0^\infty g(\nu) d\nu = 1. \qquad 4.12$$

$g(\nu)$ has a finite value over a range of frequencies. Since $g(\nu)$ is a normalized function, its maximum value is an inverse

measure of its width. A characteristic time T_2 is defined by

$$T_2 = \frac{1}{2}\left[g(\nu)\right]_{max.} \qquad 4.13$$

The factor $\frac{1}{2}$ is introduced to make this definition of T_2 consistent with another definition which will be developed in part D. Signal line width is inversely proportional to T_2.

(3) Factors Affecting Line Width, Spin-Spin Relaxation Time

Some of the factors affecting line width are discussed below. In addition, the effect of exchange upon line width will be discussed in part E.

(a) Natural line width due to spontaneous emission - The natural line width of any transition is determined by the lifetime a nuclear spin in the higher energy state. It has been found that spontaneous emission of radiation has little effect on the line width of NMR signals (135).

(b) Broadening due to spin-lattice relaxation - The lifetime of the two spin states is decided by the spin-lattice relaxation time. Line broadening occurs as a natural consequence of the uncertainty principle,

$$\Delta E \Delta t \approx \hbar. \qquad 4.14$$

Since $\Delta E = h\Delta\nu$, the uncertainty in the absorption frequency is $1/2\pi\Delta t$. Consequently the line width, on a frequency scale,

will be proportional to $1/T_1$, in the absence of other broadening mechanisms.

(c) Broadening due to spin-spin interaction - Nuclei may see a variety of local fields due to the presence of other nuclear spins. For example, the field caused by a magnetic moment μ, at a distance r from a nucleus, is of the order of μ/r^3. Therefore, a proton 1 Å from a nuclear magneton will see a local field of several gauss. The presence of local fields of this strength will alter the magnetic field seen by the various nuclei and will cause resonance to occur over a range of frequencies as large as 100Kc/s. Since g (ν) is a normalized function, the value of T_2 will be decreased due to the spin-spin interactions. For this reason, T_2 is often called the spin-spin relaxation time.

T_2 can be defined in terms of equation 4.9 and the strength of the local fields.

$$1/T_2 \propto \frac{\gamma}{2\pi} \cdot H_{local} \qquad 4.15$$

In liquids and gases, rapid molecular motions tend to average local fields to zero. Consequently, there is little broadening due to spin-spin interaction. In solids, the rigid nature of the lattice prevents motions of this type. Consequently, NMR signals of solids are usually broader than those of liquids and gases.

(d) Broadening due to magnetic field inhomogenity - If the

magnetic field is not homogeneous throughout the region in which the sample is placed, then resonance will occur over a range of frequencies because molecules in different parts of the sample see different values of the main magnetic field.

In a perfectly homogeneous field and in the absence of spin-spin interactions, T_1 and T_2 should be equal since in these circumstances the line width is determined by T_1.

(C) Spin-Lattice Relaxation Mechanisms.

A fluctuating magnetic field can induce transitions between spin states if the field has an appreciable component of frequency ν_0, the Larmor precession frequency. The extent of spin-lattice relaxation depends upon the magnitude of local fields and the rates of fluctuation of these fields.

Several mechanisms may induce fluctuating magnetic fields of the type described above. These are discussed below:

(1) Relaxation Due to Nuclear Magnetic Dipole Interactions

Lattice motions will cause fluctuating magnetic fields due to movement of nuclear spins. Early attempts to correlate lattice vibrations in solids with T_1 were unsuccessful in that the calculated values of T_1 were much too large (136). Calculations of this type are inaccurate since there are few lattice vibrations in the proper frequency range.

Bloembergen, Purcell and Pound (BPP) have examined the

influence of rotational, translational, and vibrational motions of molecules in a liquid upon relaxation times (135). Liquids can be considered to exist in definite configurations even though overall molecular chaos prevails. One can define a correlation time τ_c which measures the time for one configuration to transfer to another completely unrelated configuration. Intramolecular and intermolecular correlation times must be considered. If a molecule contains two or more nuclei with non-zero spins, then these spins will move relative to one another if the molecule rotates. This movement produces a fluctuating magnetic field which can, if it has the proper frequency, induce transitions of the spins in the molecule. The intramolecular correlation time τ_c is defined as the average time taken by the molecule to rotate through one radian. It is possible to predict a value of τ_c by making use of a modification of the theory of dielectric dispersion (137). τ_c is then related to the viscosity η by (135)

$$\tau_c = 4\pi\eta a^3/3kT \qquad 4.16$$

where a is the radius of the molecule if the molecule is assumed to be spherical. Translational molecular motions can also give rise to relaxation. From the theory of Brownian motion (138), the intermolecular correlation time is given by

$$\tau_c = \pi\eta a r^2/2kT. \qquad 4.17$$

τ_c is the time taken by a molecule to diffuse through a distance r where r is approximately equal to the molecular radius.

BPP obtained the following expression for T_1:

$$1/T_1 = \frac{C_1 \tau_c}{1 + 4\pi^2 \nu_0^2 \tau_c^2} + \frac{C_2 \tau_c}{1 + 16\pi^2 \nu_0^2 \tau_c^2}. \qquad 4.18$$

C_1 and C_2 are constants which depend upon the relation between internuclear distance and local magnetic field strength. The equations have the same form for intra- and intermolecular contributions to T_1.

If $2\pi\nu_0\tau_c \ll 1$, then equation 4.18 becomes

$$1/T_1 = (C_1 + C_2)\tau_c. \qquad 4.19$$

If $1 \ll 2\pi\nu_0\tau_c$, then equation 4.18 becomes

$$1/T_1 = \frac{4C_1 + C_2}{16\pi^2 \nu_0^2 \tau_c}. \qquad 4.20$$

Therefore, in the region where τ_c is very short, T_1 is inversely proportional to τ_c. On the other hand, if τ_c is very long, then T_1 is directly proportional to τ_c. The minimum in T_1 occurs for $\frac{1}{2} < 2\pi\nu_0\tau_c < 1$. Because τ_c is a mean value of the time for molecular reorientations, the fluctuating magnetic fields caused by molecular motions have the maximum component of frequency equal to the Larmor precession frequency when $2\pi\nu_0\tau_c = 1$, i.e. when τ_c equals the time for one nuclear precession. The minimum does not occur when $2\pi\nu_0\tau_c = 1$ because frequencies equal to $2\nu_0$ can also induce

transitions between nuclear spin states.

BPP measured T_1 of glycerine as a function of viscosity and temperature. They found that the plot showed the expected minimum. This confirmed that molecular motions in liquids were of the right order to cause spin-lattice relaxation.

The condition $\tau_c \ll (2\pi\nu_0)^{-1}$ is also the condition for spin-spin relaxation to be ineffective because molecular motions average out local fields which cause relaxation. Therefore, T_1 and T_2 are nearly equal when $\tau_c \ll (2\pi\nu_0)^{-1}$. As τ_c increases, T_1 decreases to a minimum and then increases. However, T_2 decreases continuously because local fields are no longer averaged out.

(2) Other Spin-Lattice Relaxation Mechanisms.

For nuclei with spin ≥ 1, interactions between quadrupole moments and fluctuating field gradients cause an increase in spin-lattice relaxation. Paramagnetic impurities such as oxygen cause a decrease in relaxation time due to interactions of nuclear spins with the unpaired electron spins.

(D) An Alternative Treatment of Relaxation Times, the Bloch Formulation

Bloch has developed a set of macroscopic equations for the variation of total nuclear magnetic moment per unit volume in a magnetic field (139). The macroscopic moment, M,

satisfies the following equation:

$$\frac{d\underline{M}}{dt} = \gamma(\underline{M} \times \underline{H}). \qquad 4.21$$

Consider a set of nuclei of spin $\frac{1}{2}$ in a steady field H_o. In the absence of relaxation processes, M_z will be constant. However, it is known that M_z approaches an equilibrium value M_o, because of spin-lattice relaxation. Therefore,

$$\frac{dM_z}{dt} = -\frac{(M_z - M_o)}{T_1}. \qquad 4.22$$

Bloch refers to T_1 as the longitudinal relaxation time since it measures the rate of change of the component of magnetization along the main magnetic field. If equation 4.21 is solved for the x and y components of M, it is found that, in the absence of relaxation mechanisms, the magnetic moment precesses around H_o with an angular velocity $-\omega_o$. However, interactions with local fields cause the nucleii to get out of phase and the components M_x and M_y decay to zero. The time constant T_2, for this decay, is called the transverse relaxation time. The rates of change of M_x and M_y are given by

$$\frac{dM_x}{dt} = \omega_o M_y - \frac{M_x}{T_2} \qquad 4.23$$

and

$$\frac{dM_y}{dt} = -\omega_o M_x - \frac{M_y}{T_2}. \qquad 4.24$$

Now consider the effect of a field H_1 perpendicular to H_o and rotating with angular velocity $-\omega$. The components of H_1 are $(H_1)_x = H_1 \cos\omega t$ 4.25

and

$(H_1)_y = -H_1 \sin\omega t.$ 4.26

The Bloch equations have simpler forms if one uses a new set of coordinate axes which rotate about $\underline{H}_o$ with angular velocity $-\omega$. u and v are respectively defined as the components of $\underline{M}$ perpendicular and parallel to $\underline{H}_1$. Allowing for the effect of the field H_1, equations 4.22 to 4.24 become:

$$\frac{du}{dt} + \frac{u}{T_2} + (\omega_o - \omega)v = 0 \qquad 4.27$$

$$\frac{dv}{dt} + \frac{v}{T_2} - (\omega_o - \omega)u + \gamma H_1 M_z = 0 \qquad 4.28$$

$$\frac{dM_z}{dt} + \frac{M_z - M_o}{T_1} - \gamma H_1 v = 0. \qquad 4.29$$

The steady state solutions are obtained by setting all time derivatives equal to zero. These solutions can be expressed in terms of u and v or M_x and M_y.

In actual practice, a linearly oscillating magnetic field is used in place of the rotating field H_1. The field components are: $H_x = 2H_1 \cos\omega t.$ 4.30

$H_y = 0.$ 4.31

This can be shown to be equivalent to two rotating fields with angular velocities ω and $-\omega$. Only one of the fields is effective

because appreciable resonance effects occur only when $\omega \approx \omega_0$. The effect of the linear field can be described in terms of the intensities of magnetization in phase and out of phase with H_1. These are respectively $2\chi' H_1 \cos\omega t$ and $2\chi' H_1 \sin\omega t$ where χ' and χ'' are the susceptibilities in phase and out of phase with H_1. The susceptibilities can be obtained from the steady states solutions of the Bloch equation. They are:

$$\chi' = \frac{1}{2}\chi_0\omega_0 \cdot \frac{T_2^2(\omega_0-\omega)}{1+T_2^2(\omega_0-\omega)^2+\gamma^2 H_1^2 T_1 T_2} \qquad 4.32$$

$$\chi'' = \frac{1}{2}\chi_0\omega_0 \cdot \frac{T_2}{1+T_2^2(\omega_0-\omega)^2+\gamma^2 H_1^2 T_1 T_2}. \qquad 4.33$$

The susceptibility χ'' has a maximum value when $\omega_0 = \omega$, i.e. at the Larmor frequency. The sample absorbs energy from the H_1 field at a rate (140)

$$A = 2H_1^2\chi''. \qquad 4.34$$

Therefore, maximum absorption occurs when $\omega = \omega_0$. Comparison of this value and the value of the rate of absorption of energy obtained from a calculation of the quantum mechanical transition probability gives

$$g(\nu) = \frac{2T_2}{1+4\pi^2 T_2^2(\nu_0-\nu)^2}. \qquad 4.35$$

From the form of equation 4.35 it is obvious that

$$[g(\nu)]_{max} = 2T_2. \qquad 4.36$$

Consequently, the two definitions of T_2 are equivalent. Equation 4.35 is only accurate if $H_1 \ll \frac{1}{\gamma\sqrt{T_1 T_2}}$.

(E) Effect of Exchange Upon T_2 and Signal Line Widths.

(1) General Discussion

Ordinary chemical techniques are unsuitable for the measurement of fast reactions. However, NMR techniques can be used to study chemical exchange reactions with exchange rates of the order of 1 to $10^4 sec^{-1}$.

NMR spectroscopy can be used to study exchange reactions if the nuclei which are exchanging have different magnetic environments and consequently different Larmor precession frequencies. Exchange can be considered to be a transverse relaxation process since the exchanged nuclei will be out of phase with the other nuclei in the same environment. Exchange between nuclei in the same environments has no effect upon the signal width because the nuclei have the same precession frequencies before and after exchange.

Slow exchange causes a decrease in the transverse relaxation time and consequently increases the width of the signals due to the exchanging nuclei. Alternatively, the increase in line width can be explained by the uncertainty principle, $h\Delta\nu\Delta t \approx \hbar$. The increase in line width due to exchange is inversely proportional to the average lifetime of the nuclei causing the resonance signal or directly proportional to the nuclear exchange rate.

As the exchange rate between nuclei in two non-equivalent sites increases, the signals become broader and move closer together until they finally collapse to a single peak which becomes sharper as the exchange increases. In this region the change in signal width is inversely proportional to the exchange rate.

(2) Modification of the Bloch Equations to Allow for Exchange.

The Bloch equations were modified to allow for exchange by Gutowsky, McCall and Slichter (112) and by McConnell(114). McConnell's treatment is simpler and will be followed here.

The simplest rate process which can be considered by NMR is the exchange of two uncoupled nuclei in non-equivalent environments. The Bloch equation can be modified so that exchange rates can be determined from known values of the chemical shift between the two sites and/or from the observed line widths of the resonance signals.

If H_1 is not too large, then $M_z=M_o$ and M_z can be replaced by M_o in equation 4.28. Suppose G is a complex moment such that

$$G = u + i v. \qquad 4.37$$

G can be rewritten in terms of equations 4.27 and 4.28.

$$\frac{dG}{dt} + \left[\frac{1}{T_2} - i(\omega_0 - \omega)\right] G = -i \gamma H_1 M_0. \qquad 4.38$$

If G_A and G_B are the complex moments associated with nuclei A and B, then

$$\frac{dG_A}{dt} + \alpha_A G_A = -i\gamma H_1 M_{0A} \qquad 4.39$$

$$\frac{dG_B}{dt} + \alpha_B G_B = -i\gamma H_1 M_{0B} \qquad 4.40$$

where

$$\alpha_n = \frac{1}{T_{2n}} - i(\omega_n - \omega). \qquad (n = A \text{ or } B). \qquad 4.41$$

It is necessary to assume that the time taken by a nucleus to jump from one site to another is negligible compared to its lifetime in either site. Exchange between equivalent sites will then have no effect because the nuclei will switch sites too rapidly for any significant relaxation to occur. If τ_A is the average lifetime of a nucleus in site A, then $1/\tau_A$ is the probability (per unit time) of the nucleus jumping to site B. The relative populations of the sites are then

$$P_A = \frac{\tau_A}{\tau_A + \tau_B} \quad \text{and} \quad P_B = \frac{\tau_B}{\tau_A + \tau_B} \qquad 4.42$$

where $P_B = 1 - P_A$.

The modified Bloch equations proposed by McConnel (114) are:

$$\frac{dG_A}{dt} + \alpha_A G_A = -i\gamma H_1 M_{0A} + \frac{G_B}{\tau_B} - \frac{G_A}{\tau_A} \qquad 4.43$$

$$\frac{dG_B}{dt} + \alpha_B G_B = -i\gamma H_1 M_{0B} + \frac{G_A}{\tau_A} - \frac{G_B}{\tau_B}. \qquad 4.44$$

$\frac{G_B}{\tau_B}$ is the rate of increase of G_A due to transfer of magnetization from B to A sites. $\frac{G_A}{\tau_A}$ is the rate of decrease of G_A.

For slow passage conditions,

$$\frac{dG_A}{dt} = \frac{dG_B}{dt} = 0 . \qquad 4.45$$

The total complex moment $(G_A + G_B)$ is given by

$$G = -(i\gamma H_1 M_0).\frac{\tau_A + \tau_B + \tau_A\tau_B(\alpha_A P_A + \alpha_B P_B)}{(1+\alpha_A\tau_A)(1+\alpha_B\tau_B) - 1}. \qquad 4.46$$

The intensity of absorption is proportional to the imaginary part $\mathcal{V}$. The solution of the above equation becomes simpler in the limiting cases where lifetimes are very long or very short.

(3) <u>Solutions of the Modified Bloch Equations for Different Exchange Rates</u>

(a) Slow exchange - If lifetimes τ_A and τ_B are sufficiently long compared to the inverse of the separation between the two sites, then two separate signals are observed. When the applied RF field has a frequency which is nearly equal to the Larmor precession frequency of one of the types of nuclei, the total magnitization contributed by nuclei in the other

environment is small because they precess at a frequency different than the applied field frequency. Therefore, when $\omega \approx \omega_A$,

$$G \approx G_A \approx - \frac{i \gamma H_1 M_0 P_A \tau_A}{1 + \alpha_A \tau_A}. \qquad 4.47$$

The solution for the imaginary component is (141)

$$v = \frac{-\gamma H_1 M_0 P_A \left[\frac{\tau_A \cdot T_{2A}}{\tau_A + T_{2A}}\right]}{1 + \left[\tau_A \cdot T_{2A} / (\tau_A + T_{2A})\right]^2 (\omega_A - \omega)^2}. \qquad 4.48$$

Under the same conditions, but in the absence of exchange, the value of the imaginary component (as obtained from solutions of equations 4.27 to 4.29) is

$$v = \frac{-\gamma H_1 M_0 P_A T_{2A}}{1 + T_{2A}^2 (\omega_A - \omega)^2}. \qquad 4.49$$

Therefore, T_{2A} has been replaced by $T_{2A'}$ where

$$\frac{1}{T_{2A'}} = \frac{1}{T_{2A}} + \frac{1}{\tau_A}. \qquad 4.50$$

Experimentally, the variable which is most conveniently measured is the signal width at half height. Therefore, it is necessary to determine the exact relationship between T_2 and signal width. From equations 4.35 and 4.36 it is seen that $g(\nu) = \frac{1}{2} (g(\nu))_{max}$ when

$$T_2 = \frac{2 T_2}{1 + 4\pi^2 T_2^2 (\nu_0 - \nu)^2}. \qquad 4.51$$

The obvious solution of this equation is

$$4\pi^2 T_2^2 (\nu_0 - \nu)^2 = 1 \qquad 4.52$$

or

$$(\nu_0 - \nu) = \pm \frac{1}{2\pi T_2}. \qquad 4.53$$

Therefore, the line width in c/s is equal to $1/\pi T_2$ or

$$\pi \Delta \nu = \frac{1}{T_2}. \qquad 4.54$$

Equation 4.49 becomes

$$\pi \Delta \nu = \frac{1}{\tau_A} + \frac{1}{T_{2A}}. \qquad 4.55$$

This equation is only true if the signal has Lorentzian line shape. Experimentally, this condition should be fulfilled if the resolution is good and if H_1 is small, i.e. if no saturation occurs.

(b) Very fast exchange - If exchange is not rapid enough to cause complete collapse of the two signals, then (142)

$$\frac{1}{T_2'} = \frac{P_A}{T_{2A}} + \frac{P_B}{T_{2B}} + P_A^2 P_B^2 (\omega_A - \omega_B)^2 (\tau_A + \tau_B). \qquad 4.56$$

If the lifetimes are very short, the last term of equation 4.56 becomes unimportant and

$$\frac{1}{T_2'} = \frac{P_A}{T_{2A}} + \frac{P_B}{T_{2B}}. \qquad 4.57$$

The signal is centered on a mean frequency

$$\omega_{mean} = P_A \omega_A + P_B \omega_B . \qquad 4.58$$

If one of the signals is not a single peak, then the situation becomes much more complicated. Meiboom and co-workers have investigated problems of this type in detail (127). By analogy to their results, the effect of relaxation arising from rapid exchange between acid and ammonio protons is given by

$$\frac{1}{T_2'} = \frac{P_A}{T_{2A}} + \frac{P_B}{T_{2B}} + P_A^2 P_B^2 (\omega_A - \omega_B)^2 (\tau_A + \tau_B) + (P_B) \frac{2}{3} J^2 \tau' \left(1 + \frac{1}{1 + (\tau')^2 (\omega_A - \omega_B)^2}\right). \qquad 4.59$$

J = NH coupling constant

P_B = population of the ammonio group

τ' = lifetime for transfer between components of the ammonio triplet.

The term $\frac{2}{3} J^2$ simply represents the second moment of the ammonio triplet. The line width of the ammonio triplet is determined by the N^{14} quadrupole relaxation time and the exchange rate. The signal will always be broadened due to this additional term. As the lifetime of the ammonio triplet becomes very short, this term decreases to zero.

(c) Intermediate exchange rates - The full expression for the intensity of absorption in the region of intermediate exchange rate was developed by Gutowsky and Holm (107). The expression is very complex and will not be considered here.

If it is assumed that the two types of nucleii have equal populations and lifetimes, and have large transverse relaxation times, the expressions can be considerably simplifed. Most commonly, the peak separation is measured as a function of exchange rate. The change in peak separation as a function of exchange rate is given by equation 3.25. If T_{2A}, $T_{2B} \neq 0$ then this simple equation is inaccurate. The equations for this situation have been developed in detail (107,115,143). The equations are complex and are most easily solved by use of a computer. They will not be given here.

(F) Ion Association or Ion Pair Formation

In recent years, ion association or ion pair formation has been the subject of numerous investigations. Deviations from ideal behaviour of conductances and activities of ionic solutions have provided most of the evidence which proves the existence of ion pairs in solution. Much of the work has been summarized in a recent monograph on ion association (144). Ion association will not be discussed in detail here but various facts and ideas applicable to this investigation will be pointed out.

(1) Factors Determining the Tendency Towards Ion Association

Bjerrum has developed an equation which predicts the probability of finding an ion at a given distance from an oppositely charged ion (145). The minimum probability occurs when

$$q = \frac{Z_i Z_j e^2}{2DkT} \qquad 4.60$$

where Z_i and Z_j are the electrostatic charges of the two charged ions, D is the dielectric constant of the solvent, and q is the distance of separation of the charge centres. If the sum of the ionic radii exceeds q, then it is assumed that the ions are completely dissociated. This equation should provide at least a qualitative estimate of the possibility of ion pair formation. The sizes of ions do affect ion pair dissociation constants. For example, consider the dissociation contants for ammonium picrate ion pairs (146,147). The dissociation constants for ammonium picrate, tri-n-butyl ammonium picrate and tetra-n-butyl ammonium picrate in nitrobenzene are respectively 1.5×10^{-4}, 1.9×10^{-4} and 2×10^{-1}.

Equation 4.60 also indicates that the dielectric constant affects ion association. This is understandable since the attraction between electrostatic charges depends upon the dielectric constant of the medium. In addition, the solvating power of the solvent and the tendencies of the ions to be solvated must be considered.

The sizes and charges of the ions are particularly important. Small ions or highly charged ions are most easily solvated. Increased solvation of the individual ions (relative to the ion pair) results in a decrease in tendency towards ion pair formation.

It is difficult to determine the exact nature of the interaction between charged ions in an ion pair. The attraction between ions may be purely electrostatic in nature or the two ions may be partially covalently bonded. For purposes of convenience, it is often considered that two ions have formed an ion pair if the distance between them is less than q (equation 4.60).

For TFA, q $\approx$ seven Å. The distance of closest possible approach of charge centres of anilinium ions and trifluoracetate ions is approximately two Å. Therefore, anilinium trifluoracetate can definitely exist as ion pairs. Since TFA molecules are quite bulky, it is assumed that anilinium ions and trifluoracetate ions form ion pairs only if there are no <u>directly intervening</u> solvent molecules. The two ions can be solvated, but the solvating molecules must not prevent the close approach of charge centres.

(2) <u>Thermodynamic Properties of Ion Pairs</u>

ΔF^o for ion pair dissociation can be calculated from the dissociation constant for the ion pair, K_D, by the thermodynamic equation

$$\Delta F^o = -RT\ln K_D. \qquad 4.61$$

ΔF^o is normally positive, i.e. $K_D < 1$, for ion pairs between metal cations and various anions in water and non-aqueous solvents (148). ΔF^o is negative for some ion pairs between singly charged

ions in aqueous solutions.

The sign of ΔS^o can be positive or negative. Dissociation increases the number of free particles and would be expected to cause an increase in entropy. However, solvation of the individual ions will lead to a decrease in freedom or "electrostriction" of the solvent and a decrease in entropy. In aqueous solutions the latter effect normally predominates and the entropy of ion pair dissociation is negative. In solvents with less solvating power, the entropy change may possibly be positive.

ΔH^o is determined by the thermodynamic equation

$$\Delta H^o = \Delta F^o + T\Delta S^o. \qquad 4.62$$

ΔH^o may be positive or negative. If, as is often the case, ΔF^o is positive and ΔS^o is negative, then ΔH^o is normally small. The change in the dissociation constant with temperature is given by

$$\int_{T_1}^{T_2} d \ln K_D = \int_{T_1}^{T_2} \frac{\Delta H^o}{RT^2} dT. \qquad 4.63$$

It is interesting to note that if ΔH^o is negative, then the ion pair concentration will increase with increasing temperature.

(3) <u>Effect of Ion Pair Formation Upon Observed Kinetics</u>

Consider a simple biionic reaction between oppositely

charged ions.

$$A^- + BH^+ \rightleftharpoons AH + B \qquad 4.64$$

If this is a true biionic "concerted" reaction (S_n2 reaction in physical organic chemical notation), then the formation of an ion pair must occur as an intermediate step in the reaction since ions must come together before they can react. If there is little tendency to form ion pairs and/or if the reaction of ion pairs is very rapid, then the concentration of ion pairs will be small. The reaction will then show behaviour typical of reactions between ions.

The rate of a bimolecular reaction is given by rate = $k'[X^{\ddagger}]$ where $[X^{\ddagger}]$ is the concentration of the activated complex. The equilibrium constant between the activated complex and the reactants is given by

$$K = \frac{[X^{\ddagger}]}{[A^-][BH^+]} \cdot \frac{f_{X^{\ddagger}}}{f_{A^-} \cdot f_{BH^+}} \qquad 4.65$$

where the f's are the activity coefficients. Therefore,

$$\text{rate} = k' K [A^-][BH^+] \left(\frac{f_{X^{\ddagger}}}{f_{A^-} \cdot f_{BH^+}}\right)^{-1} = k_0 [A^-][BH^+] \cdot F. \qquad 4.66$$

It may be shown that in dilute solutions (149)

$$\ln F = \frac{\varepsilon^2 Z_{A^-} Z_{BH^+}}{DkT} \cdot \frac{\kappa}{1+\kappa a} \qquad 4.67$$

where

$$\kappa = \left(\frac{8N\pi\varepsilon^2}{10^3 DkT} \cdot \mu\right)^{\frac{1}{2}}. \qquad 4.68$$

ε is the charge of the ion in esu, D is the dielectric constant of the solvent, k is the Boltzmann constant, 'a' is an empirical constant which is sometimes considered to represent the distance of closest approach of ions and μ, the ionic strength, is $\frac{1}{2}\sum_i c_i Z_i^2$. Therefore, the apparent rate constant k (= rate / $[A^-][BH^+]$) is given by

$$\log_{10} k = \log_{10} k_0 + \frac{Z_{A^-} \cdot Z_{BH^+} \cdot A\sqrt{\mu}}{1 + Ba\sqrt{\mu}} \left(\frac{1}{2.303}\right) \qquad 4.69$$

where $A = \left(\frac{8\pi N \varepsilon^6}{10^3 (DkT)^3}\right)^{\frac{1}{2}}$ and $B = \left(\frac{8\pi N \varepsilon^2}{10^3 DkT}\right)^{\frac{1}{2}}$. 4.70

Therefore, the reaction rate depends upon the ionic strength. Equation 4.69 can be used to calculate the true second order rate constants of biionic reactions.

Ion pair formation will decrease both the free ion concentrations and the ionic strength of the solution. Therefore, equation 4.69 will no longer be obeyed. Since the reaction must proceed via ion pair formation, it is possible to predict the ion pair reaction rate from the ion pair concentration. The reaction of ion pairs should be a simple first order reaction. In the limiting case where the ions exist almost entirely as ion pairs, the rate is given by

$$\text{rate} = k\,[BH^+ --- A^-] = k\,[\text{total } BH^+] \qquad 4.71$$

(if $[A^-] = [BH^+]$). Theoretically the reaction rate should be independent of ionic strength because the reactant and the

activated complex are considered to be electrically neutral. This is, of course, only an approximation and the reaction rate may be somewhat dependent upon ionic strength.

3. EXPERIMENTAL

(A) Aniline and Haloanilines in TFA

Most of the anilines used in this study were obtained from Distillation Products Ind. and were Eastman White Label grade. The p-fluoroaniline was Eastman Practical grade. m-Chloroaniline was obtained from K and K Laboratories, Inc. m-Fluoroaniline was obtained from Matheson, Coleman and Bell. m-Iodoaniline was obtained from Aldrich Chemicals. Solid anilines were used without purification. Liquid anilines were distilled under reduced pressure and small constant temperature fractions were collected for use in exchange studies. Trifluoroacetic acid was an Eastman White Label grade chemical. The aliquots of acid used in preparing the solutions were first treated with one or two drops of trifluoracetic anhydride per aliquot in order to remove any water in the acid. TFA was not further purified. Cyclohexane was a Fisher Spectro-Analyzed reagent and was used without purification.

The TFA solutions were prepared by weighing by the method described in Chapter 2. The solutions contained three mole per cent of cyclohexane and from one to three mole per cent of substituted aniline. Cyclohexane was chosen as an internal

reference because it did not react with TFA or aniline and because it gave an intense signal, even when present in low molar concentration. Whenever possible, the aniline concentration was adjusted so that exchange broadening of the acid proton signal occurred at temperatures just above room temperature.

Originally, aniline concentrations of from four to eight mole per cent were used. However, the plots of log (acid proton line width) versus (absolute temperature)$^{-1}$ were always curved in the low temperature regions (0 to 30°C). In two extreme cases, the slope of the line actually changed sign. It was found that if aniline concentrations of from one to three mole per cent were used, the plots for all but one of the aniline solutions (p-fluoroaniline) were essentially linear in the region of slow exchange.

Solutions were placed in thick-walled 5 mm OD sample tubes. The solutions were degassed and then the sample tubes were evacuated and sealed. Spectra were measured on a Varian DP-60 spectrometer. Experiments at different temperatures were carried out with the aid of an NRC-manufactured temperature device (105). The spinning air was heated by a nichrome wire heater. Temperature control was attained by variation of the air flow rate and by variation of the power supplied to the heater by a Variac. Temperatures from 10°C to room temperature were obtained by passing the spinning air through a copper coil

immersed in an ice-salt mixture before it passed through the temperature device. In order to obtain lower temperatures, it was necessary to use pre-cooled nitrogen gas to spin the sample. The nitrogen gas was cooled by a dry ice-acetone mixture. Because the pre-cooled nitrogen had to be heated by approximately 80°C and also because it was difficult to keep the nitrogen flow rate constant, it was impossible to maintain constant temperature in the temperature region below 10°C. Therefore, line widths could not be accurately measured in this region. The exchange reactions of o-iodoaniline in TFA could not be studied, because rapid proton exchange occurred below 10°C. One measurement of the line width of a m-chloroaniline solution was made at 0°C. Since the line width was nearly constant at that temperature, temperature control was not very important.

Temperatures were measured with a copper-constantan thermocouple attached to a Varian G-11 recording potentiometer. The potentiometer was regularly recalibrated to insure that there was no error in the recorder readings. The temperature was usually changed by about two to three °C between runs. Solutions were allowed to equilibrate for at least two hours at each temperature before the spectra were obtained. Usually solutions were heated slightly above the desired temperature and then allowed to cool to that temperature. It is estimated that temperature readings were accurate to within 0.5°C.

The ammonio proton signals were very broad and very weak.

Therefore, line widths of these signals could not be measured. However, the acid proton signal widths were easily measured. Because there were large concentrations of acid protons in the solutions studied, low RF power could be used, even when the protons were exchanging rapidly. Therefore, signal saturation was not a problem. This was quite important because saturation would have altered the signal width. Signal widths between one and fifteen c/s could be measured accurately. The possible error in measuring line widths of less than one c/s was quite large. If the signal was broader than fifteen c/s, it was necessary to use high RF power and the signal sometimes appeared to be partially saturated.

The resolution was carefully controlled while acid proton signal widths were measured. Before each pair of measurements of the acid proton signal, the width of the cyclohexane signal was measured twice (forward and reverse) by placing sidebands of the signal 5 c/s on both sides of itself. The sideband frequency was measured with a Hewlett-Packard 521C electronic counter which was accurate to within 0.1 c/s. The sweep rate was approximately 10 c/s/minute. The width of the acid proton signal was then measured twice (forward and reverse). Sideband frequencies of five to twenty c/s were used for signals of different widths. The width of the cyclohexane signal was then remeasured. This procedure was repeated until ten measurements of the acid proton line width were obtained. If the resolution

changed appreciably while a pair of measurements of the acid proton line width were being made, those measurements were discarded. Occasionally, the acid proton line width at room temperature was remeasured at the finish of a series of measurements at higher temperatures, in order to determine if chemical reaction or decomposition had altered the line width. In all cases, the two sets of measurements at room temperature agreed within experimental error.

Line widths were measured directly with a ruler calibrated in tenths of millimeters. In each spectrum the region to low field of the TFA proton signal was scanned because there were no peaks in that region and an accurate measurement of the base line position could be obtained. The "half-height" of the peak was then determined and the width of the signal was measured at that point. This was compared to the peak-to-peak separation of the sidebands in order to calculate the line width in c/s.

A number of specific experiments were carried out in order to determine points of interest. The line width of the acid proton signal of a solution containing only two mole per cent cyclohexane in TFA was measured as a function of temperature. The width of the acid proton signal of a similar solution which contained one drop of water was also measured.

The line width of the acid proton was also measured as a function of aniline concentration. Five solutions with

aniline concentrations from one to five mole per cent were used. The samples were not degassed because it was felt that some of the TFA might evaporate. The cyclohexane line width was not larger than in other solutions. Therefore, the signals cannot have been broadened by oxygen in solution. These experiments were carried out at 50°C because viscosity effects seemed unimportant at this temperature and also because the one mole per cent solution did not exchange appreciably below this temperature. The chemical shifts of the acid and phenyl protons of the aniline solutions were measured relative to cyclohexane at different temperatures.

Trifluoracetic anhydride was added to a series of solutions of aniline in TFA. The effect of changing anhydride concentration upon acid proton line widths at room temperature was investigated.

The UV spectrum of a one mole per cent solution of aniline in TFA was obtained, in order to determine the amount of free aniline in solution . For purposes of comparison, a 20 mole per cent solution of aniline in TFA was prepared and diluted approximately 1:100 and 1:1000 in acetonitrile. The spectra of these two solutions were obtained. A Beckmann DK spectrophotometer was used to obtain these spectra.

(B) <u>N,N-dimethylaniline in TFA</u>

TFA and N,N-dimethylaniline were Eastman White Label grade chemicals and were used without purification. A ten mole

per cent solution of dimethylaniline in TFA was used. The sample was degassed and sealed in an evacuated 5 mm O.D. sample tube.

Spectra were obtained with a Varian DP-60 spectrometer. Experiments at different temperatures were carried out with the aid of the previously mentioned temperature device. The temperature was measured with an iron-constantan thermocouple attached to a Minneapolis-Honeywell Brown recording potentiometer. The sample was allowed to equilibrate for at least two hours at each temperature before the spectrum was obtained. It is believed that the temperature was constant within 0.2°C.

The resolution was adjusted by obtaining the best possible splitting of the methyl doublet of protonated dimethylaniline. Only the apparent H^{+}-N-CH_3 coupling constant was measured. The acid proton was fairly broad, even at room temperature. The broadening was probably due to the viscosity of the solution. Consequently the acid proton line width was not measured. The separation of the methyl doublet was measured by placing sidebands of the doublet on both sides of itself, approximately 20 c/s away. The sideband frequencies were measured by a Hewlett-Packard 521C electronic counter. The doublet spacing was measured ten times at each temperature.

4. RESULTS

(A) Aniline and Haloanilines in TFA

The line widths of TFA and cyclohexane protons of two solutions of cyclohexane in TFA are given below in Table I.*

TABLE I

Concentration (mole %)			Line Width (c/s)		Temperature (°C)
TFA	C_6H_{12}	H_2O	TFA	C_6H_{12}	
98.1	1.9	-	0.44±0.03	0.43±0.03	24.5 ± 0.05
			0.45±0.04	0.46±0.06	42.5 "
97.0	2.1	0.9	0.45±0.05	0.44±0.05	24.7 "
			0.47±0.06	0.45±0.04	43.2 "

All results are the average of ten to twelve measurements. The error limits represent the RMS deviations of the measurements. Since line widths are constant, T_2 must be the same for the protons of cyclohexane and TFA, in the absence of aniline. T_2 for both types of protons appears to be independent of temperature in the temperature range studied. Water apparently has little effect upon the acid proton line width.

The widths of the acid proton signals and acid proton exchange rates of various aniline solutions are given in Table II. Included in Table II are the acid proton line widths of two of the concentrated solutions (eight mole per cent aniline and eight mole per cent m-chloroaniline in TFA). The results for these two solutions are reported in order to show the typical behavior of concentrated solutions. Other results for

---

* All other tables are given at the end of the Chapter.

concentrated solutions are not given because no useful information can be obtained from these results.

The line widths given in Table II are corrected line widths obtained by the use of equation 4.55. It was assumed that the cyclohexane line width represented $1/\pi T_2$ for acid protons. It has already been shown that this is a correct assumption for TFA and cyclohexane in the absence of aniline. Each value of line width is the average of nine or ten measurements. Quoted error limits are the RMS deviations of the sets of line width measurements. Any measurement which differed from the other nine measurements of line width at a given temperature by more than four times the RMS deviation of those measurements has been discarded. It was never necessary to discard more than one measurement.

The corrected acid proton line widths of a series of aniline solutions of different concentrations are given in Table III. It was not possible to obtain the same temperature for each solution. The exchange rates have all been corrected to the expected rate at 50.2°C from the measured activation energy for proton exchange of aniline in TFA. The value of the activation energy is given in the Discussion of Results. The quoted error limits are based on the uncertainties in the measured line widths and temperature. The calculated concentrations of the solutions in moles/liter are also given. They have been calculated by assuming the formation of ideal solutions.

The ratio of $[HA]$ to $[\emptyset NH_3^+]$ is the same for concentrations in mole fractions and moles/litre. The chemical shifts of the acid protons and phenyl protons of the various solutions are given in Table IV. The acid protons shift to high field with increasing temperature. The shifts seem to be nearly independent of aniline concentration. The phenyl proton shift is independent of temperature and aniline concentration.

The corrected line widths of solutions of aniline in TFA and trifluoracetic anhydride are given in Table V. The decrease in acid proton line width appears to be closely related to the ratio of aniline to trifluoracetic anhydride.

The UV spectra are given in Figure 1 (aniline in TFA) and Figure 2 (aniline and TFA in acetonitrile). There should be a secondary peak due to aniline at $\approx$ 280 mu and one due to anilinium ions at $\approx$ 254 mu (150). These values are those for the two substances in water and may be slightly different in other solvents. The extinction coefficients are respectively 1430 and 160. Consequently, the aniline peak should be relatively more intense. It can be seen in Figure 1 that there is a large peak in the region 270 - ? mu which partly overlaps with the solvent peak, starting at 252 mu. The peak has a "tail" in the region 320-270 mu which may or may not be due to aniline. In Figure 2 there is a large peak at approximately 285 mu which must be due to free aniline. The peak due to anilinium ions, if present, is obscured by the TFA peak. The

aniline peak is quite broad and occurs in the same region as the "tail" of the anilinium ion in Figure 1. Therefore, the tail probably represents a peak due to free aniline which partly overlaps with the anilinium ion peak. The ratio $[\emptyset NH_2] / [\emptyset NH_3^+]$ must be very small to give a spectrum of this type.

The plots of line width versus temperature^{-1} are given in Figures 3 to 16.

(B) N,N-dimethylaniline in TFA

The measured methyl doublet separations at various temperatures are given in Table VI. It will be shown in Part 6 that the collapse of the doublet was due entirely to exchange of ammonio proton spins. The lifetime of a protonated molecule with a given spin configuration of the ammonio proton and the rate of exchange of proton spins are also given. These values have been calculated by using equation 3.25. It was assumed that the doublet separation at 26.8°C represented the true value of the H^+-CH_3 coupling constant.

Equation 3.25 is accurate only if the inverse of the transverse relaxation time of the methyl protons is small compared to the separation of the methyl doublet. In the absence of exchange, the methyl proton line width was about 0.45 c/s. The maximum doublet separation was 5.26 c/s. Since the minimum doublet separation which was measured was 3.65 c/s, it is felt that very little error was introduced by the use of equation 3.25.

Even when the doublet separation was only 3.65 c/s, the spectrum consisted of two distinct peaks with a central minimum between them at about two thirds of the maximum peak height. The two peaks were nearly symmetrical and the positions of the maxima did not appear to be altered by the overlap of the peaks. Two peaks could be observed when the doublet separation was as low as 2.5 c/s. However, when the separation was less than 3 c/s overlap of the peaks appeared to appreciably decrease the observed peak separation.

The plot of log $1/\gamma$ versus 1/T is given in Figure 17.

FIGURE 1. Reproduction of the UV spectra of (1) pure TFA and (2) a one mole per cent solution of aniline in TFA.

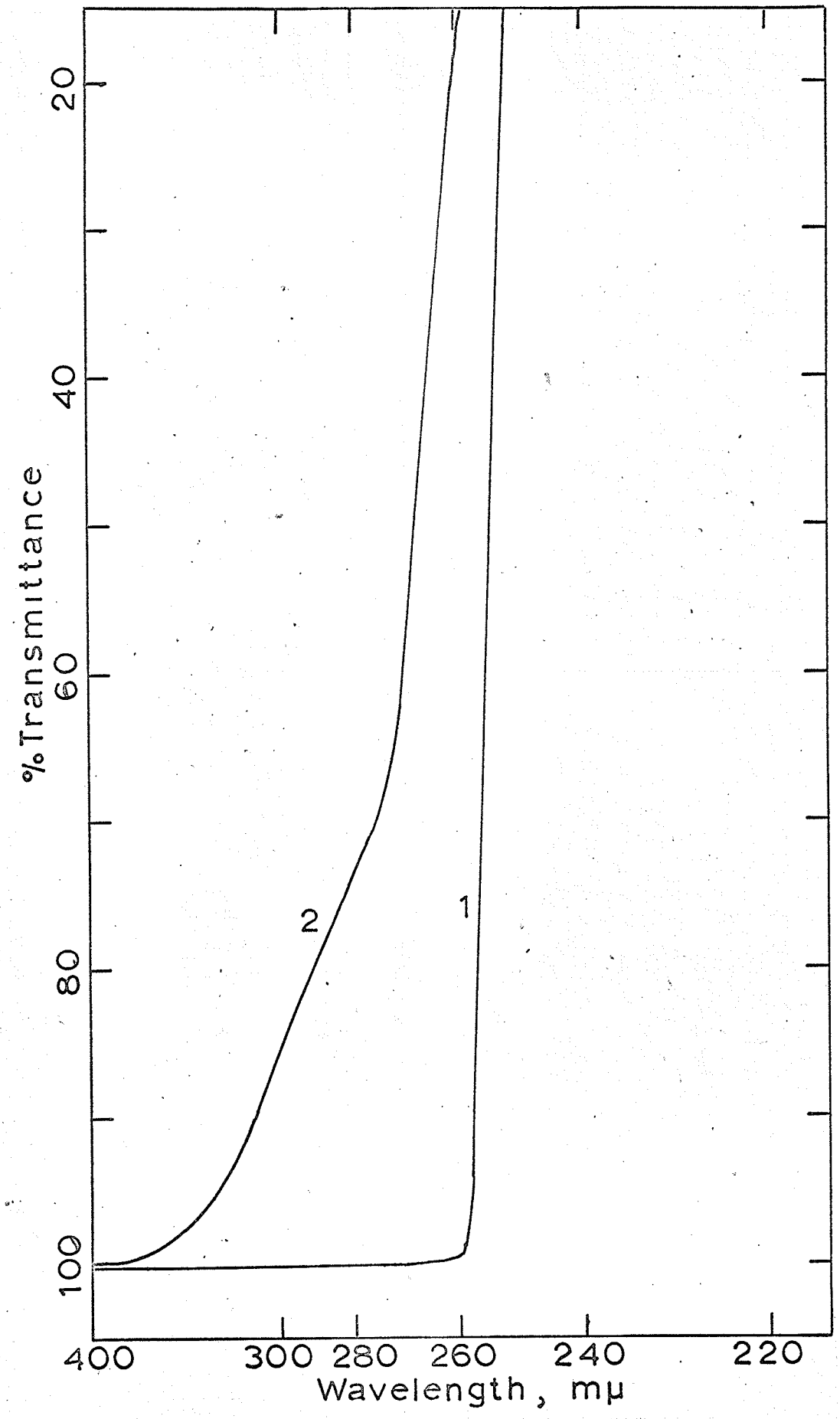
% Transmittance
20
40
60
80
100
2
1
400
300
280
260
240
220
Wavelength, mμ

FIGURE 2. Reproduction of the UV spectra of a twenty mole per cent solution of aniline in TFA diluted (2) 1:1000 in acetonitrile and (3) 1:100 in acetonitrile. Line (1) represents the base line.

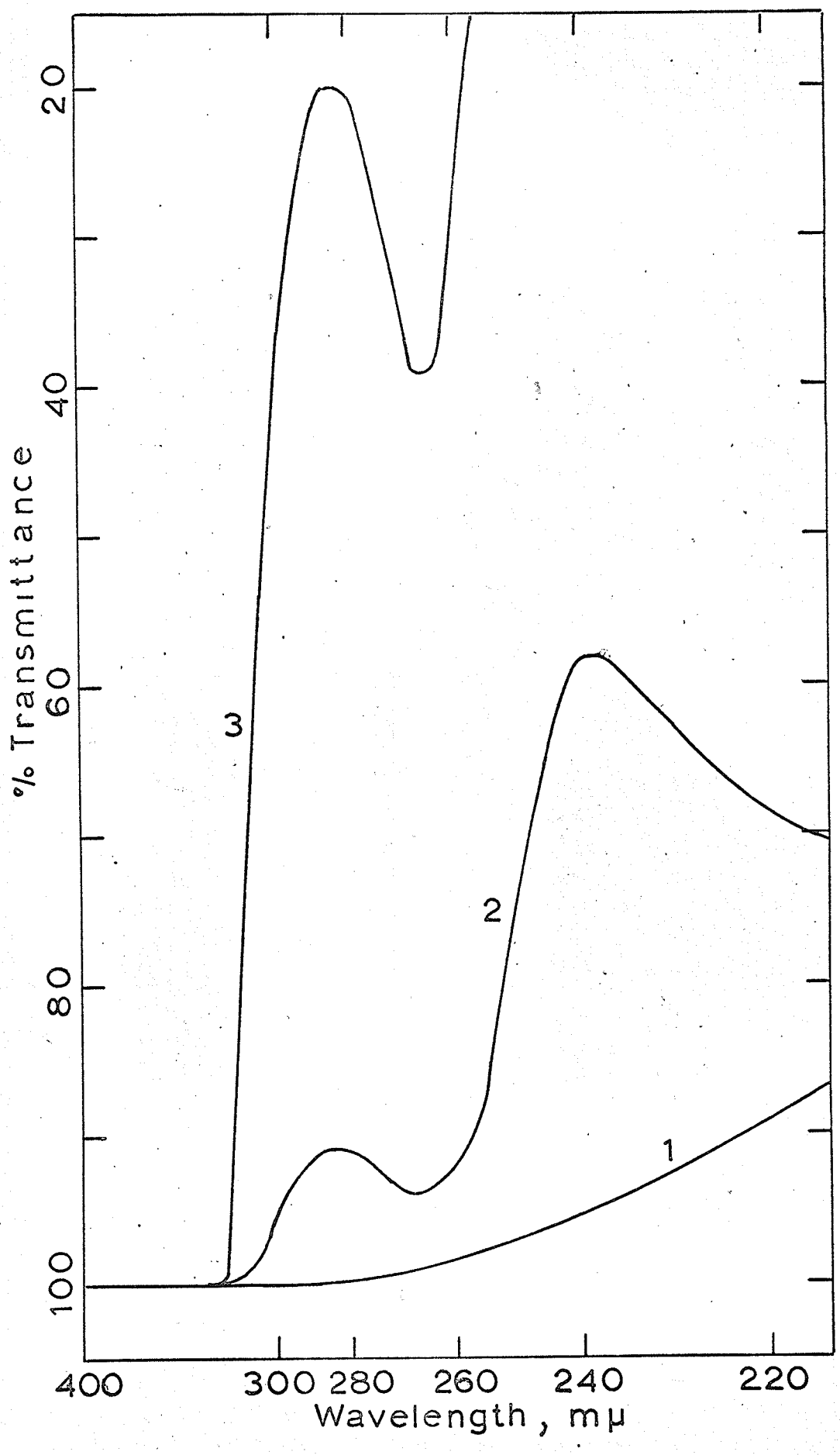
% Transmittance
20
40
60
80
100
3
2
1
400
300
280
260
240
220
Wavelength, mμ

FIGURE 3. Plot of log (TFA proton line width) versus (absolute temperature)$^{-1}$ for a four mole per cent solution of aniline in TFA. The rectangles give the uncertainties in temperature and acid proton line width.

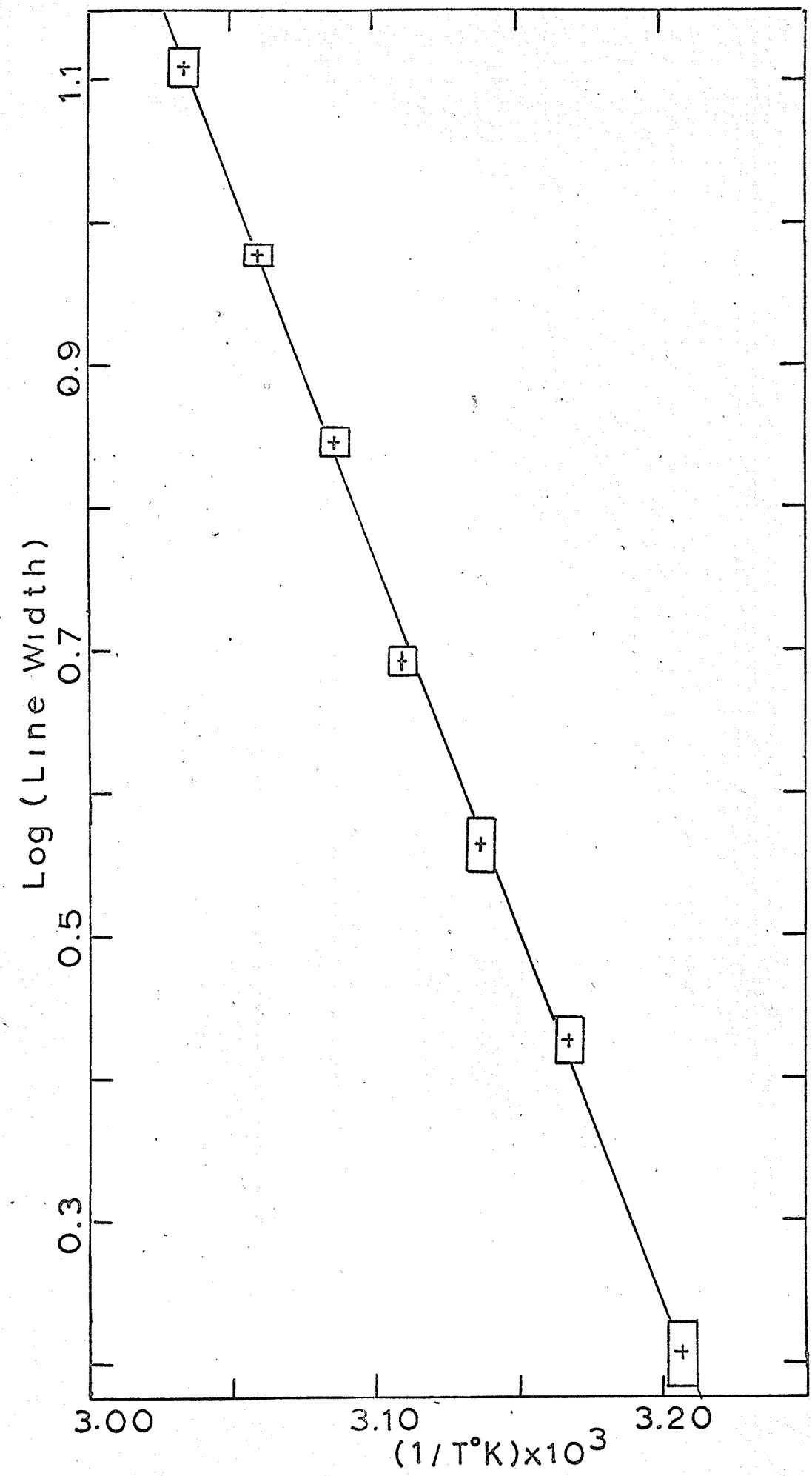
Log (Line Width)
0.3
0.5
0.7
0.9
1.1
3.00
3.10
3.20
(1/T°K)x10^3

FIGURE 4. Plot of log (TFA proton line width) versus (absolute temperature)$^{-1}$ for a two mole per cent solution of p-fluoroaniline in TFA. The circles represent the measured TFA proton line widths of the solution containing undistilled p-fluoroaniline.

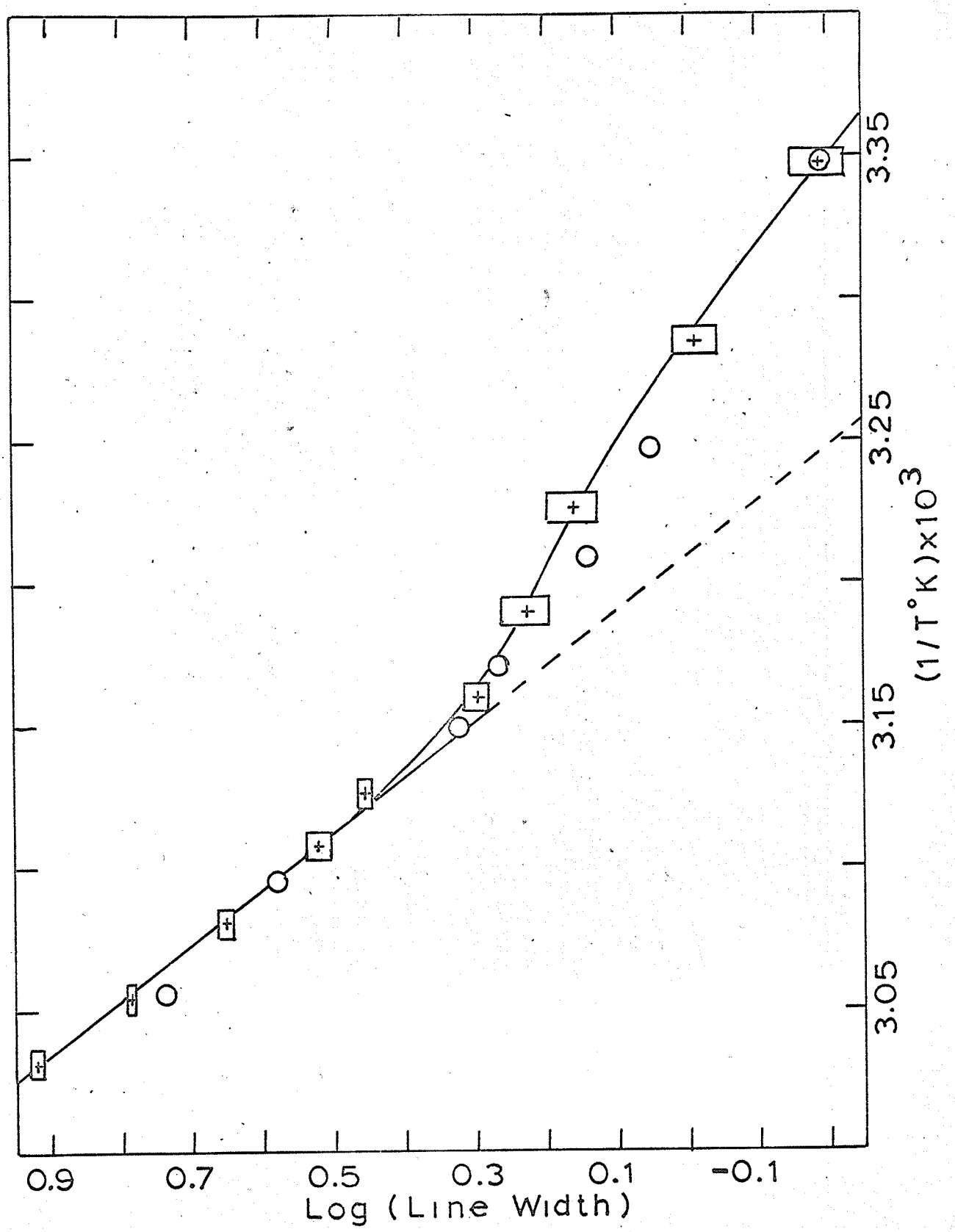
0.9
0.7
0.5
0.3
0.1
-0.1
Log (Line Width)
3.05
3.15
3.25
3.35
(1/T°K)×10^3

FIGURE 5. Plot of log (TFA proton line width) versus (absolute temperature)$^{-1}$ for a three mole per cent solution of p-chloroaniline in TFA.

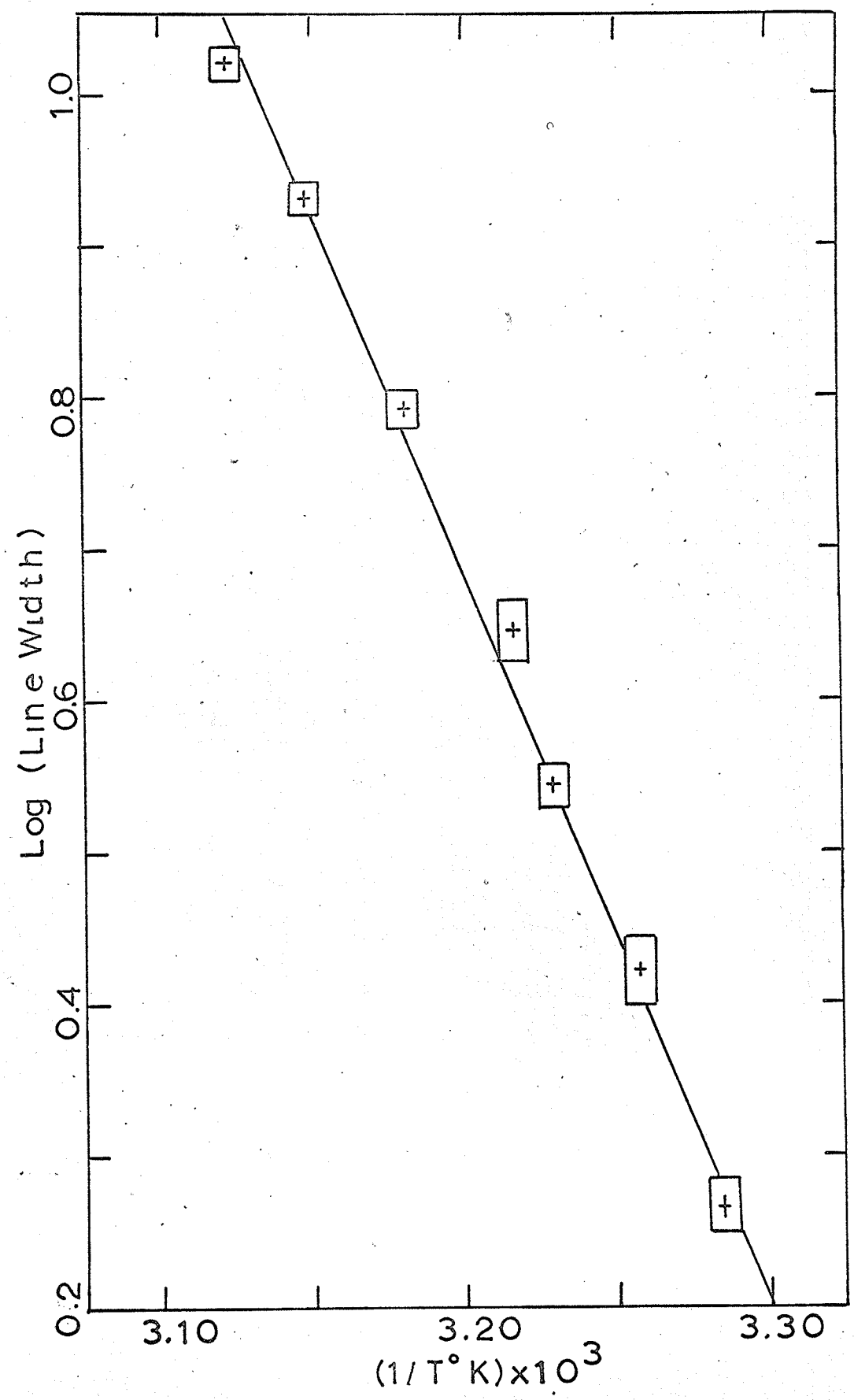
Log (Line Width)
0.2
0.4
0.6
0.8
1.0
3.10
3.20
3.30
(1/T°K)x10^3

FIGURE 6. Plot of log (TFA proton line width) versus (absolute temperature)$^{-1}$ for a two mole per cent solution of ρ-bromoaniline in TFA.

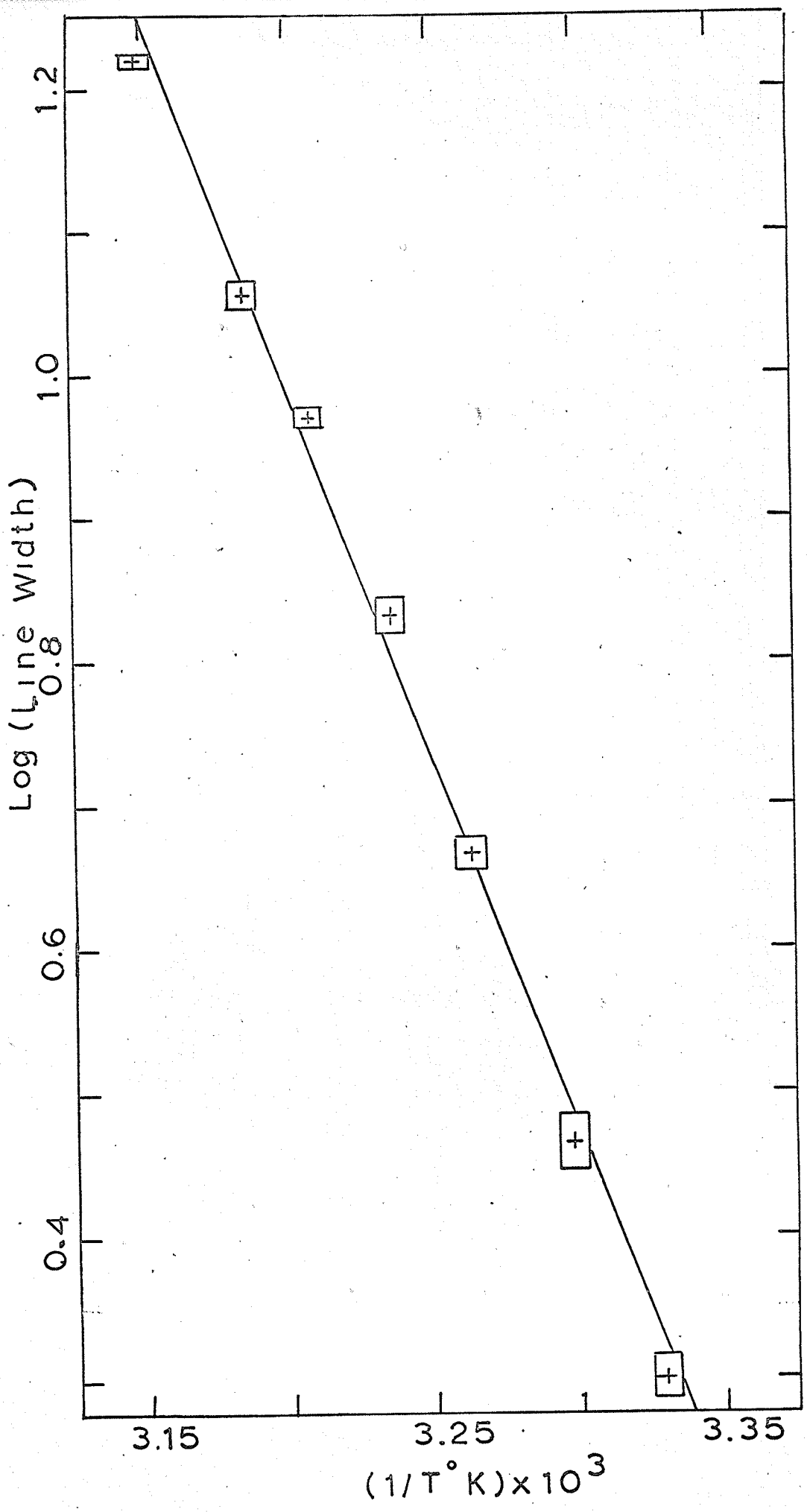
Log (Line Width)
0.4
0.6
0.8
1.0
1.2
3.15
3.25
3.35
(1/T°K)x10^3

FIGURE 7. Plot of log (TFA proton line width) versus (absolute temperature)$^{-1}$ for a two mole per cent solution of p-iodoaniline in TFA.

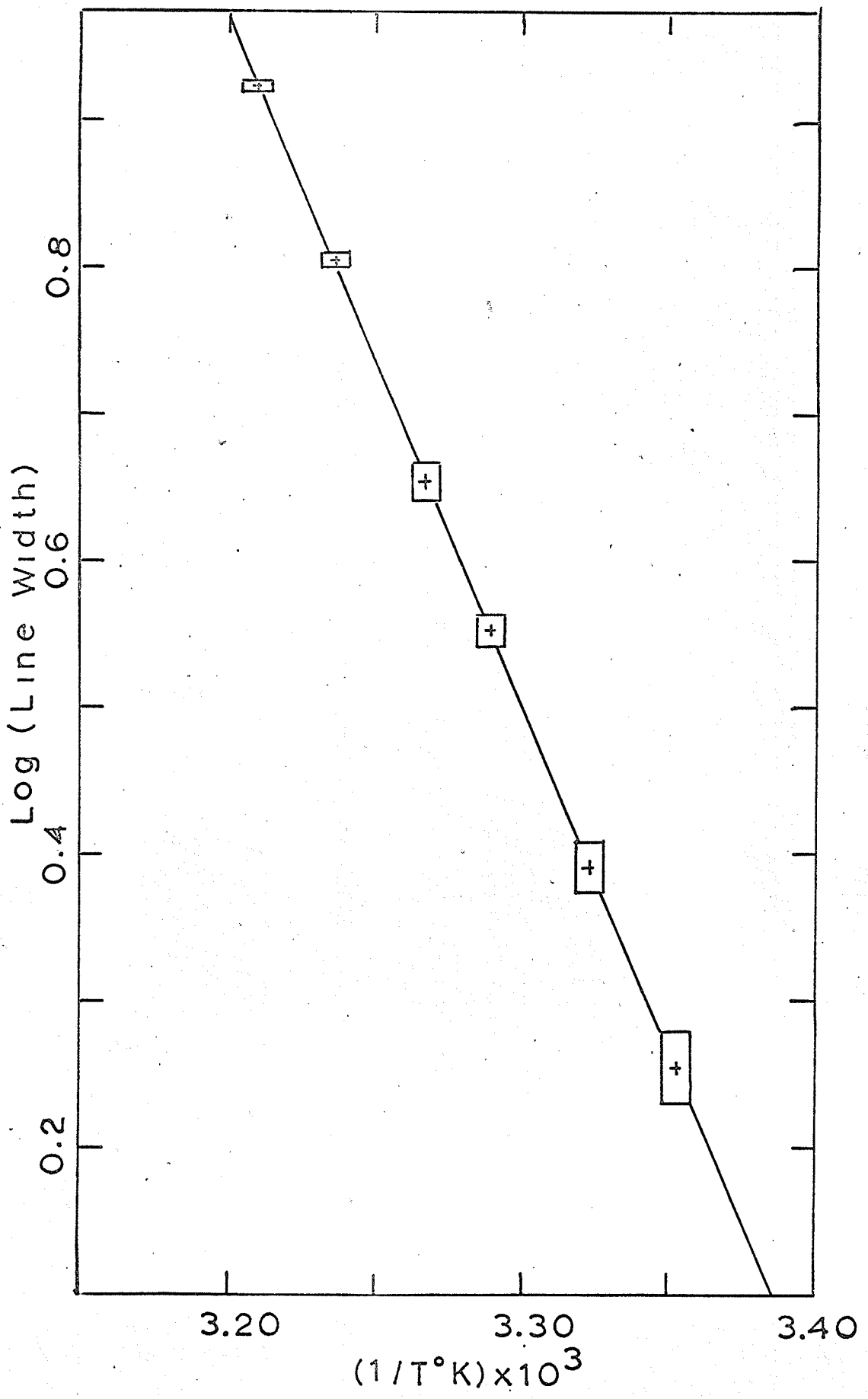
Log (Line Width)
0.2
0.4
0.6
0.8
3.20
3.30
3.40
(1/T°K)x10^3

FIGURE 8. Plot of log (TFA proton line width) versus (absolute temperature)$^{-1}$ for a two mole per cent solution of m-iodoaniline in TFA.

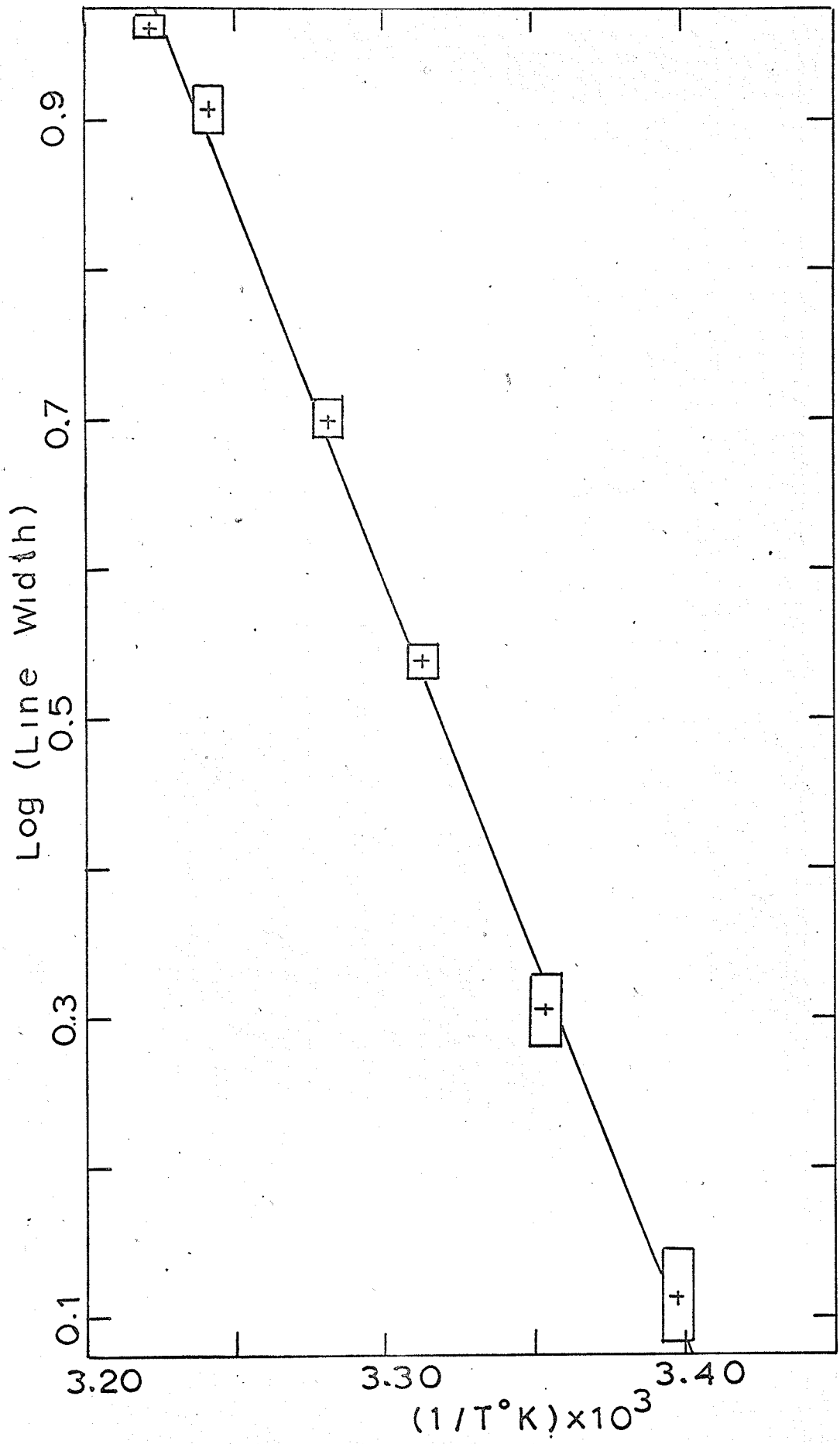
Log (Line Width)
0.1
0.3
0.5
0.7
0.9
3.20
3.30
3.40
(1/T°K)×10^3

FIGURE 9. Plot of log (TFA proton line width) versus (absolute temperature)$^{-1}$ for a two mole per cent solution of m-bromoaniline in TFA.

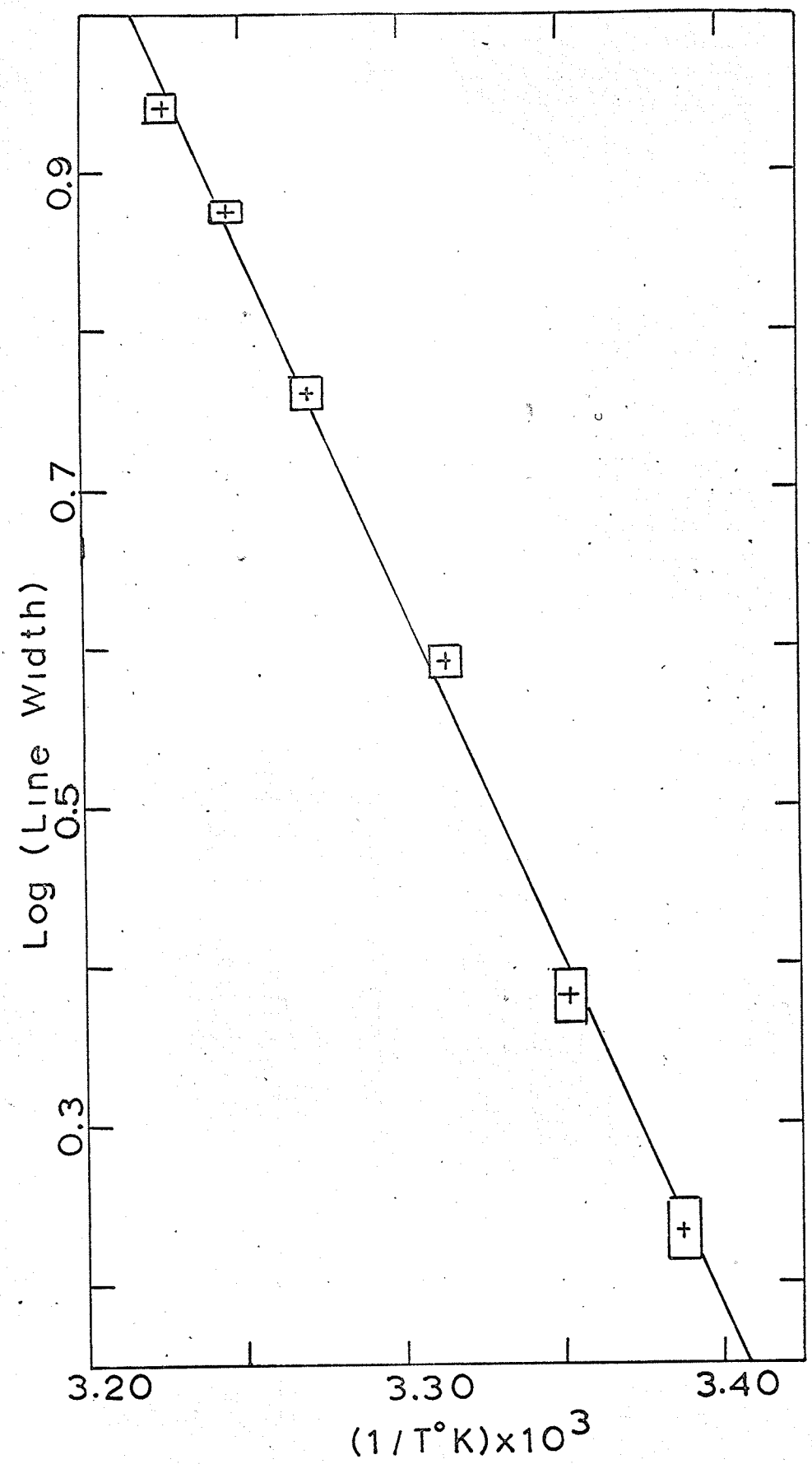
0.9
0.7
0.5
0.3
Log (Line Width)
3.20
3.30
3.40
(1/T°K)x10^3

FIGURE 10. Plot of log (TFA proton line width) versus (absolute temperature)$^{-1}$ for a three mole per cent solution of m-chloroaniline in TFA.

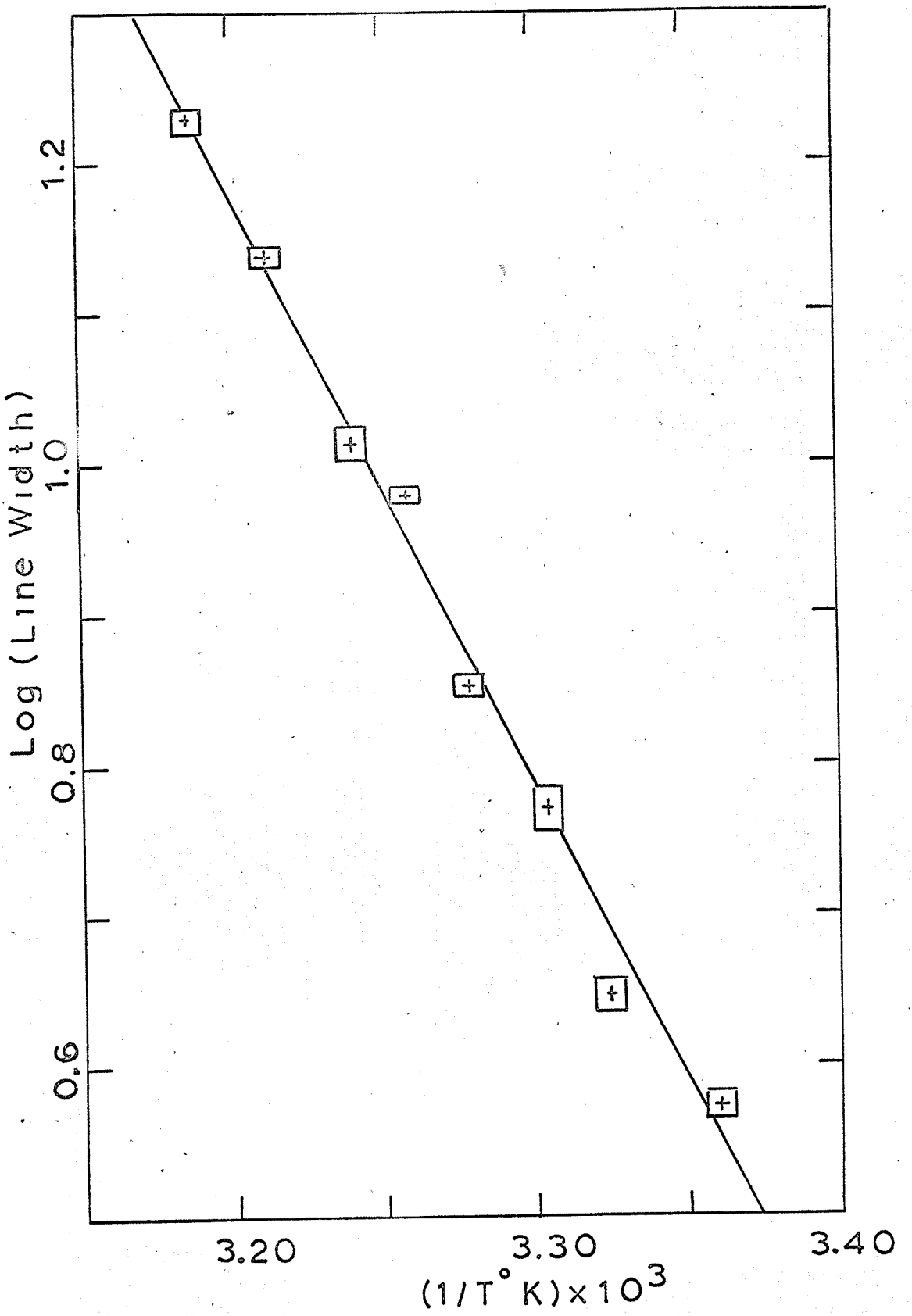
Log (Line Width)
1.2
1.0
0.8
0.6
3.20
3.30
3.40
(1/T°K)×10³

FIGURE 11. Plot of log (TFA proton line width) versus (absolute temperature)$^{-1}$ for a one mole per cent solution of m-fluoroaniline in TFA. The broken line represents the calculated TFA proton line width in the coalesced region. It has been calculated by use of equation 4.56 (see text).

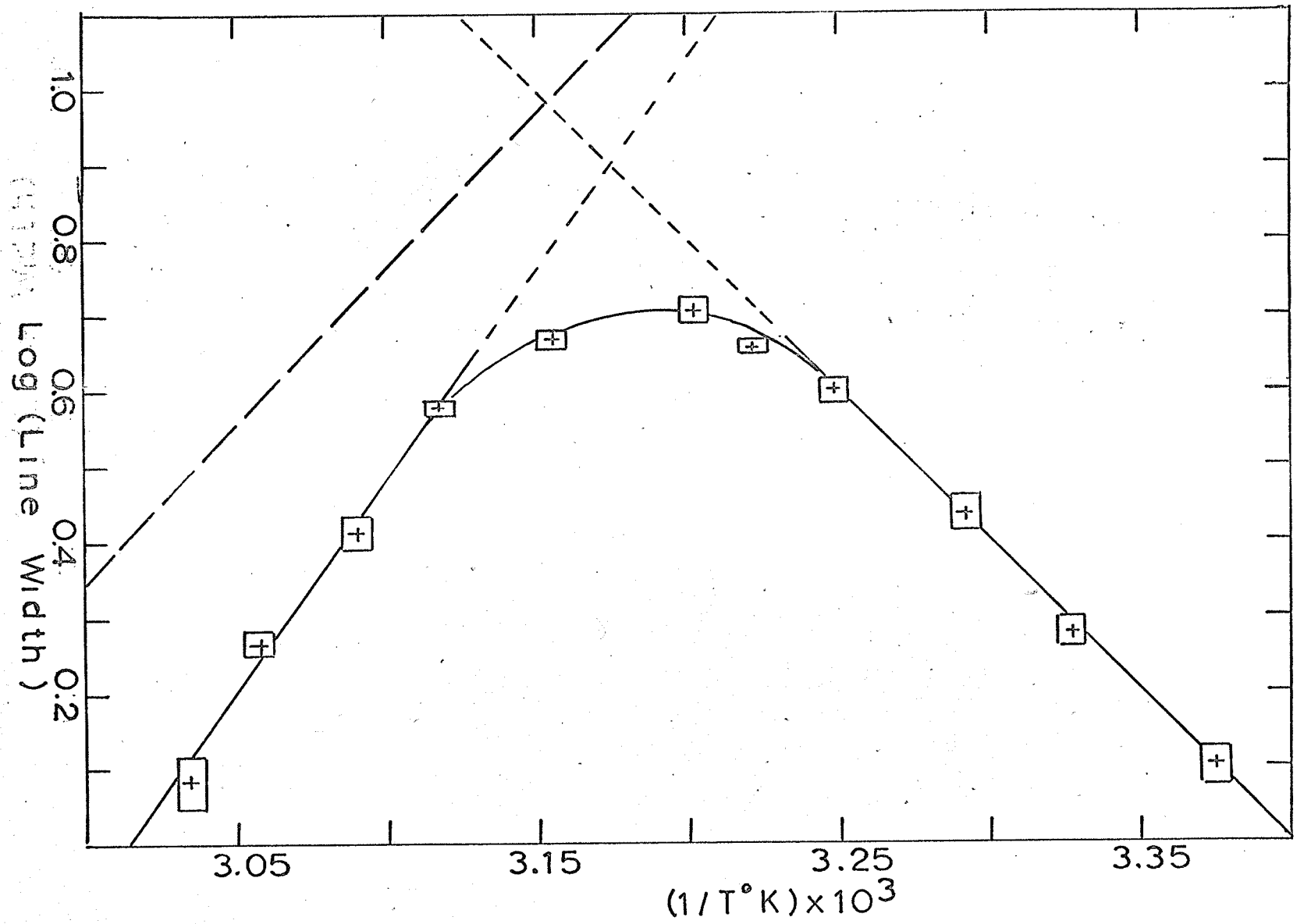
1.0
0.8
0.6
0.4
0.2
Log (Line Width)
3.05
3.15
3.25
3.35
(1/T°K)×10^3

FIGURE 12. Plot of log (TFA proton line width) versus (absolute temperature)$^{-1}$ for a one mole per cent solution of o-fluoroaniline in TFA.

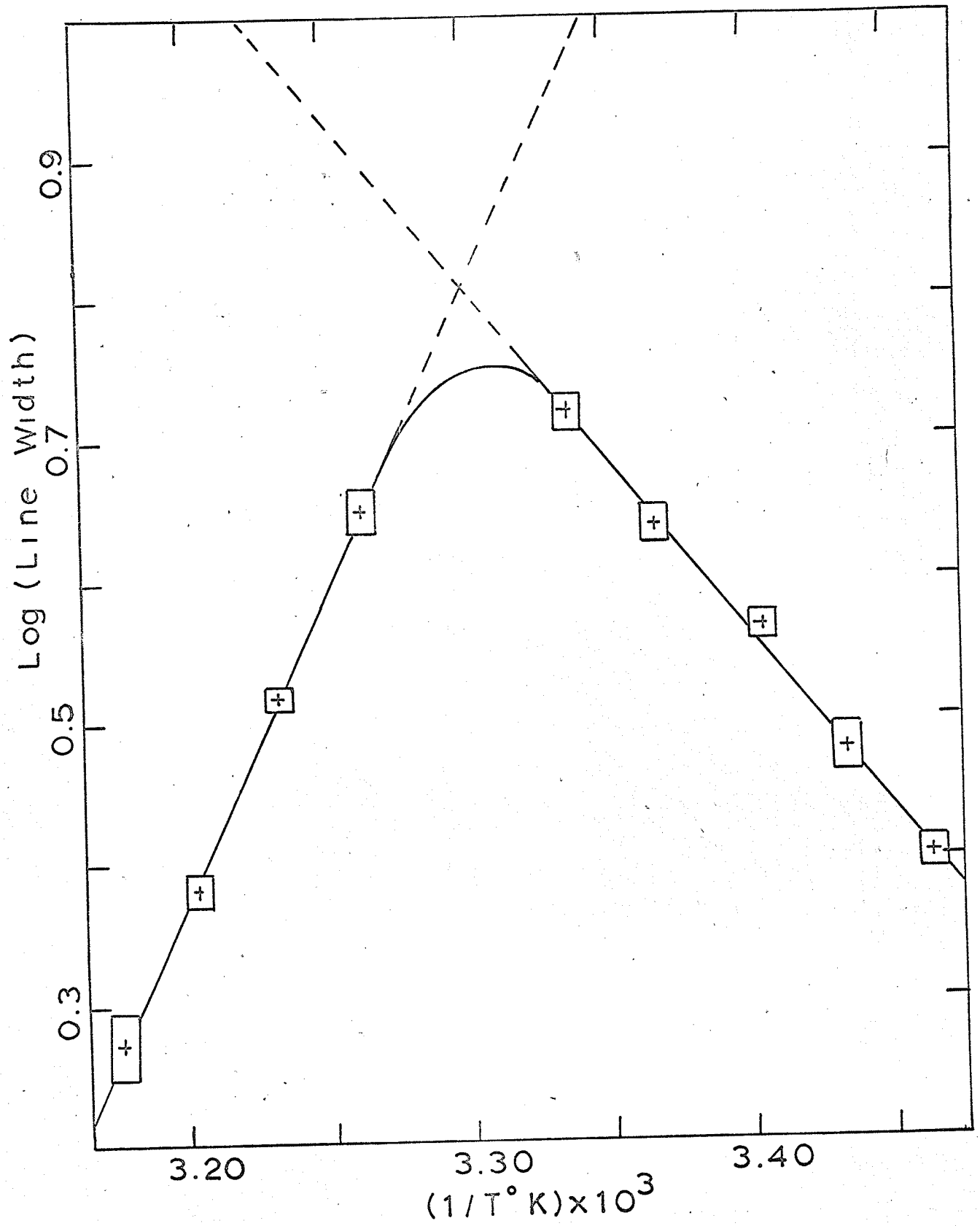
Log (Line Width)
0.3
0.5
0.7
0.9
3.20
3.30
3.40
(1/T° K)x10^3

FIGURE 13. Plot of log (TFA proton line width) versus (absolute temperature)$^{-1}$ for a two mole per cent solution of o-chloroaniline in TFA.

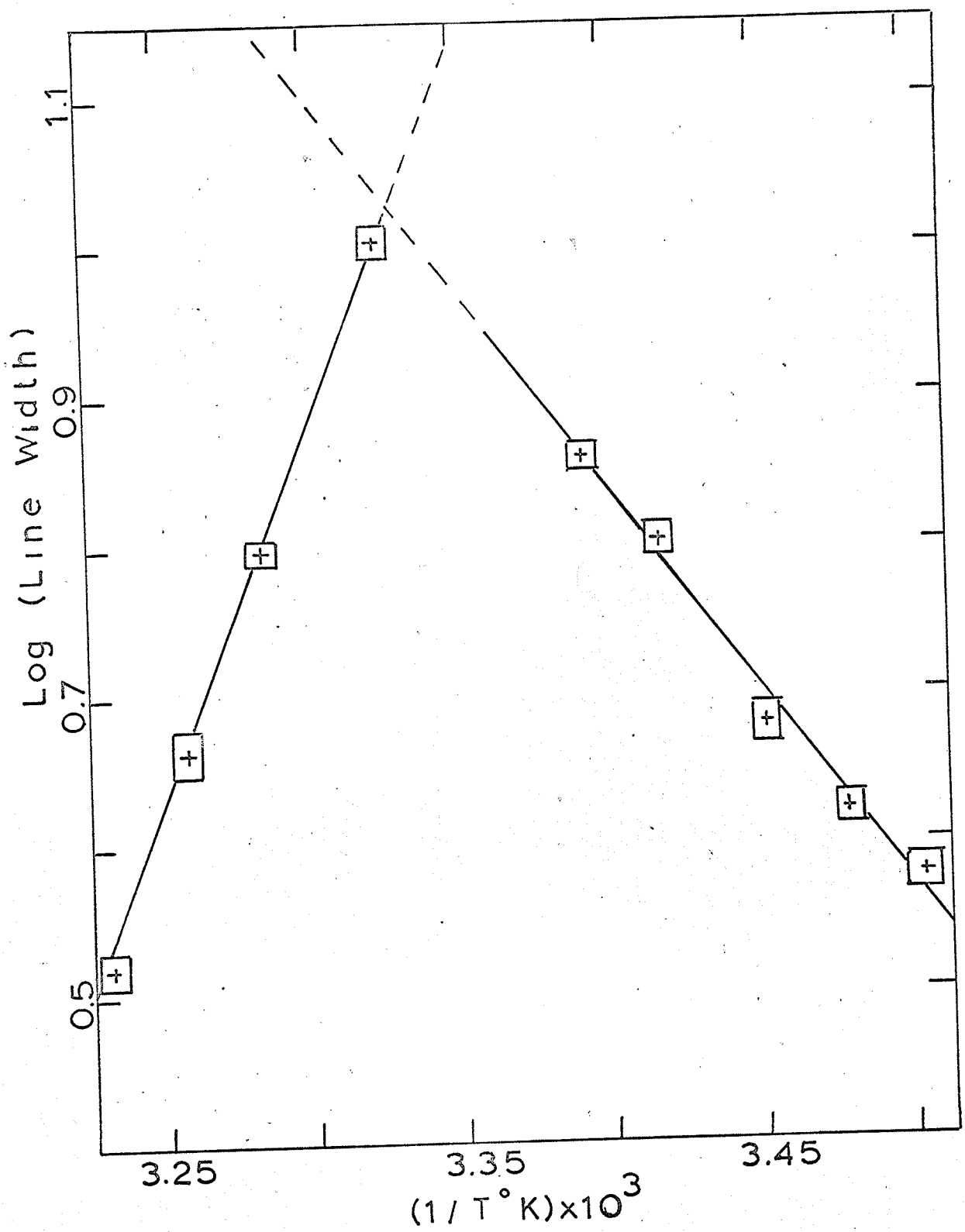
Log (Line Width)
0.5
0.7
0.9
1.1
3.25
3.35
3.45
(1/T°K)x10^3

FIGURE 14. Plot of log (TFA proton line width) versus (absolute temperature)$^{-1}$ for a one mole per cent solution of o-bromoaniline in TFA.

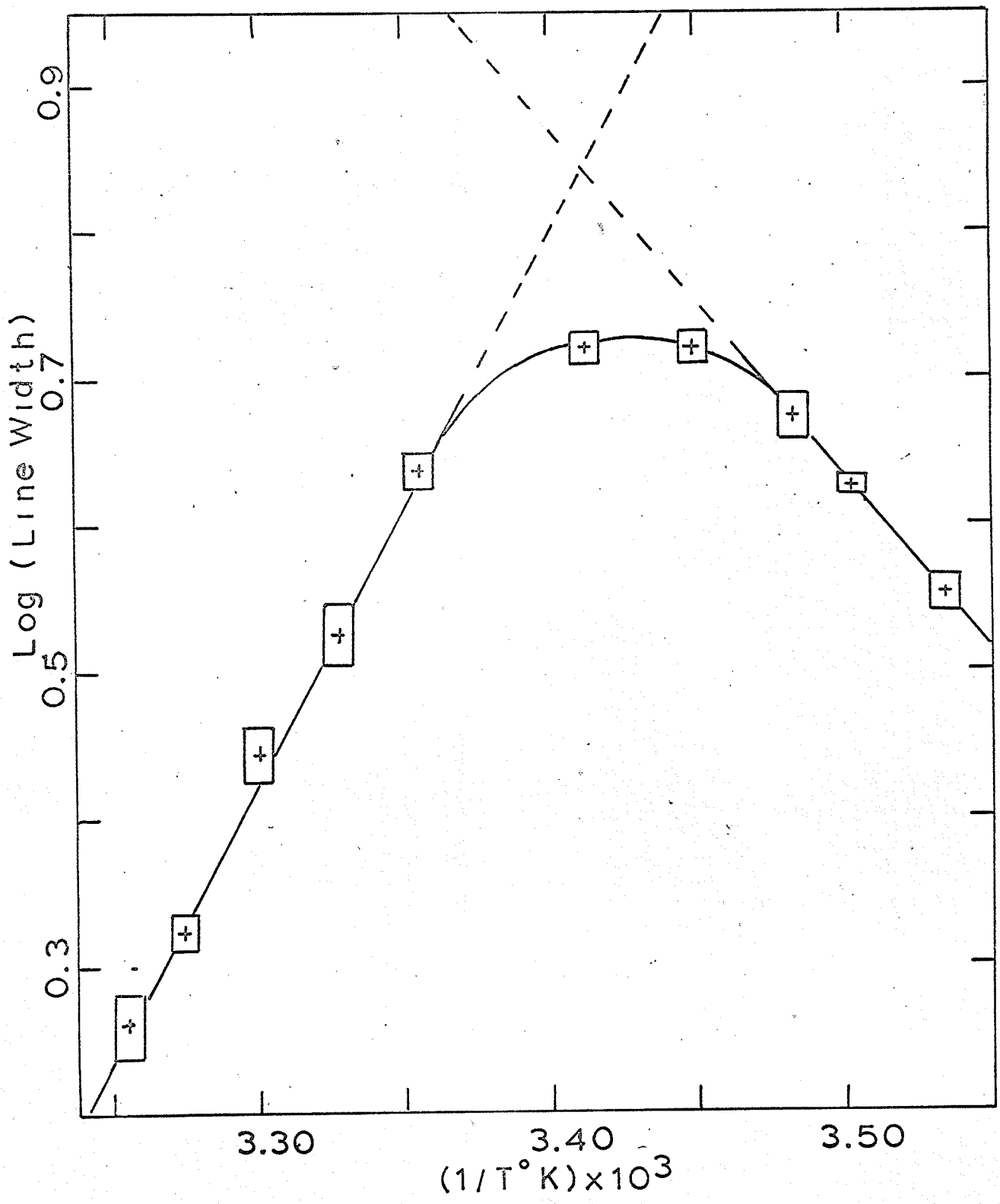
Log (Line Width)
0.9
0.7
0.5
0.3
3.30
3.40
3.50
(1/T°K)x10^3

FIGURE 15. Plot of log (TFA proton line width) versus (absolute temperature)$^{-1}$ for an eight mole per cent solution of aniline in TFA.

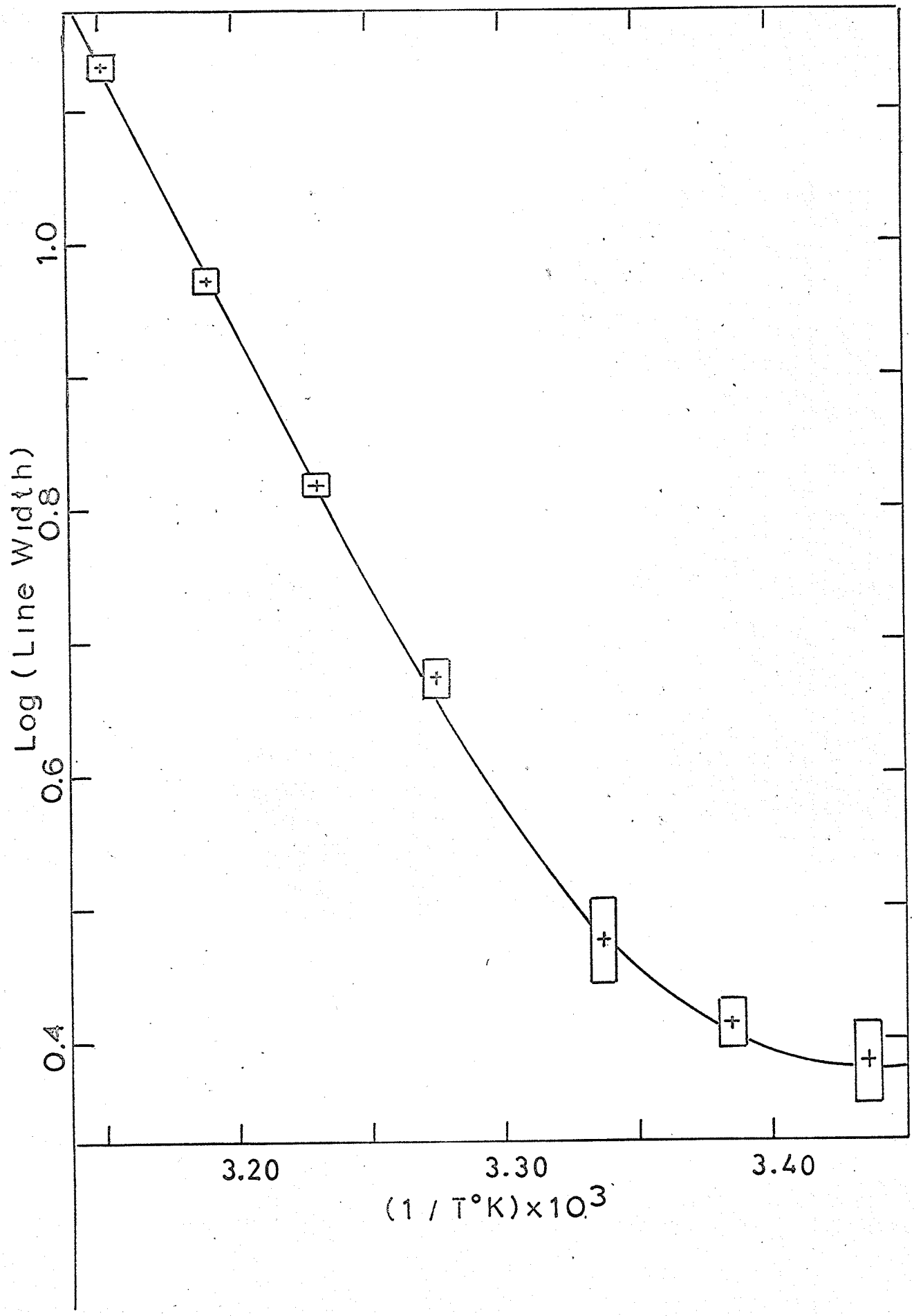
Log (Line Width)
1.0
0.8
0.6
0.4
3.20
3.30
3.40
(1 / T°K) x 10^3

FIGURE 16. Plot of log (TFA proton line width) versus (absolute temperature)$^{-1}$ for an eight mole per cent solution of m-chloroaniline in TFA.

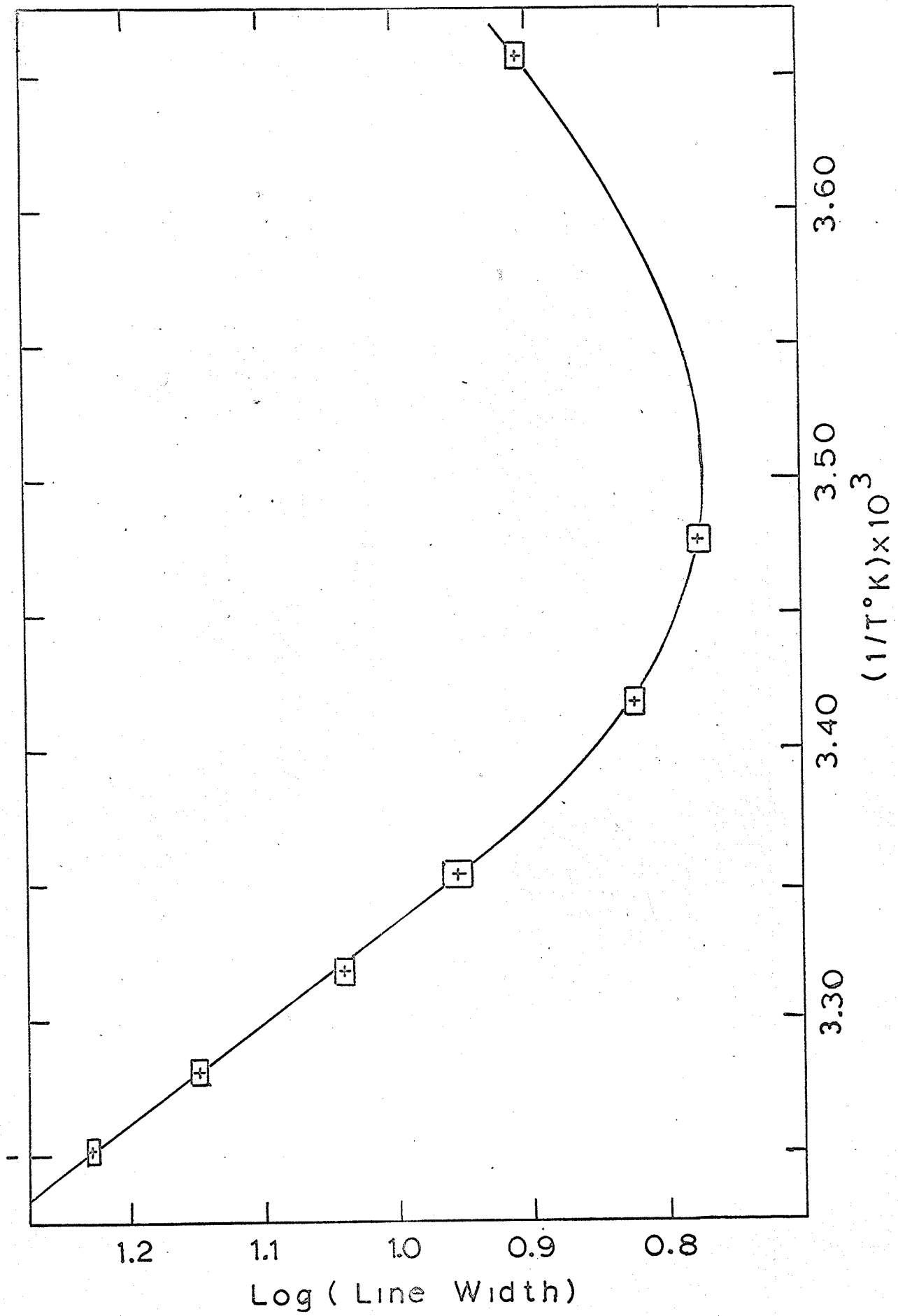
3.30
3.40
3.50
3.60
(1/T°K)×10^3
1.2
1.1
1.0
0.9
0.8
Log (Line Width)

FIGURE 17. Plot of log (calculated ammonio proton spin exchange rate) versus (absolute temperature)$^{-1}$ for a ten mole per cent solution of N,N-dimethylaniline in TFA. $J_{(H_3C-N-H^+)}$ is assumed to be equal to the measured splitting of the methyl doublet at 26.8°C. The exchange rate has been calculated from equation 3.25.

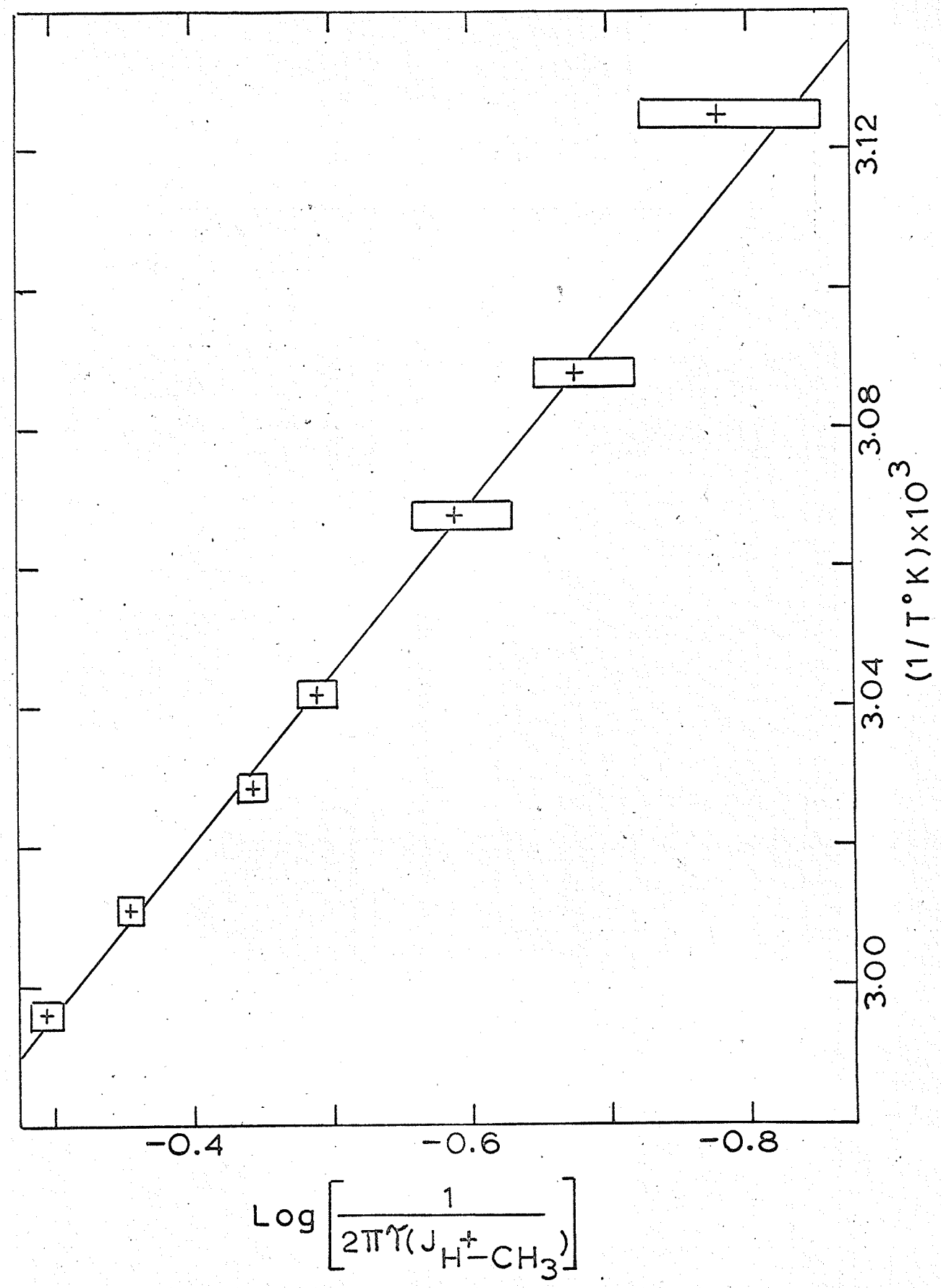
3.12
3.08
3.04
3.00
(1/T°K)×10^3
−0.4
−0.6
−0.8
Log [1 / 2πΥ(J H+−CH3)]

5. DISCUSSION OF RESULTS FOR ANILINE AND HALOANILINES

(A) Factors Affecting the Shapes of Plots of Acid Proton Line Width Versus Temperature

The plots of log ($\Delta\nu$) versus 1/T are essentially linear for all dilute aniline solutions except p-fluoroaniline (Figure 4). The non-linearity of Figure 4 is considered in Part D.

The linearity of the plots suggests that there can only be one reaction occurring in solution which affects the acid proton line width. Since the plots are linear even for very low acid proton exchange rates, the assumption that T_2 acid = T_2 cyclohexane (where T_2 acid is T_2 in the absence of exchange) must be correct for dilute solutions of aniline in TFA.

It can be considered that the acid proton exchange reactions are catalyzed by the addition of anilines and that the slopes of the plots (Figures 3 to 14) are proportional to the activation energies of the catalyzed exchange reactions.

The line widths of the acid proton signals of one mole per cent solutions of anilines in TFA (Figures 11 to 14) reach maximum values and then decrease with increasing temperature. The decreases must occur when the exchange rates are fast enough to coalesce the acid and ammonio proton signals. The acid proton exchange rate which causes this collapse depends upon the relative populations of acid and ammonio protons and upon the chemical shift between the two types of protons in the absence

of exchange (see equation 4.56). Presumably the same behaviour would be noted for the other solutions if the line widths were measured at higher temperatures.

The exchange rates at lower temperatures can be extrapolated to higher temperatures. With these values of exchange rate, equation 4.56 can be used to calculate the expected line widths at higher temperatures if a value of $(\omega_A - \omega_B)$ can be obtained. The results for such a calculation for m-fluoroaniline in TFA are shown in Figure 11. It has been assumed that $(\omega_A - \omega_B) = 2\pi(160\ c/s)$ and that the ammonio triplet is completely collapsed. The value of 160 c/s is an average value of the shifts between acid and ammonio protons obtained from Chapter 2. The experimental exchange rate is greater than the predicted rate. This may or may not be significant since 160 c/s may not be the correct value of the chemical shift between acid and ammonio protons.

What is significant is the difference in slopes of the lines in the coalesced and uncoalesced regions. If it is assumed that only acid-ammonio proton exchanges are occurring, then equations 4.55 and 4.56 can be reduced to

$$\pi \Delta \nu_{corrected} = \left(\pi \Delta \nu - \frac{1}{T_2}\right) = \frac{1}{\tau_{ACID}} \qquad 4.72$$

and

$$\pi \Delta \nu_{corrected} = A \cdot \tau_{ACID} \qquad 4.73$$

where $A = P_A P_B^2 (\omega_A - \omega_B)^2$.

$1/\tau_{acid} = k$, the rate constant for acid exchange. Therefore, it can be shown from the simple Arrhenius equation that the plots of $\log \pi\Delta\nu_{corr.}$ versus 1/T should have the same slopes (with opposite signs) in the two regions.

The different slope may be due to incomplete collapse of the ammonio triplet. It may also be due to additional reactions which affect the lifetime of the ammonio protons but not of the acid protons (see Part B). However, since the ammonio protons are present in much smaller concentrations than the acid protons, it is unlikely that either of these explanations can account for the marked difference in slope. A more probable explanation is suggested by the results in Table IV. The high field shifts with temperature of the acid protons are nearly independent of aniline concentration. There is a high field shift of 46 c/s of the acid proton in the 5 mole per cent aniline solution when the temperature is changed from 27° to 69°C. The acid protons and ammonio protons are present in a ratio of 6:1. Therefore, if the acid proton shift is caused solely by exchange, then $(\omega_A - \omega_B) > 2\pi(320$ c/s). This appears most unlikely. Most probably, the high field shift is partly due to a decrease in acid molecule hydrogen bonding with increasing temperature. This would also account for the increased slope of the line width plot in the coalesced region. If $(\omega_A - \omega_B)$ and consequently A (equation 4.73) are decreasing constantly, then $\pi\Delta\nu$ will also decrease more

rapidly than would be expected.

The curved line plots obtained for the more concentrated solutions (Figures 15 and 16) have not yet been explained. There appear to be two possible explanations. The first is that competing reactions are occurring in solution. The second is that TFA and cyclohexane protons have different relaxation times.

The first explanation appears unlikely. Since the line actually reverses slope (Figure 16) any additional reaction must have an apparent negative activation energy. Therefore, it is unlikely that simultaneous reactions are occurring.

The concentrated aniline solutions are quite viscous at low temperatures. The line width of the cyclohexane signal sometimes increases from its normal value of 0.4 c/s to as much as 0.6 c/s. However, the increase in line width of the acid protons cannot arise from bulk viscosity effects because these effects should be the same for both types of protons. However, acid molecules and cyclohexane molecules can conceivably have different correlation times. Many of the acid molecules presumably exist in solvation shells around the ions and/or ion pairs whereas the cyclohexane molecules exist in a less solvated state. Since acid protons are not as free to move, their correlation times should be longer. Presumably both solvation and correlation times increase as temperature decreases. If as a result of solvation, acid protons are held

close to atoms with nuclear spins and if $\tau_{acid} < (2\pi\nu_0)^{-1}$, then T_1 of the acid protons should decrease with decreasing temperature. This could account for the negative slope in the low temperature region of Figure 16. If T_1 broadening is greater than exchange broadening at low temperatures, then the slope of the plot of log (line width) versus $1/T$ should be negative.

If the acid proton broadening at $0^{o}C$ is assumed to be entirely due to T_1 effects, then $T_1 \approx 0.05$ sec. A decrease in the number of ions in solution or an increase in temperature will decrease the amount of solvation and decrease the correlation time of the protons. Therefore, it is probable that T_1 broadening is insignificant in dilute aniline solutions at higher temperatures.

(B) <u>Probable Reactions in Solution and Their Effect Upon the Observed Kinetics</u>

It has already been pointed out that the exchange reactions can be considered to be catalyzed proton exchange reactions. It is desirable to consider the individual exchange reactions which may be occurring, in order to correlate exchange rates and thermodynamic data with the nature of reactions and reactants.

There are a number of reactions in solutions of aniline in TFA which involve changes in the magnetic environment of protons. In some of the reactions, hydrogen bonds are made

or broken. These reactions can sometimes be detected by NMR spectroscopy while they cannot be detected by ordinary chemical methods. Reactions in which ammonio protons are involved and TFA protons are not involved will not be detected by measurement of the acid proton signal, if there are separate acid and ammonio proton signals. The probable reactions occurring in solution are listed below.

$$\phi NH_3^+ + A^- \underset{k_{-1}}{\overset{k_1}{\rightleftharpoons}} \phi NH_2 + HA \qquad \text{I}$$

$$\underline{\text{OR}} \begin{cases} \phi NH_3^+ + A^- \underset{k_{-2}}{\overset{k_2}{\rightleftharpoons}} (\phi NH_3^+ \cdots A^-) & \text{II} \\ (\phi NH_3^+ \cdots A^-) \underset{k_{-3}}{\overset{k_3}{\rightleftharpoons}} (\phi NH_2 \cdots HA) & \text{III} \\ (\phi NH_2 \cdots HA) \underset{k_{-4}}{\overset{k_4}{\rightleftharpoons}} \phi NH_2 + HA & \text{IV} \end{cases}$$

$$A^- + HA \xrightarrow{k_5} AH + A^- \qquad \text{V}$$

$$\phi NH_3^+ + H_2N\phi \xrightarrow{k_6} \phi NH_2 + {}^+H_3N\phi \qquad \text{VI}$$

$$2HA \underset{k_{-7}}{\overset{k_7}{\rightleftharpoons}} AH_2^+ + A^- \qquad \text{VII}$$

In addition, solvation reactions of TFA with ions and molecules in solution are occurring.

Reaction V involves the transfer of protons between equivalents sites and will not be detected by NMR. Reaction VI does not involve acid protons and will not be detected by measurements of acid proton line widths. However, it will affect the line width of the ammonio proton signal. Each

time an ammonio group loses a proton, the remaining two protons are transformed into amino protons and are therefore in a new magnetic environment. At the same time, two amino protons become ammonio protons. Only the proton which is transferred is not relaxed by the exchange reaction.

Reaction IV and some of the solvation reactions involve the making and breaking of acid hydrogen bonds. These reactions exchange protons between H-bonded and non-H-bonded states and consequently cause T_2 relaxation. Hydrogen bond exchange reactions are probably much faster than the other reactions in most of the solutions studied. Experimentally it has been found that many plots of line width versus temperature are linear for exchange rates as low as 5/molecule second. This indicates that the acid proton peaks of dilute aniline solutions are not appreciably broadened by hydrogen bond exchange reactions. However, it has been shown (Part A) that solvation may have caused an increase in acid proton line widths in concentrated solutions of aniline in TFA at low temperatures.

Reaction VII is an auto-protolysis reaction. Such reactions normally have very high rate constants in aqueous solutions (151). The auto-protolysis reaction of TFA cannot have contributed significantly to acid proton line widths because it should also have broadened the acid proton signal of pure TFA. This did not happen.

Acid proton exchange occurs as a result of reaction I (or II,III and IV). Therefore, the acid proton line width will alter as a result of reaction I. Since reaction I is an equilibrium reaction, the overall reaction rates in both directions must be equal. The relative values of the overall rate constants (k_1 and k_{-1}) depend upon the relative activities of the four reacting species.

It is reasonable to assume that aniline exists in solution almost entirely as anilinium ions. The large excess of TFA should alter equilibrium concentrations in favor of anilinium ions. UV spectra (Figures 1 and 2) indicated that there was little free aniline present in a one mole per cent solution of aniline in TFA.

The line width of the acid proton signal is related to the average lifetime of an acid molecule by equation 4.55. The rate constant for acid proton exchange is equal to the inverse of the lifetime. Therefore, the total proton exchange rate (expressed as either gain or loss of protons) is $k_{HA} \cdot [HA]$ where $k_{HA} = 1/\tau_{HA}$. The total proton exchange rate can also be expressed in terms of the rate of reaction I.

$$\frac{1}{\tau_{HA}}[HA] = k_1[\emptyset NH_3^+][A^-] = k_{-1}[\emptyset NH_2][HA] \qquad 4.74$$

OR

$$\frac{1}{\tau_{HA}} = k_1 \frac{[\emptyset NH_3^+][A^-]}{[HA]} = k_{-1}[\emptyset NH_2] \qquad 4.75$$

where concentrations are expressed in moles/litre and the k's are apparent rate constants.

Since the aniline concentration is very small, the reaction characterized by the rate constant k_1 can be considered to be the "rate determining" reaction for proton exchange, i.e., the rate of this reaction determines the acid proton line width. If it were possible to change k_1 without changing k_{-1}, then the overall reaction rate would change correspondingly because the concentration of anilinium ions is nearly independent of $K_{equilibrium}$ $(=k_1/k_{-1})$ if K_e is not grossly altered. On the other hand, $[\emptyset NH_2]$ is strongly dependent upon K_e. If k_{-1} were altered and k_1 were kept constant, $[\emptyset NH_2]$ would change but there would be little effect upon the overall proton exchange rate since k_1 and $[\emptyset NH_3^+]$ would be only slightly changed.

The lifetime of TFA protons has been measured as a function of anilinium ion concentration (Table III). It was assumed that all the aniline was in the form of anilinium ions. A series of plots of $[\text{total}\,\emptyset NH_3^+]^n/[HA]$ versus the lifetime of TFA protons have been constructed. The best fit is obtained for n = 1.2 (Figure 18) although reasonable straight lines can be obtained for n = 1.0 to 1.4. Concentrations are in moles/litre.

The rate of reaction I can be expressed in terms of the activities of anilinium ions and trifluoracetate ions and the

FIGURE 18. Plot of TFA proton exchange rate versus

$$\frac{[\emptyset NH_3^+]^{1.2}}{[HA]} \times 10^2.$$

Concentrations are expressed in moles/litre. It is assumed that aniline is completely protonated in TFA.

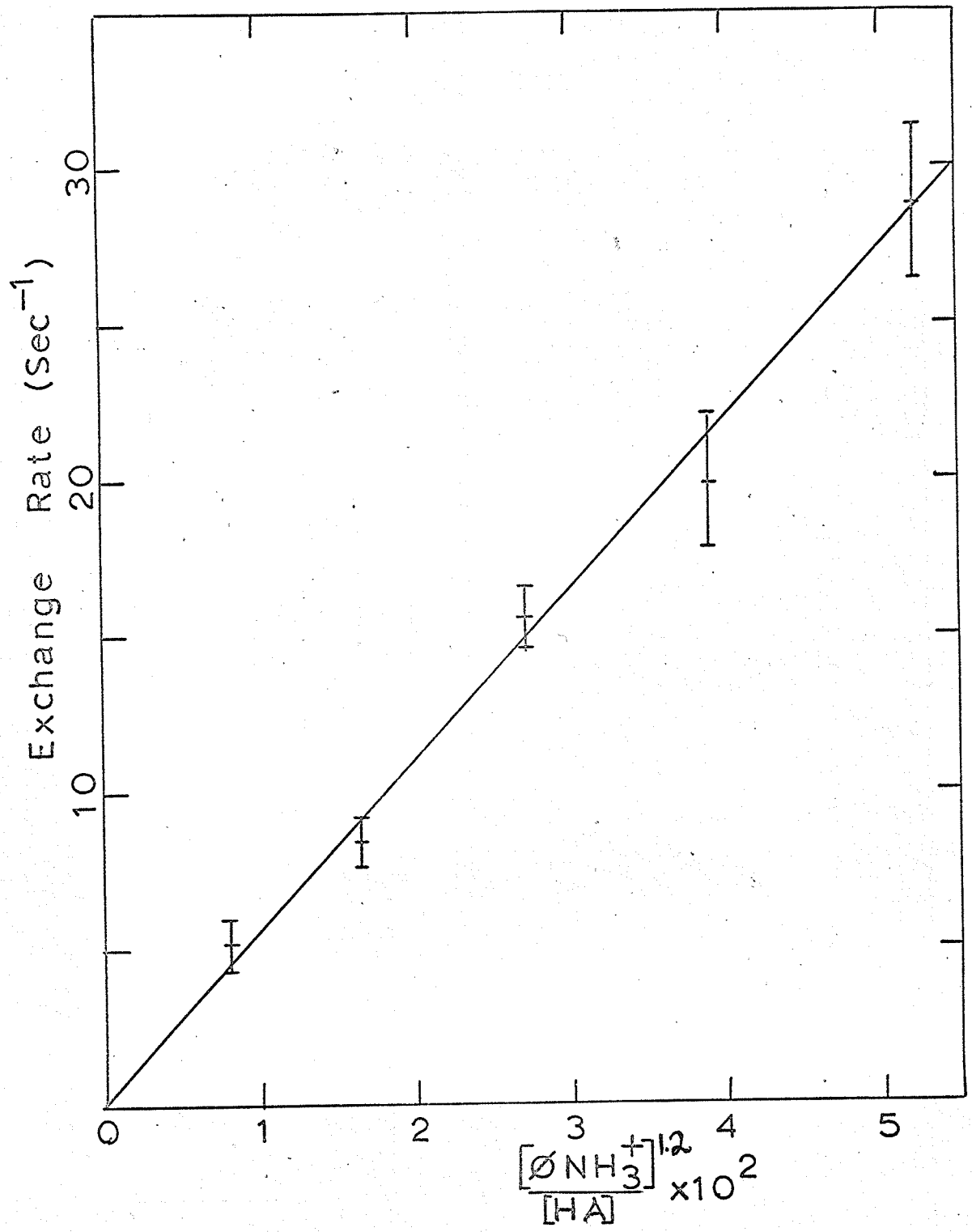
Exchange Rate (Sec^{-1})
10
20
30
0
1
2
3
4
5
$\frac{[\emptyset NH_3^+]^{1.2}}{[HA]} \times 10^2$

true second order rate constant k_o.

$$(1/\tau_{HA}) \cdot [HA] = k_o[\phi NH_3^+][A^-] \cdot F = k_o[\phi NH_3^+]^2 F \qquad 4.76$$

because $[\phi NH_3^+] = [A^-]$. k_o should be independent of aniline concentration if no ion pairs are formed in solution. The experimental rate constants have been corrected by the technique described in the theoretical discussion (equations 4.67 to 4.69). 'a' (equation 4.69) is often considered to represent the distance of closest approach of ions. If 'a' is considered to be the distance of closest possible approach of charge centres ($\approx 2\mathring{A}$) and the dielectric constant of TFA at 50°C is assumed to 39.5, then the corrected second order rate constant is given by

$$\log k_o = \log k_1 + \frac{2.52\sqrt{\mu}}{1+0.889\sqrt{\mu}} . \qquad 4.77$$

The apparent and corrected second order rate constants are given in Table III. Both experimental values of exchange rate and values estimated from Figure 18 have been used. The calculated rate constants vary slightly as concentration changes. Since the Debye-Hückel theory usually gives too small values of activity coefficients for concentrated solutions (152), the true rate constants probably vary by a larger amount than do the corrected rate constants shown in Table III.

If the ions form ion pairs, then the activities of the

ions in solution will be reduced. The free ion concentrations and the activity coefficients can be calculated if a value of the ion pair dissociation constant is assumed and a new set of rate constants can also be calculated. If the molar dissociation constant (uncorrected for ionic activities) is equal to one, then the new corrected rate constants of the one and five mole per cent aniline solutions are nearly equal. This suggests that the molar dissociation constant is approximately equal to one. Because the Debye-Hückel correction terms are probably too large, the actual molar dissociation constant is probably less than one.

Reaction I can be considered to occur in steps (shown in Reactions II,III and IV). If an ion pair is considered to be any two oppositely charged ions in close proximity, then the reaction can be considered to consist of formation of an ion pair followed by internal proton transfer by the ion pair. It is difficult to visualize any true biionic concerted reaction between oppositely charged ions which does not involve the approach of the two ions as a first step. A possible second order non-concerted reaction will be considered later.

The exchange rate can be expressed in terms of the concentration of ion pairs in solution. If $K_D = \frac{[\emptyset NH_3^+][A^-]}{[\emptyset NH_3^+ \cdots A^-]}$, then

$$[HA]\frac{1}{\tau_{HA}} = k_1 [\emptyset NH_3^+][A^-] = k_1 K_D [\emptyset NH_3^+ \cdots A^-] = k_3 [\emptyset NH_3^+ \cdots A^-] \quad 4.78$$

K_D is the apparent molar dissociation constant. Consider (1) a 0.25 molar solution and (2) a 0.50 molar solution of aniline in TFA. The ratios of $[\emptyset NH_3^+ \ldots A^-]$ and $[\text{total } \emptyset NH_3^+]$ for the two solutions can be compared. If $K_D = 10^{-1}$, then

$$\frac{[\emptyset NH_3^+ \cdots A^-]_2}{[\emptyset NH_3^+ \cdots A^-]_1} = \left[\frac{[\text{total } \emptyset NH_3^+]_2}{[\text{total } \emptyset NH_3^+]_1}\right]^{1.3} \qquad 4.79$$

If $K_D = 10^{-2}$, then

$$\frac{[\emptyset NH_3^+ \cdots A^-]_2}{[\emptyset NH_3^+ \cdots A^-]_1} = \left[\frac{[\text{total } \emptyset NH_3^+]_2}{[\text{total } \emptyset NH_3^+]_1}\right]^{1.1} \qquad 4.80$$

Therefore, the plot of acid proton lifetime versus anilinium ion concentration can be explained by assuming that the reaction is bimolecular and that the apparent ion pair dissociation constant has a value of about 10^{-1} to 10^{-2}. The true dissociation constant is probably smaller than the apparent dissociation constants because the ions presumably have lower activity coefficients than the ion pair.

From the consideration of the results given in Table III, it has been shown that the ion pair dissociation constant is probably less than one. Unfortunately the results are too inaccurate to justify any definite conclusions. However, an ion pair dissociation constant of from 1 to 10^{-2} appears reasonable in view of the results of other workers. Fraenkel has shown that anilinium trifluoracetate exists partly as ion pairs even in water and aqueous acids (8). It is also known that ammonium salts have small ion pair dissoc-

iation constants (152). This is usually attributed to hydrogen bonding. Hydrogen bonding can also occur between anilinium and trifluoracetate ions. Finally, it has been shown in Chapter 2 that the ring proton shifts of protonated anilines could be rationalized by field effect calculations based on the assumption that anilinium trifluoracetate exists as ion pairs in TFA.

Another type of proton transfer reaction could occur in solution. The anilinium ion could lose a proton which would then react with a trifluoracetate ion. Since there is a definite probability that the proton would recombine with the aniline molecule before it could combine with a trifluoracetate ion, the rate of proton transfer would depend upon the concentrations of anilinium ions and trifluoracetate ions. Presumably, the anilinium ion would lose a proton more easily if it were adjacent to a trifluoracetate ion because the proton would be attracted by the negative charge of the anion. Therefore, there would be a much greater probability of the reaction occurring if the oppositely charged ions existed as ion pairs. Therefore, the reaction would be essentially equivalent to the bimolecular reaction which has already been discussed. The only possible difference between the two reactions would be in the nature of the activated complex. The values of entropy of activation obtained in part C indicate that a partial neutralization of charge probably occurs

when an ion pair forms an activated complex. This suggests that the proton is partially bonded to both ions in the activated complex. Therefore, it appears probable that the proton transfer reaction is not an ionization reaction.

Meiboom and coworkers have found that a reaction of the type $R_3NH^+ + H_2O + NR_3 \rightarrow R_3N + H_2O + H^+NR_3$ 4.81 contributed appreciably to the proton exchange rate of alkylamines in acidic aqueous solutions (118-120). A similar reaction occurred between carboxylic acids and their anions in methanol (154). The rate determining step was assumed to be a proton transfer to the solvent. Since it is most unlikely that TFA will accept an additional proton, this type of reaction very probably does not occur to any appreciable extent in solutions of aniline in TFA.

Proton exchange reactions can also occur between acid molecules and ring protons. It has been shown that exchange reactions between heavy water and ring protons of protonated N,N-dimethylanilines are very slow. Several hours elapse before equilibrium is established (155).

Similar reactions between TFA and anilinium ion ring protons must also be slow. If any appreciable ring proton exchange occurs in solution, then the ring proton signal should be shifted to low field (closer to the TFA proton signal). It has been shown that the ring proton shifts of anilinium protons in TFA did not exchange when the temperature changed.

In summary, it appears that ion pair formation between anilinium ions and trifluoracetate ions followed by internal proton transfer is the most probable mechanism for the proton transfer reaction which broadens the acid proton peak.

(C) Calculation and Discussion of Thermodynamic Data

(1) Activation Energies and Enthalpies of Activation

The experimental activation energies of acid proton exchange are given in Table VII. The activation energies have been calculated from the least squares plots of log (corrected acid proton line width) versus 1/T by using the logarithmic form of the Arrhenius equation:

$$\log k = \log A - E_A/2.303\ RT \qquad 4.82$$

The line widths are directly related to the acid proton lifetime and the rate constant for acid proton exchange (equation 4.55). The error limits are 95 per cent confidence limits which have been calculated by standard statistical methods (156). There appears to be a general correlation between position of ring substitution and activation energies. The activation energy is greatest for *para*-substituted anilines and least for *ortho*-substituted anilines. There is no specific correlation between types of substituents and activation energies, although the activation energies of the *meta*-substituted anilines do seem to be crudely related to substituent electronegativity.

It is necessary to carefully consider the reactions which are occurring in solution before one can decide what activation energy is actually being measured. There is an activation energy for proton transfer by ion pairs and an activation energy for the overall biionic reaction. If ΔH^{o}_{D} for ion pairs is zero, then the ratio of populations of ion pairs and free ions is independent of temperature and the experimental value of E_A is equal to the values of the activation energy for the overall reaction and for the ion pair reaction, (see figure 19). However, if ΔH^{o}_{D} is not zero, then the concentrations of free ions and ion pairs change when the temperature is changed. If ΔH^{o}_{D} is positive, then the concentration of ion pair decreases when the temperature is increased. Therefore, the apparent rate of change of the calculated rate constant for the ion pair reaction is too small and the measured activation energy is smaller than the true activation energy for proton transfer by ion pairs. On the other hand, if ΔH^{o}_{D} is negative, then the measured activation energy is larger than the activation energy of the overall reaction because the concentration of free ions decreases as the temperature increases. If anilinium trifluoracetate exists in solution almost entirely as ion pairs ($K_D \ll 1$), then $E_A \approx$ the activation energy for the reaction of ion pairs. If the salt exists almost entirely as ions, then $E_A \approx$ the activation energy for the complete biionic reaction.

The difference in activation energies is equal to ΔH_D^o. The enthalpies of dissociation of ion pairs between univalent ions are usually less than 3 kcal/mole (148). Therefore, the experimental value of E_A probably does not differ much from the activation energy of either reaction. If $|\Delta H_D^o| <$ 2 kcal/mole, then E_A will usually agree, within the estimated experimental error, with both values of activation energies.

Enthalpies of activation at 25°C have been obtained from E_A values. The two thermodynamic variables are related by

$$E_A = \Delta H^{\ddagger} + RT \qquad 4.83$$

Values of enthalpies of activation are given in Table VII.

(2) Free Energies of Activation

According to the theory of activated complexes (157),

$$k_{rate} = \kappa \frac{kT}{h} e^{-\Delta F^{\ddagger}/RT} \qquad 4.84$$

where κ, the transmission coefficient, is the probability that the activated complex formed between reactants will decompose to form products rather than reactants. κ is normally equal to one. The specific rate constant must be expressed in terms of activities of reactants.

Theories for the calculation of free energies of activation for reactions of ions in dilute solutions have been developed in detail (149). The apparent rate constants for ionic reactions can be corrected by use of the Debye-Hückel

FIGURE 19. Hypothetical plot of relative enthalpies of ions, ion pairs, activated complex and free molecules for a solution of anilinium trifluoracetate in TFA. It is assumed that the ions and ion pairs have equal enthalpies.

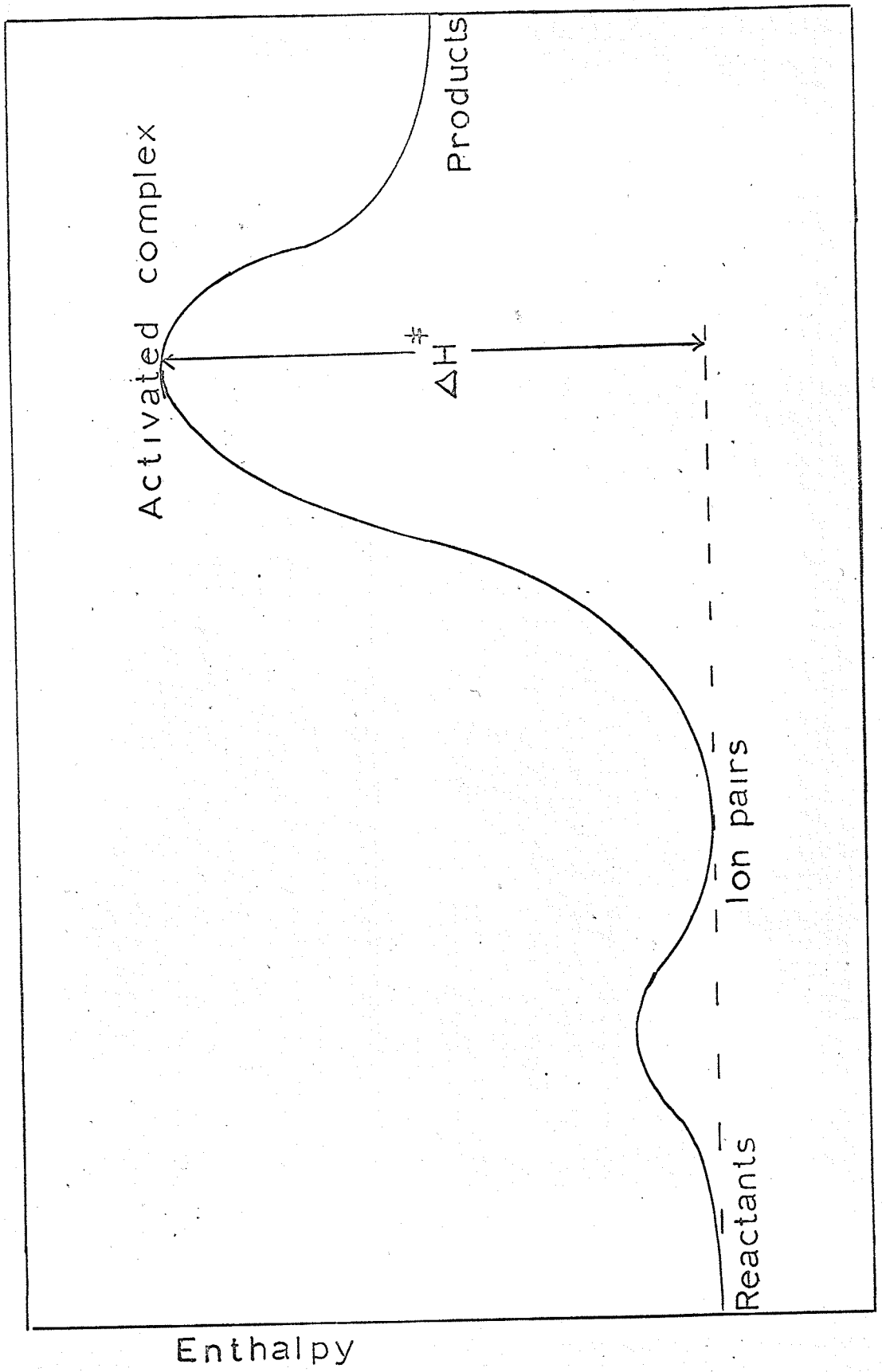
Activated complex
Products
$\Delta H^{\ddagger}$
Ion pairs
Reactants
Enthalpy

correction term (equation 4.69). The free energy of activation of an ionic reaction is equal to the free energy change which occurs when the two ions are brought together plus the free energy which is required to activate the ion pair.

The free energy of activation for a reaction of ion pairs does not include the free energy change which occurs when the ion pair is formed. In order to calculate the free energy of activation of the ion pair, it is necessary to know the activity coefficient of the ion pair. The simplest procedure is to assume that the ion pair is a neutral group unaffected by the ionic strength of the solution. This is obviously only an approximation. However, since the ion pair and the activated complex are both polar in character, this assumption should not introduce drastic errors. Even if the activity coefficients differ by a factor of two there will only be an error of approximately 0.4 kcal/mole in the calculated free energies (see equation 4.84). The error should be approximately the same for the different substituted anilines and should therefore not alter the relative values of $\Delta F^{\ddagger}$.

Four different sets of rate constants have been calculated for the exchange reactions between substituted anilines and TFA at 25°C. They are given in Table VIII. The first set are the corrected second order rate constants for the biionic reaction, assuming that no ion pairs exist in solution.

The apparent second order rate constants have been calculated by inserting values of the acid proton lifetimes at 25°C into equation 4.75. The values of acid proton lifetimes at 25°C have been obtained from Figures 3 to 14. If the exchange rate had not been measured at 25°C, then the plot of line width versus temperature was extrapolated to 25°C. In the case of p-fluoroaniline, the straight line portion of the graph was extrapolated to 25°C. The estimated exchange rate of p-fluoroaniline probably is too high. Except possibly in the case of p-fluoroaniline, it is believed that the estimated exchange rates are accurate to within 20 per cent. This allows for a 5 per cent error in concentration and a 10 per cent error in measuring exchange rate. Most of the exchange rates are probably accurate to within 10 per cent. The apparent rate constants have been corrected by equation 4.69. It was assumed that 'a' = 2Å. The correction factor was $\frac{2.86\sqrt{\mu}}{1+0.926\sqrt{\mu}}$. The corrected rate constants are given in column one. Since the Debye-Hückel theory gives only approximate estimates of the mean activity coefficients of concentrated salt solutions, these rate constants may possibly be incorrect by as much as a factor of two.

The calculated rate constants for the reactions of ion pairs are given in column 2. These have been calculated by inserting the values of acid proton lifetimes at 25°C. into equation 4.78. It was assumed that the aniline salts existed

in solution entirely as ion pairs and that the ion pairs had the same activity coefficients as the activated complexes. The first two sets of rate constants are the rate constants for the two limiting situations which can exist in solution. In addition, the concentrations of the ion pairs and free ions have been calculated, assuming an ion pair dissociation constant of one. When $K_D = 1$, the apparent rate constants of the overall reaction and the ion pair reaction are the same because $[\emptyset NH_3^+][A^-] = [\emptyset NH_2....A]$. The rate constants of the ion pair reactions have been calculated for the new concentrations of ion pairs. They are given in column 3.

The ionic strengths of the solutions have been calculated. It was assumed that the ion pairs did not contribute to the ionic strength. The corrected rate constants of the overall reaction have been calculated, using equation 4.75. They are given in column 4. Since the experimental evidence suggests that $K_D < 1$, the true ion pair reaction rate constants probably lie between the two sets of calculated rate constants. The overall reaction rate constants are presumably equal to or larger than the calculated rate constants listed in column 4.

Equation 4.84 may be written as

$$\Delta F^{\ddagger} = 2.303\ RT\ (\log \frac{kT}{h} + \log K - \log (k_{rate}))\ . \qquad 4.85$$

At 25°C,

$$\Delta F^{\ddagger} = 1.365\ (12.79 + \log K - \log(k_{rate}))\ \text{kcal/mole}. \qquad 4.86$$

It can be seen from the form of equation 4.86 that the calculated values of $\Delta F^{\ddagger}$ are relatively insensitive to small changes in rate constants.

Free energies of activation have been calculated by inserting calculated rate constants into equation 4.86. The results are given in Table IX. It was assumed that the transmission coefficient was equal to one. This assumption is correct if every ion pair which becomes activated decomposes into acid molecules and aniline molecules. This decomposition is detected by NMR spectroscopy, even if the molecules instantaneously react to reform ions.

Although the values of $\Delta F^{\ddagger}$ predicted from the different sets of rate constants are somewhat different, they all appear to be definitely related to the types of substituents and their positions. The free energies of activation of p-haloanilines increase from p-iodoaniline to p-fluoroaniline. The free energies of m-iodo-, bromo- and chloroanilines are approximately equal while the free energy of m-fluoroaniline is lower. The free energy of o-bromoaniline is lower than either o-chloro- or fluoroaniline. These results can be accounted for by reasonable combinations of inductive and mesomeric effects. The free energies are in general lowest for <u>ortho</u>-substituted anilines and highest for <u>para</u>-substituted anilines and always less than $\Delta F^{\ddagger}$ for aniline. This is reasonably explained by assuming that free energies of activation

are largely determined by inductive effects. The free energies of ortho- and para-substituted anilines are probably also affected by mesomeric interactions of substituents with the phenyl rings. The free energies of activation of the ortho-substituted anilines may also be decreased by steric repulsion of the ammonio protons.

The overall pattern of free energies of activation can be explained by assuming that the inductive effect of halogens increases in the order iodine < bromine < chlorine < fluorine and that the mesomeric effect increases in the same order. The halogens withdraw electrons inductively and donate electrons mesomerically. Any deviations from this pattern are small enough to be attributed to either experimental errors or inaccurate correction factors. In no case is it necessary to assume an error of greater than 0.3 kcal/mole in order to fit the values of $\Delta F^{\ddagger}$ into the postulated pattern. Although there is no real justification for doing so, it is tempting to assume that the results in column 2 are the most accurate because they fit the above-postulated patterns better than the other results.

The overall consistency of the calculated $\Delta F^{\ddagger}$ values and their correlation with inductive and mesomeric properties of the halogens, suggests that the assumptions which were made in calculating these values were not drastically inaccurate.

The free energies of activation of the reactions of ion pairs are presumably greater than the values in column 3 and less than or equal to the values in column 2. The free energies of activation of the overall reactions are presumably equal to or less than the free energies given in column 4.

(3) Entropies of Activation

Entropies of activation are related to enthalpies and free energies of activation by

$$\Delta S^{\ddagger} = (\Delta H^{\ddagger} - \Delta F^{\ddagger})/T \qquad 4.87$$

The calculated values of $\Delta S^{\ddagger}$ for the ion pair reactions are given in columns 1 and 2 of Table X. These values represent the probable upper and lower limits of entropies of activation for the ion pair reactions. The error limits are determined by the estimated uncertainties in the values of enthalpies of activation.

In general aniline and the para-substituted anilines have the largest entropies of activation and the ortho-substituted anilines have the lowest entropies of activation. The individual values of entropy are too inaccurate to allow any interpretation of the relative effects of halogens upon entropies.

There are two possible explanations which can account for the increase in entropy which occurs when an anilinium

trifluoracetate ion pair forms an activated complex. The ion pair is probably solvated. The opposite charges of the ion pair are partially neutralized by formation of an activated complex and solvation decreases. In addition, the charges on the ion pair form an effective dipole. Presumably, TFA molecules in the vicinity of dipole, tend to be aligned in its field. Formation of an activated complex decreases the dipole field by partial charge neutralization. Therefore, disorder in the solvent molecules surrounding an ion pair is increased when it forms an activated complex. These two effects must be more important than the increased ionic order which occurs when an ion pair forms an activated complex.

Para-substitution of aniline should have little effect upon $\Delta S^{\ddagger}$ values. The substituent groups will be too far removed from the reaction centre to have any steric or electrostatic effect upon the solvation of the reaction centre. Also, the extent of solvation of the substituent group should not be altered very much by formation of an activated complex. As the substituent is moved closer to the reaction centre, there is an increased probability that the substituent will affect the reaction centre and vice-versa. In o-haloanilinium trifluoracetate ion pairs, the negative substituent group can sterically and electrostatically inhibit solvation of the ammonio group. Similarly, it should be more difficult to solvate the substituent. Therefore, the ion pair

will be less completely solvated and there will be a smaller increase in entropy upon formation of the activated complex. It is quite possible that the ortho substituent is more extensively solvated in the activated complex than in the ion pair because the positive charge of the ammonio group is smaller and it is easier for the positive ends of TFA molecules to approach the substituent. There is also a decrease in entropy when the activated complex is formed because the two ions are "tied" together. The negative entropy of activation of o-haloanilinium trifluoracetate ion pairs must be due to these two factors.

In summary, the decrease in entropy of activation which occurs when a substituent is moved closer to the reaction centre can be explained by assuming that there is a decrease in solvation of the substituent and the reaction centre due to steric and electrostatic effects.

Calculated values of $\Delta S^{\ddagger}$ for the overall reactions have not been given, since they do not yield any further information. In general, they are larger than the values of $\Delta S^{\ddagger}$ for the ion pair reaction and show the same overall trends.

(D) Probable Errors in Measurements of Line Widths and Calculation of Exchange Rates

Because accurate values of ion pair dissociation constants of the various anilinium salts at different temperatures

are not known, there is some uncertainty in the calculated values of exchange rates and in the calculated thermodynamic data. Also, the applied correction factors for ionic activities are only approximate. Since the calculated free energies can be related directly to substituent effects, the ion pair dissociation constants of all the anilinium salts are probably approximately equal. However, it is impossible to decide from the available data which of the calculated values of the thermodynamic variables are correct. The probable ranges within which the values lie have been indicated.

Uncertainties in the sample temperature represented the main potential source of experimental error in the measurement of line widths. It is believed that measured temperatures were accurate to within 0.5°C. Part of the uncertainty in temperature measurement was due to the poor reproducibility of temperature readings by the Varian G-11 temperature recorder. The Minneapolis-Honeywell Brown recording potentiometer which was used to measure temperature during the investigation of the exchange reactions of protonated N,N-dimethylaniline gave much more consistent readings. For this reason it is believed that the temperature measurements in that investigation were accurate to within 0.2°C.

Sample temperatures reached equilibrium very slowly. This was shown by alternately increasing and decreasing temperatures for a series of measurements. A different line

width was obtained for a sample when it was heated to a given temperature than when it was cooled to the same temperature. If the sample was allowed to equilibrate for at least two hours before each set of measurements, then the measured line widths were equal, within experimental error.

The thermocouple junction in the NRC temperature probe was located in the returning air stream at a distance of four inches from the sample. If the sample temperature differed greatly from room temperature, then there may have been a significant temperature gradient within the apparatus. If the sample temperature was above room temperature, then the measured temperature may have been lower than the sample temperature. Where possible, aniline concentration was adjusted so that the sample exchanged at a measurable rate in a temperature range close to room temperatures. It was felt that this would decrease the possibility of errors in temperature measurement.

There probably were some impurities present in the compounds used to prepare the solutions. Only for the solution containing p-fluoroaniline was there any evidence that exchange was occurring between TFA and impurities. The plot of acid proton line width versus temperature (Figure 4) is nearly linear in the high temperature region. If the straight line is extrapolated to lower temperatures (dotted line), then deviations from expected behavior can be plotted against

1/T (Figure 20). The additional exchange rate increases then decreases with increasing temperature. This is exactly the behaviour one would expect for exchange between acid and an impurity. Distillation apparently concentrated the impurity since there were larger deviations from expected behaviour in the solution containing redistilled p-fluoroaniline. Whatever the impurity was, it must have been present in appreciable quantities ($\approx$10 per cent of the total aniline concentration) since it broadened the acid proton peak by as much as 0.6 c/s (Figure 20). Since the exchange took place in the vicinity of room temperature, the impurity was quite probably some other substituted aniline.

It has been reported by Paterson that exchange occurred between aqueous solutions of alcohols and protons from glass sample tubes (131-133). This cannot have been a serious problem in this study because any exchange between TFA and the glass sample tubes should have broadened the acid proton signal of the pure TFA solution. This did not happen (Table I).

The absence of any other evidence of proton exchange between TFA and impurities is understandable, even though some impurities may have been present. Impurities will appreciably affect acid proton line widths only if they fulfill the following three conditions:

(1) They must contain exchangeable protons or be able to accept protons.

FIGURE 20. Plot of log (additional acid proton line width) versus (absolute temperature)$^{-1}$ for a one mole per cent solution of ρ-fluoroaniline in TFA. The additional acid proton line width has been determined by extrapolating log (acid proton line width) in the high temperature region to the low temperature region. The additional line width due to the impurity has been determined from this plot (Figure 4).

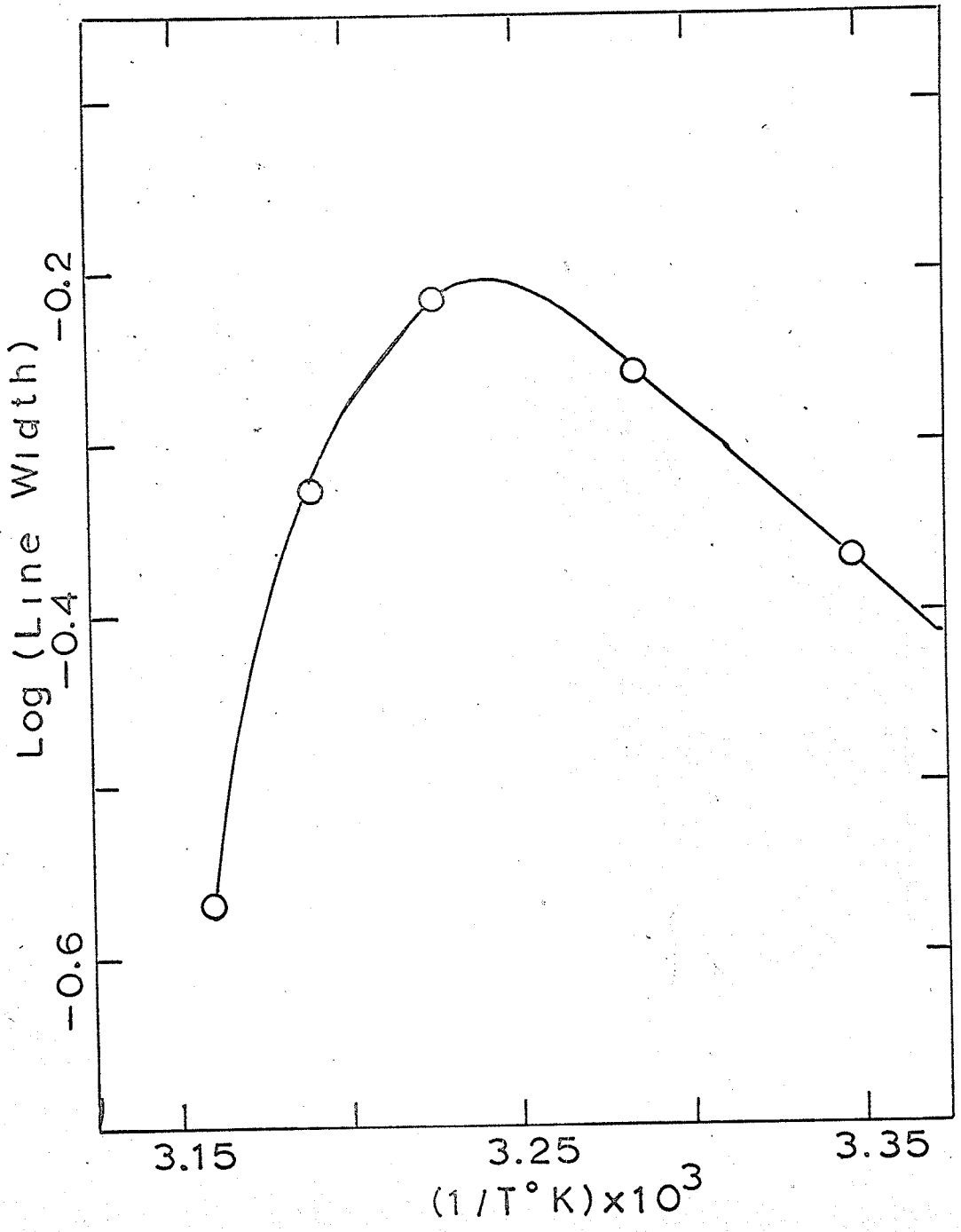
Log (Line Width)
-0.2
-0.4
-0.6
3.15
3.25
3.35
(1/T°K)x10^3

(2) They must be present in significant amounts.

(3) They must exchange with acid at an intermediate rate at the same temperature at which the protonated aniline exchanges with TFA or else they must catalyze the anilinium ion exchange reaction. These three points can be dealt with in order. Firstly, any impurity which does not exchange protons with TFA will have no effect upon the acid proton line width since it will not alter the proton lifetime. Secondly, the maximum width of the acid proton signal depends upon the concentration of the substance with which it exchanges. For example, 3 mole per cent solutions of substituted anilines broadened the acid proton signal by as much as 15 c/s while the maximum line width of acid proton signals in 1 mole per cent solutions of substituted anilines was about 6 c/s. If there is only a very low concentration of impurity in solution, then its relative exchange rate will be so much greater than that of the acid that the two signals will coalesce before the acid proton signal is appreciably broadened. Thirdly, there will normally be little broadening of the acid proton signal if the exchange rate of the reaction between the impurity and TFA is either very slow or very fast in the region of interest. However, this is not necessarily true if the impurity catalyses the exchange reaction between anilinium ions and trifluoracetate ions. For example, consider the effect of water in solution. It has been shown

that water has little effect upon the acid proton line width (Table I). This probably indicates that water is rapidly exchanging protons with TFA. It is conceivable that unprotonated water molecules could accept protons from anilinium ions and donate them to trifluoracetate ions. Such a transfer would introduce a proton with a different Larmor precession frequency into the system of acid and water molecules and cause a broadening of the coalesced acid-water peak. There are three reasons why it is considered unlikely that catalysis reactions of this type occurred in the solutions studied. Firstly, it has been shown that the exchange reaction between ammonium ions and water has an activation energy of 12.2 kcal/mole (123). Since aniline is a weaker base, the corresponding exchange reaction between anilinium ions and water should have a lower activation energy. The experimental activation energy of proton transfer of the solution of aniline in TFA was 23.8 kcal/mole. Secondly, any water in the TFA was presumably almost completely protonated. Consequently, the concentration of free water molecules which could exchange with anilinium ions must have been small. Thirdly, if the measured exchange reactions had been catalyzed by water or other impurities, then there should have been no correlation between exchange rate and structure because the exchange rate would have depended upon the catalyst concentration.

Swarts showed that the reaction between aniline and TFA to form trifluoracetanilide occurred after the reactants had been heated for 8 hours at 120°C in a sealed tube (158). Therefore, it is unlikely that any appreciable reaction between aniline and TFA occurred at the temperatures used in this study. However, the decrease in acid proton line width which was observed when trifluoroacetic anhydride was added to solutions of aniline in TFA was probably due to formation of trifluoracetanilide. This would explain the observed relationship between the concentration ratio of aniline and trifluoracetic anhydride and the acid proton line width. Less than 0.01 gm of trifluoracetic anhydride was added to each sample of TFA which was used to prepare a solution for exchange studies. It was added to the acid several minutes before the acid was added to the aniline. It possibly reacted with any water in the acid before the acid was added to the aniline. Because of the time interval and because only a very small amount of anhydride was added, it is considered unlikely that any appreciable reaction occurred between the anhydride and aniline.

6. DISCUSSION OF RESULTS FOR N,N-DIMETHYLANILINE

In the investigation of the exchange reactions of ring-substituted anilines, the acid proton lifetimes were measured

and the rate constants for anilinium proton exchange were calculated. However, the lifetime of protonated N,N-dimethylaniline was measured directly. It was considered possible that additional reactions which did not affect the acid proton lifetime would be measured. For example, the reaction

$$\emptyset N(CH_3)_2 + H^+(CH_3)_2N\emptyset \longrightarrow \emptyset N(CH_3)_2H^+ + (CH_3)_2N\emptyset \qquad 4.88$$

would not affect the acid proton line width while it would cause collapse of the methyl proton doublet. However, the calculated thermodynamic data are quite consistent with those calculated in section 5. Therefore, it is very probable that the same type of reaction was measured in both sets of experiments.

The derived thermodynamic data are given in Tables VII to X . The lifetime of protonated N,N-dimethylaniline molecules at 25°C was obtained by extrapolation of the plot of dimethylanilinium ion lifetime versus temperature (Figure 17). Collapse of the methyl doublet was assumed to occur only as a result of reactions in which ammonio protons were replaced by protons which had spins opposite to those of the original protons. The proton exchange rate was assumed to be twice as large as the calculated spin exchange rate. These assumptions are discussed below.

If it were possible for proton exchange to occur without

change of proton spins (without T_1 relaxation), then the observed splitting of the spin-spin doublet of protonated N,N-dimethylaniline would be altered by exchange only if the solution contained an appreciable amount of free N,N-dimethylaniline. This can be shown in the following manner. Consider a solution containing both protonated and unprotonated N,N-dimethylaniline with relative populations P_A and P_B ($P_A + P_B = 1$). Assume that any ion which loses a proton must later acquire a proton with the same spin. This assumption effectively divides the dimethylanilinium ions into two groups; those which always have an ammonio proton with spin + $\frac{1}{2}$ and those which always have an ammonio proton with spin - $\frac{1}{2}$. The expected methyl proton NMR spectrum is shown in Figure 21.

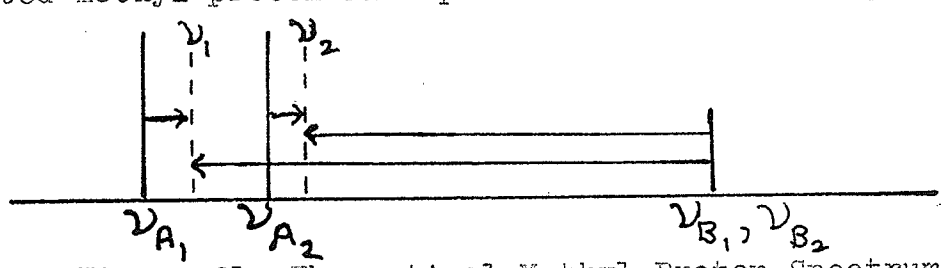

Figure 21: Theoretical Methyl Proton Spectrum of Protonated N,N-dimethylaniline

ν_{A_1} is the resonance frequency of the methyl protons coupled to ammonio protons in one spin state and ν_{A_2} is the resonance frequency of the methyl protons coupled to ammonio protons in the other spin state. In the unprotonated molecule the two types of methyl protons will resonate at the same frequency. Suppose dimethylanilinium ions are rapidly losing and gaining protons of the same spin. Since one is observing

the methyl protons, it does not matter what types of ions or molecules are exchanging protons with the dimethylanilinium ions. The two pairs of methyl proton signals (A_1,B_1 and A_2, B_2) collapse together and only two coalesced peaks remain. The resonance frequencies of the two peaks are $\nu_1 = (P_{A_1}\nu_{A_1} + P_{B_1}\nu_{B_1})/(P_{A_1}+P_{B_1})$ and $\nu_2 = (P_{A_2}\nu_{A_2} + P_{B_2}\nu_{B_2})/(P_{A_2}+P_{B_2})$. The populations of the ammonio protons in the two spin states are very nearly equal. Therefore, $P_{A_1} = P_{A_2} = P_A/2$ and $P_{B_1} = P_{B_2} = P_B/2$. Because $\nu_{B_1} = \nu_{B_2}$,

$$(\nu_1 - \nu_2) = P_A(\nu_{A_1} - \nu_{A_2}). \qquad 4.89$$

If N,N-dimethylaniline is almost completely protonated then the measured peak separation ($\nu_1 - \nu_2$) of the coalesced peaks is almost equal to the coupling constant ($\nu_{A_1} - \nu_{A_2}$). K_A for protonated N,N-dimethylaniline in water is smaller than 10^{-5}(159). Even if K_A for N,N-dimethylaniline were as large as 10^{-2}, a 10 mole per cent solution would be approximately 99.9 per cent protonated and the observed coupling constant would be altered by only 0.1 per cent as a result of exchange. Therefore, it is felt that the collapse of the observed H^+-N-CH_3 coupling constant was due only to exchange of ammonio proton spins because chemical exchange without change of proton spins probably decreased the observed coupling constant by less than 0.01 c/s.

Collapse of a proton spin-spin doublet is normally caused by T_1 relaxation of the proton which is responsible for the splitting. The T_1 relaxation may be due to any normal spin-

lattice relaxation mechanism or it may be due to replacement of the proton by another proton which is in the opposite spin state to the first proton. It has been shown in Chapter 3 that the H^+-N-CH_3 coupling constants of two protonated benzylamines were constant over a temperature range of about 100°C. The T_1 relaxation times of the ammonio protons in the two compounds must have been constant over that temperature range. Since the ammonio protons of the dimethylanilinium ion and of the protonated benzyl amines were in essentially the same type of magnetic environments, it is believed that only exchange contributed to the temperature-dependent decrease in the spin-lattice relaxation time of the ammonio protons of N,N-dimethylanilinium ions.

If the average lifetime of unprotonated N,N-dimethylaniline molecules was long compared to the average lifetime of $\emptyset N(CH_3)_2 \cdots HA$ hydrogen bonds, then the proton exchange rate must have been twice as large as the spin exchange rate. If this condition were not fulfilled, then the dimethylaniline molecule would often regain the same proton which it had lost. Therefore, less than half of the protons which were added to dimethylaniline molecules would have had different spins than the protons which were lost. It has been shown that amine-water hydrogen bonds have lifetimes of approximately 10^{-10} seconds (160). Therefore, it is probable that the condition which has been assumed was fulfilled, since the acid-

amine hydrogen bonds probably had very short lifetimes.

It was assumed that K_D had a value between zero and one. If K_D is not equal to zero, then the rate constant is given by

$$k = \frac{1}{\tau_{\emptyset N(CH_3)_2H^+}} \cdot \frac{[\text{total } \emptyset N(CH_3)_2H^+]}{[\emptyset N(CH_3)_2H^+ \cdots A^-]} . \qquad 4.90$$

The rate constants were calculated for the two values of K_D. Values of $\Delta F^{\ddagger}$ and $\Delta S^{\ddagger}$ were calculated from the rate constants. The calculated concentration of N,N-dimethylanilinium trifluoracetate was 1.32 moles/litre. Values of $\Delta F^{\ddagger}$ and $\Delta S^{\ddagger}$ for the overall reaction were not calculated because it was felt that any calculated activity coefficient for a very concentrated solution would probably have been grossly inaccurate. The activation energy was calculated from the slope of the least squares plot shown in Figure 17. Only the last six points were used in the least squares calculation. The quoted error limit is the 95 per cent confidence limit for the calculated value of activation energy.

The activation energy of proton transfer by protonated N,N-dimethylaniline is much lower than the activation energy of proton transfer by protonated aniline. Since N,N-dimethylaniline is a stronger base than aniline one might naively expect its conjugate acid to have a higher energy of activation of proton transfer than the conjugate acid of aniline. This is not necessary, however. The N,N-dimethylanilinium ion has a larger free energy of activation than the anilinium

ion, as would be expected. However, it has a much smaller entropy of activation. Probably the two methyl groups sterically hinder solvation of the ion pair. There will then be very little change in the extent of solvation when the activated complex is formed and consequently the entropy of the solution will only be slightly changed.

7. SUMMARY AND CONCLUSIONS

(1) The same reaction is measured when one measures the lifetime of acid protons as when one measures the lifetime of ammonio protons.

(2) The reaction is probably a biionic reaction between anilinium ions and trifluoracetate ions. The two ions form an ion pair. The anilinium ion then transfers a proton to the trifluoroacetate ion.

(3) There is a definite correlation between values of free energy of activation and the nature of the substituents bonded to aniline. Alkylation of the ammonio group increases $\Delta F^{\ddagger}$. Halogen substitution generally decreases $\Delta F^{\ddagger}$. The decrease is greatest for <u>ortho</u>-substitution and least for <u>para</u>-substitution. The values of $\Delta F^{\ddagger}$ for haloanilines can be related to the inductive and mesomeric effects of the halogens. The results indicate that both the inductive and the mesomeric effects are smallest for

iodine and largest for fluorine and that the inductive effect is larger than the mesomeric effect.

(4) The size of the entropy of activation depends largely upon the position of the substituent. The entropy of activation is largest for aniline and *para*-substituted anilines and least for *ortho*- and N-substituted anilines. The size of the entropy of activation is apparently determined by the extent of steric and electrostatic hindrance of solvation of the ions and ion pairs.

TABLE II

Measured Acid Proton Line Widths and Acid Proton Exchange Rates of Solutions of Substituted Anilines in TFA

	CONCENTRATIONS							
	Mole % as weighed			Moles/litre assuming (1) Ideal solutions (2) Complete Protonation of aniline		Corrected acid proton line width (c/s)	Acid proton exchange rate (sec^{-1})	Temperature (°C)
	TFA	$\emptyset NH_2$	C_6H_{12}	TFA	$\emptyset NH_3^+$			
Aniline	92.7	4.03	3.24	11.7	0.530	1.61 ± 0.08	5.1 ± 0.25	38.6 ± 0.5
						2.67 ± 0.10	8.4 ± 0.3	42.5
						3.66 ± 0.16	11.5 ± 0.5	45.6
						4.93 ± 0.11	15.5 ± 0.3	48.1
						7.02 ± 0.16	22.1 ± 0.5	50.8
						9.50 ± 0.17	29.8 ± 0.5	53.6
						12.86 ± 0.38	40.4 ± 1.2	56.4
p-F Aniline (distilled)	95.0	2.00	3.03	12.2	0.265	0.65 ± 0.06	2.05 ± 0.2	25.5
						0.97 ± 0.07	3.05 ± 0.2	31.2
						1.45 ± 0.12	4.55 ± 0.4	36.8
						1.69 ± 0.13	5.3 ± 0.4	40.3
						1.98 ± 0.08	6.2 ± 0.25	43.3
						2.85 ± 0.06	9.0 ± 0.2	46.7
						3.33 ± 0.13	10.5 ± 0.4	48.6
						4.49 ± 0.12	14.1 ± 0.4	51.4
						6.12 ± 0.17	19.2 ± 0.5	54.2
						8.32 ± 0.17	26.15 ± 0.5	56.7
p-F Aniline (Undistilled)	95.3	2.00	2.73	12.3	0.264	0.65 ± 0.05	2.05 ± 0.15	25.7
						1.13 ± 0.08	3.55 ± 0.25	34.8
						1.39 ± 0.05	4.4 ± 0.15	38.5
						1.87 ± 0.09	5.9 ± 0.3	42.2
						2.12 ± 0.10	6.7 ± 0.3	44.4
						3.81 ± 0.06	12.0 ± 0.2	49.8
						5.49 ± 0.13	17.25 ± 0.4	54.0

TABLE II CONTINUED

p-Cl Aniline	93.7	2.98	3.17	12.1	0.393	1.17 ± 0.06	3.7 ± 0.2	27.8
						1.84 ± 0.08	5.8 ± 0.25	31.2
						2.64 ± 0.14	8.3 ± 0.4	33.8
						3.50 ± 0.12	11.0 ± 0.4	36.5
						4.43 ± 0.20	13.9 ± 0.65	37.7
						6.19 ± 0.17	19.45 ± 0.55	41.2
						8.55 ± 0.21	26.9 ± 0.65	44.4
						10.38 ± 0.34	32.6 ± 1.1	47.3
p-Br Aniline	94.8	2.02	3.14	12.5	0.272	2.00 ± 0.07	6.3 ± 0.2	27.2
						2.92 ± 0.13	9.2 ± 0.4	30.0
						4.64 ± 0.12	14.6 ± 0.4	33.2
						6.80 ± 0.19	21.4 ± 0.6	35.8
						9.36 ± 0.15	29.4 ± 0.5	38.4
						11.38 ± 0.25	35.75 ± 0.8	40.7
						16.59 ± 0.19	52.1 ± 0.6	44.4
p-I Aniline	94.6	2.06	3.35	12.4	0.276	1.80 ± 0.10	5.65 ± 0.3	25.0
						2.46 ± 0.10	7.7 ± 0.3	27.7
						3.57 ± 0.09	11.2 ± 0.3	30.8
						4.51 ± 0.13	14.2 ± 0.4	32.9
						6.38 ± 0.07	20.0 ± 0.3	35.8
						8.39 ± 0.07	26.4 ± 0.3	38.4
m-F Aniline	95.9	1.00	3.11	12.7	0.134	1.26 ± 0.07	3.95 ± 0.2	23.0
						1.90 ± 0.09	6.0 ± 0.3	27.1
						2.73 ± 0.15	8.6 ± 0.5	30.5
						3.96 ± 0.15	12.45 ± 0.5	34.4
						4.55 ± 0.11	14.3 ± 0.35	37.2
						5.09 ± 0.19	-	39.2
						4.65 ± 0.12	-	43.9
						3.79 ± 0.12	-	47.6
						2.59 ± 0.13	-	50.3
						1.85 ± 0.07	-	53.8
						1.21 ± 0.10	-	56.4

TABLE II CONTINUED

m-Cl Aniline	94.0	2.97	3.06	12.4	0.392	3.74	± 0.08	11.8	± 0.25	24.6
						4.69	± 0.12	14.7	± 0.4	27.6
						5.90	± 0.20	18.5	± 0.6	29.4
						7.12	± 0.12	22.4	± 0.4	31.8
						9.54	± 0.11	30.0	± 0.35	33.7
						10.33	± 0.25	32.45	± 0.8	35.4
						13.75	± 0.21	43.2	± 0.7	38.1
						16.93	± 0.32	53.2	± 1.0	40.6
m-Br Aniline	95.0	1.95	3.05	12.3	0.258	1.71	± 0.08	5.4	± 0.25	22.0
						2.41	± 0.09	7.6	± 0.3	25.1
						3.91	± 0.09	12.6	± 0.3	28.6
						5.77	± 0.13	18.1	± 0.4	32.5
						7.50	± 0.11	23.6	± 0.35	34.8
						8.72	± 0.18	27.4	± 0.55	36.7
m-I Aniline	94.5	2.17	3.37	12.2	0.287	1.30	± 0.09	4.1	± 0.3	21.1
						2.02	± 0.11	6.35	± 0.35	25.0
						3.46	± 0.09	10.9	± 0.3	28.6
						5.02	± 0.14	15.8	± 0.4	31.3
						8.08	± 0.30	25.4	± 0.95	35.3
						9.16	± 0.15	28.8	± 0.5	37.2
o-F Aniline	95.8	1.01	3.24	12.7	0.135	2.52	± 0.07	7.9	± 0.2	15.5
						3.00	± 0.12	9.4	± 0.4	18.0
						3.68	± 0.09	11.6	± 0.3	20.4
						4.35	± 0.14	13.7	± 0.4	23.8
						5.23	± 0.17	16.4	± 0.5	26.5
						4.46	± 0.16		-	33.3
						3.29	± 0.07		-	36.2
						2.41	± 0.06		-	39.1
						1.87	± 0.10		-	41.8

TABLE II CONTINUED

o-Cl Aniline	94.4	2.00	3.59	12.2	0.264	3.77 ± 0.10	11.85 ± 0.3	12.5
						4.18 ± 0.10	13.1 ± 0.3	14.8
						4.77 ± 0.15	15.0 ± 0.5	17.0
						6.35 ± 0.15	19.95 ± 0.5	19.9
						7.24 ± 0.18	22.75 ± 0.6	22.2
						10.11 ± 0.27	-	27.7
						6.25 ± 0.13	-	31.3
						4.60 ± 0.16	-	33.8
						3.30 ± 0.09	-	36.3
						2.47 ± 0.08	-	39.3
						1.97 ± 0.07	-	41.6
o-Br Aniline	95.9	1.02	3.13	12.3	0.135	3.57 ± 0.10	11.2 ± 0.3	9.7
						4.23 ± 0.06	13.3 ± 0.2	12.2
						4.72 ± 0.17	14.8 ± 0.5	14.0
						5.26 ± 0.13	-	16.7
						5.30 ± 0.29	-	19.8
						4.33 ± 0.13	-	24.8
						3.36 ± 0.16	-	27.4
						2.78 ± 0.13	-	29.8
						2.10 ± 0.06	-	32.2
						1.82 ± 0.09	-	34.0
Aniline	89.8	8.09	2.14	10.7	1.05	2.42 ± 0.17	-	18.0
						2.59 ± 0.11	-	22.2
						2.99 ± 0.12	-	26.5
						3.74 ± 0.11	-	32.1
						6.58 ± 0.13	-	36.3
						9.37 ± 0.14	-	40.3
						13.58 ± 0.29	-	44.1

TABLE II CONTINUED

m-Cl Ani-Line	89.5	8.22	2.26	10.6	1.075	8.06 ± 0.13	-	0.2
						5.95 ± 0.11	-	14.4
						6.65 ± 0.10	-	19.4
						9.00 ± 0.23	-	25.0
						10.94 ± 0.17	-	28.2
						14.06 ± 0.20	-	31.6
						16.90 ± 0.17	-	34.1

TABLE IIIa

Acid Proton Exchange Rates of Different Solutions of Aniline in TFA

	Concentrations: Mole % as weighed			Concentrations: Moles/litre assuming (1) Ideal solutions (2) Complete protonation of aniline		Temperature (°C)	Line Width (c/s)	Exchange Rate (sec^{-1})	Exchange Rate at 50.2°C
	TFA	$\emptyset NH_2$	C_6H_{12}	TFA	$\emptyset NH_3^+$				
(1)	95.9	1.01	3.09	12.6	0.1345	50.2±0.5	1.63±0.15	5.1±0.5	5.1±0.8
(2)	95.2	2.01	2.78	12.3	0.266	49.6	2.48±0.08	7.8±0.25	8.4±0.75
(3)	93.7	2.98	3.35	11.9	0.392	48.8	4.23±0.10	13.3±0.3	15.6±1.2
(4)	93.0	3.95	3.10	11.7	0.520	50.2	6.30±0.29	19.8±0.9	19.8±2.05
(5)	91.9	4.95	3.20	11.4	0.650	49.5	8.47±0.21	26.6±0.65	28.8±2.4

TABLE IIIb

Apparent and Corrected Rate Constants* of Proton Exchange of Solutions of Aniline in TFA at 50.2°C.

	Apparent Rate Constants ($K_D=\infty$): (a) Calculated from Measured Acid Proton Line Widths	Apparent Rate Constants ($K_D=\infty$): (b) Calculated From Fig.18	Corrected Rate Constants ($K_D=\infty$): (a) Calculated from Measured Acid Proton Line Widths	Corrected Rate Constants ($K_D=\infty$): (b) Calculated From Fig.18	Corrected Rate Constants ($K_D=1$) Calculated from Figure 18.
(1)	3.58×10^3	2.83×10^3	1.86×10^4	1.47×10^4	1.69×10^4
(2)	1.46×10^3	1.56×10^3	1.14×10^4	1.22×10^4	-
(3)	1.21×10^3	1.15×10^3	1.25×10^4	1.19×10^4	-
(4)	8.57×10^2	9.10×10^2	1.09×10^4	1.16×10^4	-
(5)	7.77×10^2	7.65×10^2	1.18×10^4	1.17×10^4	1.72×10^4

* All rate constants have units of (litres/mole second)

TABLE IV

Chemical Shifts of TFA Protons and Anilinium Ion Ring Protons in Different Solutions of Aniline in TFA at Different Temperatures

Concentration (Mole % Aniline) as weighed	Temperature (°C)	Chemical Shift in c/s (Relative to cyclohexane)	
		TFA Protons	Anilinium ion ring protons
2.01	25.2 ± 0.5	- 602 ± 1	- 364 ± 1
	49.8	- 585.5	- 365
2.98	24.5	- 609.5	- 363
	49.5	- 593	- 364
3.95	24.8	- 611.5	- 365
	50.2	- 593	- 365
4.95	26.8	- 612.5	- 365
	32.0	- 609	- 364
	38.4	- 605	- 365
	44.0	- 600.5	- 365
	49.5	- 596	- 365
	54.5	- 591.5	- 364
	60.2	- 586	- 364
	64.6	- 579.5	- 364
	69.4	- 566.5	- 364

TABLE V

Acid Proton Line Width of Solutions of Aniline and Trifluoracetic Anhydride in TFA at 25°C.

Concentration (mole %)				Acid proton line width (c/s)	$\frac{[\text{Anhydride}]}{[\text{ØNH}_2]}$	Change in line width when anhydride added / Original line width
ØNH_2	C_6H_{12}	TFA Anhydride	TFA			
5.1	2.0	0.0	93.0	3.70 ± 0.17	-	-
5.9	2.1	0.0	90.8	4.79 ± 0.14	-	-
7.0	2.2	0.0	90.8	6.40 ± 0.19	-	-
5.0	2.3	0.2	92.5	3.55 ± 0.12	-	-
5.8	2.2	0.2	91.8	4.67 ± 0.06	-	-
6.9	1.9	0.3	90.9	6.30 ± 0.13	-	-
5.1	2.1	2.0	90.9	2.52 ± 0.11	0.4	0.3
5.8	2.0	2.1	90.1	3.12 ± 0.09	0.35	0.35
7.0	2.2	2.1	88.7	4.29 ± 0.14	0.3	0.3

TABLE VI

Measured Peak Separation of the Methyl Doublet of Protonated N,N-dimethylaniline and calculated Values of the Ammonio Proton Spin Exchange Rate of N,N-dimethylanilinium Ions

Temperature (°C.)	Doublet Separation (cycles/sec.)	Lifetime of Protonated Molecules (sec.)	Exchange Rate ($sec.^{-1}$)
17.6±0.2	5.26±0.03	-	-
26.8	5.26±0.03	-	-
46.8	5.11±0.04	0.189 ± .029	5.3 ± 0.9
50.6	5.02±0.03	0.143 ± .010	7.0 ± 0.5
52.8	4.90±0.06	0.118 ± .010	8.5 ± 0.8
55.5	4.67±0.04	0.093 ± .003	10.8 ± 0.4
57.0	4.52±0.03	0.084 ± .002	11.9 ± 0.3
58.9	4.11±0.05	0.069 ± .001	14.6 ± 0.3
60.6	3.65±0.10	0.060 ± .001	16.8 ± 0.4

TABLE VII

Measured Activation Energies of Proton Transfer and Calculated Enthalpies of Activation of Proton Transfer of Solutions of Aniline and Substituted Anilines in TFA

Substituent	Activation Energy (Kcal/mole)	Enthalpy of Activation (Kcal/Mole) at 25°C.
H	23.85 ± 0.75	23.25 ± 0.75
p-F	> 22.8	> 22.2
p-Cl	21.7 ± 1.55	21.1 ± 1.55
p-Br	23.7 ± 2.15	23.1 ± 2.15
p-I	21.35 ± 0.4	20.65 ± 0.4
m-F	18.3 ± 0.9	17.7 ± 0.9
m-Cl	18.0 ± 1.1	17.3 ± 1.1
m-Br	20.3 ± 1.15	19.6 ± 1.15
m-I	22.5 ± 2.1	21.9 ± 2.1
o-F	11.3 ± 1.5	10.7 ± 1.5
o-Cl	11.7 ± 3.9	11.1 ± 3.9
o-Br	10.4 ± 3.3	9.8 ± 3.3
N,N-diMe	18.8 ± 1.1	18.2 ± 1.1

TABLE VIII

Calculated Rate Constants for the Overall Reactions and the Ion Pair Reactions of Solutions of Aniline and Substituted Anilines in TFA at 25°C.

Substituent	Rate constant for overall reaction if $K_D = \infty$ (litres/mole sec.)	k_3 (4.78) Rate constant for ion pair reaction if $K_D=0$ (sec.$^{-1}$)	4.73 Rate constant for ion pair reaction if $K_D=1$ (sec.$^{-1}$)	Rate constant for overall reaction if $K_D=1$ (litres/mole sec.)
H	7.2×10^2	2.2×10^1	7.8×10^1	1.1×10^3
p-F	$< 1.1 \times 10^3$	$< 2.9 \times 10^1$	$< 1.6 \times 10^2$	$< 1.4 \times 10^3$
p-Cl	3.0×10^3	8.8×10^1	2.2×10^2	4.1×10^3
p-Br	8.5×10^3	2.3×10^2	1.2×10^3	1.0×10^4
p-I	9.3×10^3	2.5×10^2	1.4×10^3	1.2×10^4
m-F	2.0×10^4	4.6×10^2	4.4×10^3	2.0×10^4
m-Cl	1.3×10^4	3.7×10^2	1.6×10^3	1.8×10^4
m-Br	1.4×10^4	3.6×10^2	2.0×10^3	1.7×10^4
m-I	1.0×10^4	2.8×10^2	1.5×10^3	1.3×10^4
o-F	6.3×10^4	1.4×10^3	1.3×10^4	5.8×10^4
o-Cl	5.1×10^4	1.3×10^3	7.6×10^3	6.5×10^4
o-Br	1.1×10^5	2.6×10^3	2.4×10^4	1.1×10^5
N,N-diMe	-	1.1×10^0	2.7×10^0	-

TABLE IX

Calculated Values of Free Energies of Activation* for the Overall Reactions and the Ion Pair Reactions of Solutions of Aniline and Substituted Anilines in TFA at 25°C.

Substituent	$\Delta F^{\ddagger}$ for overall reaction if $K_D=\infty$	$\Delta F^{\ddagger}$ for ion pair reaction if $K_D=0$	$\Delta F^{\ddagger}$ for ion pair reaction if $K_D=1$	$\Delta F^{\ddagger}$ for overall reaction if $K_D=1$
H	13.55	15.65	14.9	13.3
p-F	>13.3	>15.45	>14.45	>13.2
p-Cl	12.7	14.8	14.0	12.5
p-Br	12.1	14.25	13.25	12.05
p-I	12.05	14.2	13.15	11.9
m-F	11.6	13.8	12.5	11.6
m-Cl	11.85	13.95	13.1	11.65
m-Br	11.8	14.0	12.95	11.7
m-I	12.0	14.1	13.1	11.8
o-F	10.9	13.15	11.8	10.9
o-Cl	11.0	13.2	12.15	10.9
o-Br	10.55	12.8	11.45	10.6
N,N-diMe	-	17.4	16.9	-

* The units of $\Delta F^{\ddagger}$ are kcal/mole.

TABLE X

Calculated Values of Entropies of Activation of the Ion Pair Reactions of Solutions of Aniline and Substituted Anilines at 25°C

Substituent	$\Delta S^{\ddagger}$ (eu) if $K_D=0$	$\Delta S^{\ddagger}$ (eu) if $K_D=1$
H	25.5 ± 2.5	33 ± 2.5
p-F	21	26
p-Cl	21 ± 5	29 ± 5
p-Br	29.5 ± 7	33 ± 7
p-I	22 ± 1	25 ± 1
m-F	13 ± 3	17.5 ± 3
m-Cl	12 ± 4	14 ± 4
m-Br	19 ± 4	22 ± 4
m-I	26 ± 7	29.5 ± 7
o-F	-8 ± 5	-4 ± 5
o-Cl	-7 ±13	-3.5 ±13
o-Br	-10 ±11	-5.5 ±11
N,N-diMe	3 ± 4	4 ± 4

CHAPTER 5

RECOMMENDATIONS FOR FUTURE RESEARCH

(1) It has been shown in Chapter 2 that there appears to be a definite relationship between substituent effects and amino proton shifts. Accurate measurements of the amino proton shifts of a large number of mono- and di-substituted anilines in cyclohexane or some other inert solvent might provide much interesting information about substituent effects. It would be particularly interesting to measure the amino proton shifts of ortho-substituted anilines in order to determine the magnitudes of dispersive and/or anisotropic effects. If the equipment becomes available, it would also be useful to measure the N^{14} chemical shifts of ortho-substituted anilines.

(2) The ring proton spectra of the hydrofluoride, hydrochloride, hydrobromide, and hydroiodide salts of pyridine and aniline should be measured in different polar solvents at different concentrations. The ring proton spectrum will not be appreciably altered by exchange if there is only a small concentration of unprotonated base in solution (see Chapters 3 and 4).

If the ring proton shifts of the hydrohalide salts of the two bases in water are extrapolated to infinite dilution, then these shifts should be the true ring proton shifts in the absence of any effect due to the field of the anion. This can be checked by comparing the extrapolated shifts of the different

salts. These ring proton shifts can be compared to those obtained from M.O. calculations and field effect calculations. The pyridinium salts will probably provide more information than the anilinium salts because the pyridinium ion ring proton shifts are larger.

If there are any deviations from these limiting shifts in another solvent of lower dielectric constant, they can be attributed to the effect of the anion upon the ring proton spectra and to the different reaction field effect of the solvent (assuming that specific solvent effects do not alter the ring proton shifts). The effect of the counter ion can be estimated by field effect calculations.

If no exchange is occurring, the shift of the proton(s) bonded to the nitrogen should provide a definite indication of the extent of ion pair formation. The expected effect of the counter ion can be calculated.

This study would firstly provide accurate values of anilinium ion and pyridinium ion shifts in the absence of counter ion effects. Secondly, it would provide data which can be used to test the accuracy of field effect calculations.

(3) If an N^{14} decoupling apparatus becomes available the shifts of the other protonated benzylamines could be studied. It would be particularly interesting to study the ammonio proton spectra of protonated D(-)-N,α- dimethylphenethylamine

and other similar compounds. This compound would give an ABX spectrum with the A and B protons bonded to the nitrogen. Therefore, a value of J_{H-N-H} could be obtained.

(4) The exchange rates of solutions of other substituted anilines could be measured at 25°C. These exchange rates could be used to calculate values of $\Delta F^{\ddagger}$ for the exchange reactions. Exchange rates could be measured with minimum experimental difficulty because it would not be necessary to use the temperature probe. However, only those protonated anilines which have measurable exchange rates at 25°C could be investigated by this method.

(5) Hindered rotation of benzylamines could be studied in some other strong non-aqueous acid such as chlorosulphonic acid. This acid freezes at -80°C and boils at 158°C. Therefore, the NMR spectra of protonated benzylamines could be investigated over a much larger range of temperatures. N^{14} spin decoupling could also be used so that the ammonio proton spectra could be investigated.

BIBLIOGRAPHY

1. J.A. Pople, W.G. Schneider and H.J. Bernstein, "High-resolution Nuclear Magnetic Resonance", McGraw-Hill Book Company, Inc., New York, 1959.

2. E.R. Andrew, "Nuclear Magnetic Resonance", Cambridge University Press, London, 1955.

3. The Varian Staff, "NMR and EPR Spectroscopy", Permagon Press, New York, 1960.

4. J.D. Roberts, "Nuclear Magnetic Resonance", McGraw-Hill Book Company, Inc., New York, 1959.

5. L.M. Jackman, "Nuclear Magnetic Resonance Spectroscopy", Permagon Press, New York, 1959.

6. W.G. Schneider, Private Communication to T. Schaefer, (1959).

7. T. Isobe, T. Ikenove, and G. Hazato, J. Chem. Phys., 30, 1371 (1959).

8. (a) G. Fraenkel, Abstracts, Summer Symposium on High-Resolution NMR Spectroscopy, Boulder, Colorado, 1962.

   (b) G. Fraenkel, J. Chem. Phys., 39, 1614 (1963).

9. P. Diehl, Helv. Chim. Acta, 44, 829 (1961).

10. P. Diehl, Helv. Chim. Acta, 45, 568 (1962).

11. (a) J.S. Martin, Thesis, Columbia University, 1962.

    (b) J.S. Martin and B.P. Dailey, J. Chem. Phys., 39, 1722 (1963).

12. B. Bak, J.B. Jensen, A. Larsen, and J. Rastrup-Andersen, Acta Chem. Scand., 16, 1031 (1962).

13. H. Spiesecke and W.G. Schneider, J. Chem. Phys., 35, 731 (1961).

14. R.R. Fraser, Can. J. Chem., 38, 226 (1960).

15. W.G. Paterson and N.R. Tipman, Can. J. Chem., 40, 2122 (1962).

16. A.D. Buckingham, Can. J. Chem., 38, 300 (1960).

17. W.G. Schneider, J. Phys., Chem., 66, 2653 (1962).

18. J.A. Pople, Proc. Roy. Soc., A239, 541 (1957).

19. J.A. Pople, Proc. Roy. Soc., A239, 550 (1957).

20. W.E. Lamb, Phys. Rev., 60, 817 (1941).

21. Reference 1, page 175.

22. J.S. Waugh and P. Fessenden, J. Am. Chem. Soc., 79, 846 (1957).

23. M.J.S. Dewar and P.J. Grisdale, J. Am. Chem. Soc., 84, 3539 (1962).

24. J. Lennard-Jones, Advanc. Sci., London, 11, 136 (1954).

25. O. Exner, Tetrahedron Letters, 4, 815 (1963).

26. J.N. Murrell, Roy. Inst. of Chem. Lecture Series No.2. (1963).

27. H.H. Jaffé and M. Orchin, "Theory and Applications of Ultraviolet Spectroscopy", John Wiley and Sons, Inc., New York, 1962, page 409.

28. J. Cavanaugh, and B.P. Dailey, J. Chem. Phys., 34, 1094 (1961).

29. L. Meyer and H.S. Gutowsky, J. Phys. Chem., 57, 481 (1953).

30. B.P. Dailey and J. Shoolery, J. Am. Chem. Soc. 77, 3977, (1955).

31. A. Allred and E. Rochow, J. Am. Chem. Soc., 79, 5361 (1957).

32. A. Bothner-By and C. Naar-Colin, J. Am. Chem. Soc., 80, 1728 (1958).

33. A. Bothner-By and C. Naar-Colin, Ann. N.Y. Acad. Sci., 70, 833 (1958).

34. P. Lauterbur, Ann. N.Y. Acad. Sci., 70, 841 (1958).

35. H. Spiesecke and W.G. Schneider, J. Chem. Phys., 35, 722 (1961).

36. J. Goldstein and H. Reddy, J. Chem. Phys., 36, 2644 (1962).

37. J. Goldstein and H. Reddy, J. Chem. Phys., 38, 2736 (1963).

38. N.A. Matwiyoff and R.S. Drago, J. Chem. Phys., 38, 2583 (1963).

39. R.S. Drago, Private Communication (1963).

40. H.S. Gutowsky and C. Juan, J. Am. Chem. Soc. 84, 307 (1962).

41. J. Hinze and H.H. Jaffé, J. Am. Chem. Soc., 84, 540 (1962).

42. H.A. Bent, Chem. Revs., 61, 275 (1961).

43. C.J.F. Böttcher, "Theory of Electrical Polarisability" Elsevier Publishing Company, Amsterdam, 1962, Chapters 1 and 2.

44. L.P. Hammett, "Physical Organic Chemistry", McGraw-Hill Book Company, Inc., New York, 1940, Chapter 7.

45. R.W. Taft and I.C. Lewis, J. Am. Chem. Soc., 81, 5343 (1959).

46. R.W. Taft, S. Ehrenson, I.C. Lewis and R.E. Glick, J. Am. Chem. Soc., 81, 5352 (1959).

47. R.W. Taft, J. Phys. Chem., 64, 1805 (1960).

48. M.J.S. Dewar and P.J. Grisdale, J. Am. Chem. Soc., 84, 3548 (1962).

49. H. van Bekkum, P.E. Verkade and B.M. Wepster, Rec. Trav. Chim., 78, 815 (1959).

50. G.W. Wheland and L. Pauling, J. Am. Chem. Soc., 57, 2086 (1935).

51. H.H. Jaffé, J. Chem. Phys., 20, 279 (1952).

52. H.H. Jaffé, J. Chem. Phys., 20, 778 (1952).

53. H.M. McConnel, J. Chem. Phys., 27, 226 (1957).

54. J. Guy and J. Tillieu, J. Chm. Phys., 24, 1117 (1956).

55. J.A. Pople, Disc. Faraday Soc., No.34, 7 (1962).

56. R.F. Zürcher, J. Chem. Phys., 37, 2421 (1962).

57. P.T. Narasimhan and M.T. Rogers, J. Phys. Chem., 63, 1388 (1959).

58. J.I. Musher, J. Chem. Phys., 35, 1159 (1961).

59. R.J. Abraham, Disc. Faraday Soc., No.34, 67 (1962).

60. Reference 1, Page 179.

61. J. Cavanaugh and B.P. Dailey, J. Chem. Phys., 34, 1099 (1961).

62. T. Schaefer, W.F. Reynolds and T. Yonemoto, Can. J. Chem. In Press.

63. A.J.R. Bourn, D.G. Gillies and E.W. Randall, Proc. Chem. Soc., 200 (1963).

64. E. Pitcher, A.D. Buckingham and F.G.A. Stone, J. Chem. Phys., 36, 124 (1962).

65. G.V.D. Tiers, J. Am. Chem. Soc., 78, 2914 (1956).

66. A.D. Buckingham, T. Schaefer and W.G. Schneider, J. Chem. Phys., 32, 1227 (1960).

67. F. London, Z. Phys., 63, 245 (1930).

68. H.A. Stuart, "Die Physik der Hochpolymeren, Band I, Die Struktur des Freien Moleküls", Springer-Verlag, Berlin, (1952), Page 72.

69. C.J. Creswell and A.L. Allred, J. Am. Chem. Soc., 85, 1723 (1963).

70. B.B. Howard, B. Linder and M.T. Emerson, J. Chem. Phys., 36, 485 (1962).

71. D.P. Stevenson and G.M. Coppinger, J. Am. Chem. Soc., 84, 149 (1962).

72. J.Hine, "Physical Organic Chemistry", McGraw-Hill Book Company, Inc., New York, 1962, Page 93.

73. J.C. Schug and J.C. Deck, J. Chem. Phys., 37, 2618, (1962).

74. A. Streitwieser, "Molecular Orbital Theory for Organic Chemists", John Wiley and Sons, Inc., New York, 1961.

75. H.S. Gutowsky, G.E. Pake and R. Bersohn, J. Chem. Phys., 22, 643 (1954).

76. C.J. Brown, Acta Crystall., 2, 228 (1949).

77. L.E. Sutton, Chapter 13 in "Determination of Organic Structures by Physical Methods". Edited by E.A. Braude and F.C. Nachod. Academic Press Inc., New York, 1955.

78. M. Karplus and T.P.Das, J. Chem. Phys., 34, 1683 (1961).

79. H.M. Hutton, W.F. Reynolds and T. Schaefer, Can. J. Chem., 40, 1758 (1962).

80. Reference 27, Page 413.

81. Reference 72, Page 87.

82. R.W. Taft, Chapter 13 in "Steric Effects in Organic Chemistry". Edited by M.S. Newman. John Wiley and Sons, New York, 1956.

83. D.M. Graham and J.S. Waugh, J. Chem. Phys., 27, 968 (1957).

84. J.N. Shoolery and B.L. Crawford, J. Mol. Spectroscopy, I, 270 (1957).

85. J.A. Pople, W.G. Schneider and H.J. Bernstein, Can. J. Chem., 35, 1060 (1957).

86. J.J. Drysdale and W.D. Phillips, J. Am. Chem. Soc., 79, 319 (1957).

87. P.M. Nair and J.D. Roberts, J. Am. Chem. Soc., 79, 4565 (1957).

88. J. Schug, P. McMahon and H.S. Gutowsky, J. Chem. Phys., 33, 843 (1960).

89. H.S. Gutowsky, G.G. Bedford and P. McMahon, J. Chem. Phys. 36, 3353 (1962).

90. R.W. Fessenden and J.S. Waugh, J. Chem. Phys., 37, 1466 (1962).

91. N. Sheppard and J.J. Turner, Proc. Roy. Soc. A252, 506 (1959).

92. R.K.Harris and N. Sheppard, Trans. Faraday Soc., 59, 606 (1963).

93. J.S. Waugh and F.A. Cotton, J. Phys. Chem., 65, 562 (1961).

94. E.O. Bishop, Annual Reports, Chem. Soc. London, 58, 67 (1961).

95. H.S. Gutowsky, J. Chem. Phys., 37, 2196 (1962).

96. S. Mizushima, "Structure of Molecules and Internal Rotation", Academic Press Inc., New York, 1954, Page 64.

97. Reference 1, page 378.

98. W.S. Brey and K.C. Ramey, J. Chem. Phys., 39, 844 (1963).

99. L. Petrakis and C.H. Sederholm, J. Chem. Phys., 36, 1087 (1962).

100. M. Karplus, J. Chem. Phys., 30, 11 (1959).

101. Reference 1, page 117.

102. R.R. Fraser, R.U. Lemieux and J.D. Stevens, J. Am. Chem. Soc., 83, 3901 (1961).

103. H.J. Bernstein, J.A. Pople and W.G. Schneider, Can. J. Chem., 35, 65 (1957).

104. H.M. McConnel, A.D. McLean and C.A. Reilly, J. Chem. Phys., 23, 1152 (1955).

105. Reference 1, page 73.

106. Reference 5, page 57.

107. H.S. Gutowsky and C.H. Holm, J. Chem. Phys., 25, 1228 (1956).

108. P.C. Lauterbur and R.J. Kurland, J. Am. Chem. Soc., 84, 3405 (1962).

109. R.E. Glick and A.A. Bothner-By, J. Chem. Phys., 25, 362 (1956).

110. C.N. Banwell and N. Sheppard, Disc. Faraday Soc., No.34, 118 (1962).

111. M. Barfield and D.M. Grant, J. Am. Chem. Soc., 85, 1899 (1963).

112. H.S. Gutowsky, D. McCall and C. Slichter, J. Chem. Phys., 21, 279 (1953).

113. H.S. Gutowsky and A. Saika, J. Chem. Phys., 21, 1668 (1953).

114. H.M. McConnel, J. Chem. Phys., 28, 430 (1958).

115. M. Takeda and E. Stejskal, J. Am. Chem. Soc., 82, 25 (1960).

116. R.A. Ogg, Disc. Faraday Soc., No.34, 215 (1954).

117. R.A. Ogg, and J.D. Ray, J. Chem. Phys., 26, 1339 (1957).

118. E. Grunwald, A. Loewenstein and S. Meiboom, J. Chem. Phys., 27, 630 (1957).

119. A. Loewenstein and S. Meiboom, J. Chem. Phys., 27, 1067 (1957).

120. S. Meiboom, A. Loewenstein and S. Alexander, J. Chem. Phys., 29, 969 (1958).

121. M.T. Emerson, E. Grunwald and R. Kromhout, J. Chem. Phys., 33, 547 (1960).

122. E. Grunwald, P.J. Karabatos, R. Kromhout and E. Purlee, J. Chem. Phys., 33, 556 (1960).

123. T. Connor and A. Loewenstein, J. Am. Chem. Soc., 83, 560 (1961).

124. S. Meiboom, J. Chem. Phys., 34, 375 (1961).

125. A. Loewenstein and A. Szoke, J. Am. Chem. Soc., 84, 1151 (1962).

126. M. Anbar, A. Loewenstein and S. Meiboom, J. Chem.Phys., 80, 2630 (1958).

127. E. Grunwald, S. Jumper and S. Meiboom, J. Chem. Phys., 84, 4664 (1962).

128. E. Grunwald, S. Jumper and S. Meiboom, J. Chem. Phys., 85, 522 (1963).

129. E. Grunwald and C. Jumper, J. Chem. Phys., 85, 2051 (1963).

130. E. Grunwald and S. Meiboom, J. Chem. Phys., 85, 2047 (1963).

131. W.G. Paterson, Can. J. Chem., 41, 714 (1963).

132. W.G. Paterson, Can. J. Chem., 41, 2472 (1963).

133. W.G. Paterson and H. Spedding, Can. J. Chem., 2477 (1963).

134. Reference 1, Chapters 1 and 3.

135. N. Bloembergen, E.M. Purcell and R.V. Pound, Phys. Rev., 73, 679 (1948).

136. I. Waller, Z. Phys. 79, 370 (1932).

137. P. Debye "Polar Molecules", Dover Publications, New York, 1945. Chapter 5.

138. S. Chandrasekar, Rev. Mod. Phys., 15, 1 (1943).

139. F. Bloch, Phys. Rev., 70, 460 (1946).

140. T. Schaefer, Thesis, Lincoln College, Oxford, 1958.

141. R.E. Richards, Chapter 4 in "Advances in Spectroscopy", Volume 2. Edited by H.W. Thompson. Interscience Publishers, Inc., New York, 1961.

142. Reference 1, page 222.

143. J.C. Woodbrey, "Calculation of the Positions and Relative Intensities for the Maxima and Central Minimum of Exchange-Averaged, Lorentzian-Type NMR Doublets, by Bendix G-15 Program", W.R. Grace and Co., Research Division, Bulletin WRC No.101, 1961.

144. C.W. Davies, "Ion Association", Butterworths, London, 1962.

145. N. Bjerrum, Kgl. Danske Videnskab Selskab Mat-Fys. Medd., 7, No.9 (1926).

146. C.W. Davies, J. Chem. Soc., 460 (1945).

147. C.A. Kraus, Ann. N.Y. Acad. Sci., 51, 789 (1949).

148. Reference 144, pages 96, 98 and 169.

149. K.J. Laidler, "Chemical Kinetics", McGraw-Hill Book Company, Inc., New York, 1950. Chapter 5.

150. L. Doub and J.M. Vandenbelt, J. Am. Chem. Soc., 69, 2714 (1947).

151. H. Eyring and E.M. Eyring, "Modern Chemical Kinetics", Reinhold Publishing Corp., New York, 1963. Chapter 6.

152. S. Glasstone, "Textbook of Physical Chemistry", Van Hostrand Company Inc., New York (1946). Page 967.

153. Reference 144, page 97.

154. C.G. Swain, J.T. McKnight, M.M. Labes and V.P. Kreiter, J. Am. Chem. Soc., 76, 4243 (1954).

155. B. Tice, I. Lee and F.H. Kendall, J. Am. Chem. Soc., 85, 329 (1963).

156. J.E. Freund, P.E. Livermore and I. Miller, "Manual of Experimental Statistics", Prentice-Hall, Inc., Englewood Cliffs, N.J. 1960. Part IID.

157. Reference 149, Chapter 3.

158. F. Swarts, Bull. Sci. Acad. Roy. Belg., 8, 343 (1922).

159. Reference 77, page 607.

160. M.T. Emerson, E. Grunwald, M.L. Kaplan and R.A.Kromhout, J. Am. Chem. Soc., 82, 6307 (1960).